Dragline Gear Monitoring under Fluctuating Conditions

by

Berndt Leonard Eggers

Submitted in partial fulfilment of the requirements for the degree

Master of Engineering

In the Faculty of

Engineering, Built Environment and Information Technology

University of Pretoria, Pretoria

October 2007

Dragline Gear Monitoring under Fluctuating Conditions

Berndt Leonard Eggers

Supervisor: Prof. P.S. Heyns
Co-Supervisor: Dr. C.J. Stander
Department: Mechanical and Aeronautical Engineering
Degree: Master of Engineering

Abstract

The aim of this study is to apply computed order tracking with subsequent rotation domain averaging and statistical analysis to typical mining environments. Computed order tracking is a fault detection method that is unaffected by varying speed conditions often found in industry and has been proven effective in laboratory conditions.

However in the controlled environment of a laboratory it is difficult to test the robustness of the order-tracking procedure. The need thus exists to adjust the order tracking procedure so that it will be effective in the mining environment. The procedure needs to be adjusted to function with a two pulse per revolution speed input. The drag gear aboard a dragline rotates in two directions. This gives the unique opportunity to observe the performance of the order tracking method in a bi-directional rotating environment allowing relationships between the results of each operating direction to be investigated.

A monitoring station was set up aboard a dragline and data was captured twice daily for a period spanning one year. The data captured consisted of accelerometer and proximity sensor data. The key on the shaft triggers the proximity sensors allowing speed and direction to be measured. The rudimentary measured speed is interpolated using various documented speed interpolation techniques and by a newly developed speed interpolation technique. The interpolated speed is then used to complete the order tracking procedure that re-samples the vibration data with reference to the speed.

The results indicate that computed order tracking can be successfully implemented in typical mining environments. Furthermore there is a distinct relationship between vibration data taken in both rotational directions: one direction provides a better indication of incipient failure. It is thus important not to choose a direction randomly when monitoring rotating machinery of this kind.

Keywords: Computed order tracking, gear condition monitoring, varying speed, rotation domain averaging.

Acknowledgments

- SASOL Mining for the access and use of the dragline.
- Johann Swart and Wollie Wolhuther for their assistance in setting up the monitoring system and keeping it running.

CONTENTS

LIST OF TABLES

LIST OF FIGURES

LIST OF SYMBOLS

θ	Angular displacement
$\dot{\theta}$	Angular velocity
$\ddot{\theta}$	Angular acceleration
Θ	Matrix formed of angular- displacement and velocity vectors
$\dot{\Theta}$	Matrix formed of angular- velocity and acceleration vectors
I	Moment of inertia
C_T	Angular damping coefficient
K_T	Angular spring coefficient
t	Time
j,n,η	Integers
L	Length
f	Force
Y	Data set
$\hat{Y}$	Fitted curve
a , b	Filter coefficient
y	Filter transfer function

LIST OF ABBREVIATIONS

A/D	Analogue to Digital
AR	Autoregressive
BSS	Blind Source Separation
CM	Condition Monitoring
COT	Computed Order tracking
CPU	Central Processing Unit
DC	Direct Current
DDVI	Displacement Driven Velocity Interpolation
DSG	Dynamic Systems Group
FFT	Fast Fourier Transform
GMF	Gear Mesh Frequency
ICP	Integrated Circuit Piezoelectric
MLE	Maximum Likelihood Estimation
MM	Method of Moments
MWOT	Moving Window Order Tracking
NN	Neural Network
PCA	Principal Component Analysis
RAM	Random Access Memory
RDA	Rotation Domain Averaging
RMS	Root Mean Square
STFT	Short-time Fourier Transform
SVM	Support Vector Machines
TDA	Time Domain Averaging
UPS	Uninterrupted Power Supply

CHAPTER 1 INTRODUCTION

1.1 Background

Condition Monitoring (CM) has become popular in modern industry to improve reliability, plant availability, to reduce maintenance cost and increase plant efficiency. According to Poste (2001), companies in the United Kingdom that have introduced a CM program on average spend 25% less on maintenance than those that had no CM program in place. This considerable decrease in expense is due to a number of factors:

- CM allows for planned plant shut down, pre-ordering of parts and allows time to get the right personnel in place to carry out shut down work.
- CM lowers labour costs since the work can be focussed on identified problem areas.
- CM prevents secondary damage caused by unforeseen break down, thus decreasing down time.
- CM can reduce or eliminate routine machine shut down, depending on the maintenance strategy employed.

CM usually employs vibration, temperature and sound measurements as well as thermal imaging and oil-debris analysis. Of these, vibration is most commonly used to detect changes in the operating condition of rotating machinery. In the case of critical machinery, online monitoring is often done. This provides the opportunity to keep a close eye on the machine's condition at all times.

However, many of the vibration analysis techniques require that the machine cycles at a constant speed in order to be effective. This means that the machine must either break from its normal routine so that measurements can be taken, or the measurements must be taken at a time when the machine is cycling relatively constantly. This creates a niche for improvement as breaking the operating routine of the machine entails losing production and timing the measurements requires human intervention and does not necessarily yield a

constant cycle sample. Thus it becomes necessary for a vibration analysis procedure to be developed that can indicate deterioration under varying speed conditions.

A method to do this, entailing order tracking, rotational domain averaging, load normalisation, pseudo Wigner-Ville distribution with extracted statistical parameters and fault recognition by neural networks, was developed by Stander et al. (2002). Order tracking entails the re-sampling of the vibration data with reference to the cycling speed of the machinery. It is the aim of this dissertation to modify the method so that it can be implemented in a mining environment aboard a dragline, where the challenge is to overcome the limited speed data from a once per revolution key phasor.

1.2 Literature review

Since the development of the computer, rapid strides have been made in the creation of new methods to approach and analyse mechanical failure. The computer is capable of performing rapid calculations allowing sophisticated fault-detection techniques to become viable. As the computer industry develops faster computers, so a large variety of more complex vibration based CM techniques are being implemented. To get a global view of the methods being used, a structured approach is necessary to avoid confusion.

A good approach to the literature review is to group the myriads of different techniques that have been developed into families of related work. Statistical methods, synchronous averaging, demodulation techniques, autoregressive modelling, order tracking, short-time Fourier transforms, time-frequency analysis, wavelet transforms and neural networks are all fault-detection families in which varying levels of activity have taken place. Each group will be introduced and work that falls within the group will be discussed. Any shortfalls within each group will be discussed so that the niche into which this research fits is clearly highlighted.

1.2.1 Statistical methods

Statistical methods are often used in conjunction with Time Domain Averaging (TDA). Typical methods include techniques such as kurtosis, skewness, form- and crest-factor. Often a comparison is made between a reference signal and the measured signal to detect the presence of a fault. These methods have however only recently taken a hold in gear tooth failure detection.

A conventional statistical method seeks to fit a statistical distribution to the recorded data. The kurtosis is then calculated to predict the system's health. Oguamanam et al. (1995) investigate the effectiveness of the Method of Moments (MM) and the Maximum Likelihood Estimation (MLE) techniques when determining the shape parameters of the beta distribution. On a healthy gear, MM and MLE produce the same kurtosis. However the MLE technique is superior to the MM technique when damage is present even though it is computationally more expensive.

Parker et al. (2000) introduce a technique using bispectral analysis. After the vibration data is phase synchronised, the statistical change in the bispectral domain is shown to be capable of detecting faults in bearings and gears.

Andrade et al. (2001) introduce the Kolmogorov-Smirnov test, which can be used to detect early signs of spur gear fatigue cracks. This test uses the cumulative density function to compare two signals. A change can then be linked to the presence of a fatigue crack. The vibration signature of the signal can then be compared to template signatures allowing the condition of the gear to be estimated.

Baydar et al. (2001) state that although methods such as TDA, spectrum and modulation techniques are capable of indicating a faulty condition, they do not provide much information about the location or severity of faults. However they suggest that a multivariate statistical approach based on Principal Component Analysis (PCA) will be capable of relaying such information. PCA is a method in which a new set of variables that represent the maximal

variability in the data is gleaned from the data with minimal loss of information. Multivariate statistics then detect any deviation when comparing PCA data to a reference set.

Roan et al. (2002) present a Blind Source Separation (BSS) approach. This entails measuring the output of an unknown system, and by assuming some characteristics of the input, learn the system and find the input. It is shown that BSS performs best when compared to previous methods but can be effective without comparison. This method was tested on a test rig and showed the capability to detect single, adjacent and non-adjacent tooth failure.

Since most statistical methods entail TDA they are also suspect when it comes to performing under varying load and speed conditions. Parker et al. (2000) however correct for shaft speed variations by re-sampling time-series data to achieve phase-synchronous samples. Andrade et al. (2001) mention that the Kolmogorov-Smirnov test is strongly dependent on the gear loading and rotational speed variations. Baydar et al. (2001) state that in CM the speed and load should remain constant so that a change in the vibration signal can be attributed to fault conditions. Roan et al. (2002) claim that the BSS approach detects a fault regardless of how the gear is being driven.

1.2.2 Synchronous averaging

Synchronous averaging or TDA, a pre-processing method, runs hand in hand with most vibration analysis techniques. It is capable of removing noise elements out of a periodic signal typically encountered in rotating machinery, thus improving the signal to noise ratio. In TDA successive samples of a repetitive signal such as a gear mesh frequency (GMF) are ensemble averaged. This method has a similar effect as that of a comb filter that has pass bands at multiples of the rotation frequency of the gear of interest. The estimate of the desired signal is improved as more averages are taken. In itself TDA can only detect severe fault conditions.

McFadden (1987i) however points out that the existing comb filter model is flawed due to the assumption that the signal is known over an infinite period of time when in reality it is finite. A revised model is presented which only requires finite knowledge of the signal. It is also shown that the number of averages need not be a power of two to optimise noise rejection. Rather the number of averages should be chosen so that the nodes of the comb filter coincide with the frequency of the noise. McFadden however acknowledges that this will not always be possible.

It is possible to improve on the analysis of TDA if all tooth meshing vibrations and its harmonics are removed from the TDA leaving the 'residual' signal. This signal often shows evidence of a defect before it can be detected on TDA. The eliminated components are known as the 'regular' signal. McFadden (1987ii) states that though this technique has been used for many years, there had been no satisfactory explanation of what regular and residual signals actually represent. It is then shown that the regular signal defines the TDA of the meshing vibration of a single gear tooth. The residual however gives the departure of the vibration from the average, indicating a fault. McFadden (1987ii) however mentions that the amplitude modulation is affected by a change in loading conditions and thus complicates the fault identification process.

After TDA and subsequent comb filtering, diagnostic parameters are often used to quantify the damage on a gear. Threshold values are determined and decisions to overhaul or inspect the gear are based on these values. Dempsey (2000) investigated two such parameters applied to the residual of the TDA signal, NA4 and FM4. FM4 is the ratio of the kurtosis to the standard deviation of the difference signal. NA4 is similar to FM4 but takes the first order sidebands into account when calculating the regular meshing components of the signal. After extensive testing FM4 indicated pitting damage sooner than NA4. It was also noted that NA4 is very sensitive to load changes that occurred during testing causing false alarms.

Hongxing et al. (2000) note that care must be taken when cutting samples from the vibration data for TDA. They state that often a period cutting error is incorporated into the TDA procedure. This period cutting error is cumulative over the number of periods removed from the vibration signal. An improved method to avoid this error is suggested and tested using 28 averages. A significant improvement in the clarity of the meshing frequency and its harmonics is shown.

McFadden (2000) introduces a new approach whereby subsequent TDAs are compared and matched by making small adjustments to amplitude and phase after the largest difference between the two TDAs is removed. The removed part, called the difference signal, is deemed indicative of a gear tooth fault. The difference signal is then decomposed into known transient components. A selection of these components is then put through a simple scoring system to give a clear indication of gear fault.

Since TDA is designed to filter out noise it is not effective in removing the amplitude and phase modulation produced by a varying load and speed condition. The TDA is likely to produce a slight smear of the frequency spectrum around the meshing frequency and its harmonics. McFadden (1987ii) assumes that constant speed and load conditions apply, leaving the problem of varying conditions largely ignored. McFadden (2000) matched difference approach could possibly be successful for small variations in speed and load.

1.2.3 Demodulation techniques

Two types of modulations typically occur within the realm of vibration analysis, amplitude and phase modulation. Both have relevance in determining fault conditions on gears. Fatigue cracks at the root of the gear teeth reduce the gear meshing stiffness. This leads to an increased amplitude and phase modulation in the measured vibration signal. The modulation appears as sidebands of the meshing frequency in the spectrum of the measured signal. Analysing modulation and demodulating signals is thus a commonly used CM

method. To understand the principles of demodulation it is first necessary to consider modulation.

Amplitude modulation is most effectively demonstrated when two signals of similar amplitude but with different frequencies are multiplied. The low frequency signal is called the modulating signal and the high frequency signal is called the modulated frequency or the 'carrier' signal. When a fast Fourier transform (FFT) is computed from the modulated signal, the amplitude modulation is represented by sidebands around the carrier frequency. The frequency difference between the carrier and either one of the sidebands is equivalent to the frequency of the modulating signal. A typical carrier, modulating and modulated signal are shown in Figure 1.1.

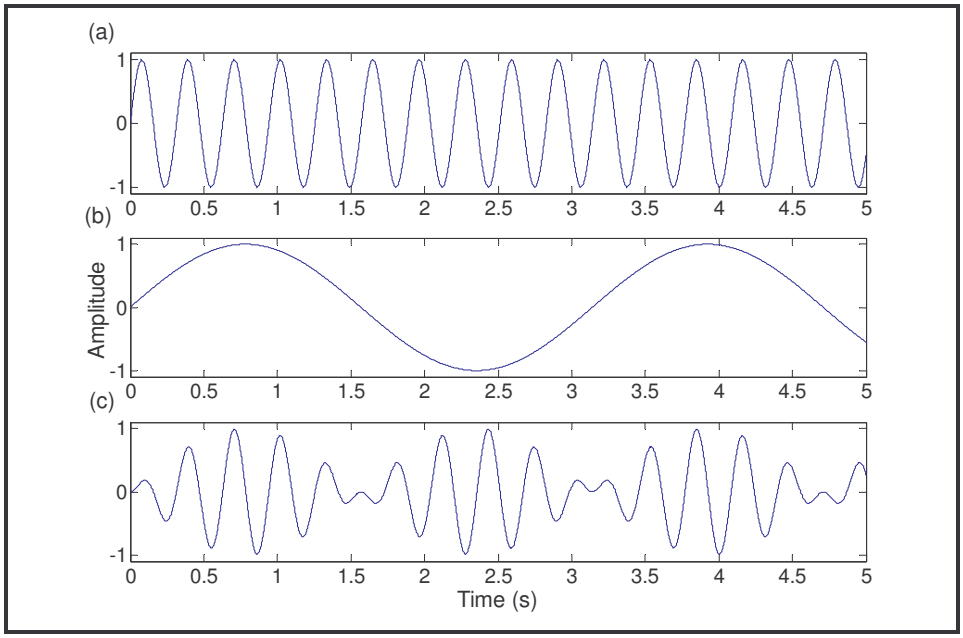

Figure 1.1: (a) The carrier signal, (b)The modulating signal, (c) The modulated signal.

The process of separating these two signals from one another is called demodulation. To be able to recover the modulating frequency from the carrier, the carrier's frequency must first be determined. Once it is determined then all that is necessary is to full-wave rectify the modulated waveform and pass it through a low-pass filter, removing the high frequency carrier signal. The dc component produced by the rectification process is easily negated, making the resulting modulating signal clearly visible. Other ways and methods also exist to demodulate a signal.

According to White (1991) frequency modulation of the tooth mesh frequency in gears can occur due to a gear that is eccentric on its shaft causing it to drive the other gear at varying speeds. When driving a load the varying speed also causes variations in the tooth forces, resulting in amplitude modulation. A gearbox driving a varying load will cause a fluctuation in the rotation speed with the resulting modulation. If the load varies significantly but the speed remains relatively constant then amplitude modulation will be more pronounced than frequency modulation.

McFadden and Smith (1985) state that in complicated gear systems the identification of modulation sidebands is more difficult and requires the resolution of the spectrum to be increased. Even then the severity of the defect is not always apparent. To improve detection the samples are synchronised with the rotation of the gear. Multiple samples are then averaged. This technique removes all signals that are asynchronous with the rotation of the gear. The data is then band pass filtered around the dominant meshing harmonics, eliminating the harmonics. An envelope is calculated from the residual signal and kurtosis is applied to detect faults.

McFadden (1986) introduces another approach whereby the data around a dominant harmonic of the meshing frequency is band pass filtered, after applying signal averaging, removing every signal that is not part of the dominant harmonic. He shows that each time a tooth meshes with the other gear a phase lag is incurred. As the damage severity increases, the phase and amplitude modulations become more pronounced demonstrating that both phase and amplitude modulation give clear indications of a fatigue crack.

Ma and Li (1996) however point out that using only a single tooth meshing harmonic and its sidebands to find the modulation signal, blunts the effectiveness of the procedure, since all meshing harmonics carry information about modulation signals. They propose a procedure whereby a mathematical model is set up describing the vibration of a damaged gear. An iterative approach to the model together with signal-averaged data captured from an

experimental set-up yields an estimation of the phase and amplitude modulations. The results of this procedure was compared to that of McFadden (1986) and yielded better sensitivity to gear damage.

Wang (2001) investigates another feasible demodulation approach. This approach is based upon the fact that structural resonance will be excited by impacts caused by gear tooth cracks. The modulation of this structural resonance will therefore carry information related to gear tooth fault. Again the GMF and its harmonics are removed from the synchronous averaged signal and the residual signal is band pass filtered around a structural harmonic. The band passed residual signal is then demodulated. Wang (2001) suggests that McFadden's (1986) approach works better if the harmonic that is analysed happens to coincide with a structural resonance.

Although it is abundantly clear that there are applications in which amplitude and phase demodulation techniques will be successful, the fact that both load and speed fluctuations also cause modulations is largely ignored. The closest to mentioning this problem is the assumption that load and speed should be constant. McFadden and Smith (1985), McFadden (1986), and Ma and Li (1996) made this assumption. Only Wang (2001) tested a method under varying load, constant speed conditions. Though this is an improvement, the effects of varying speeds on the success of demodulation techniques are not investigated.

1.2.4 Autoregressive modelling

Wang and Wong (2000) have proposed the use of a stationary Autoregressive (AR) process to detect and diagnose gear faults. A TDA signal is modelled using AR. This model is then used to predict the next point in a time signal given a number of previous points; the error between the predicted point and a signal from an unhealthy gear will be significant. In this way a change in the signal is detected. The advantage of this method of fault detection is that no knowledge of the number of teeth on the monitored gear is required. Wang and Wong (2000) also showed that the AR model based on an already faulty signal was also effective in detecting a fault condition.

Padovese (2004) introduces four hybrid time-frequency methods based on the AR model to calculate the time-frequency coordinates of the signal spectral pattern and the Capon method to estimate the power density associated with each coordinate. These hybrids are constructed by calculating the frequencies present at each time instant, leading to a time-frequency distribution and then to calculate the amplitudes associated with each time-frequency point. Four hybrid time-frequency methods are then reached depending on how the time-frequency distribution and amplitude calculation is achieved. These hybrid methods present excellent high-frequency resolution and better time and frequency resolution than the Wigner-Ville methods.

Though Wang and Wong (2000) indicate that AR models could perform under varying load conditions, their tests were performed in constant speed conditions. The testing done by Padovese (2004) was also conducted in constant speed conditions. Neither addressed effects of varying speeds on AR.

1.2.5 Order tracking

Order tracking is a method that uses special analogue hardware to sample vibration data at a rate proportional to the shaft speed. This then allows frequency analysis based on multiples of the running speed (orders), instead of frequency. According to Fyfe and Munck (1997) this approach is prone to have problems following rapidly changing shaft speeds. Computed Order Tracking (COT) samples at a constant rate and then uses software to resample the data at constant angular increments. This cuts the cost and complexity of the equipment required. Order tracking is useful in machine CM because it can easily identify speed-related vibrations and eliminates the deleterious effect of speed on almost all of the vibration methods mentioned in this chapter.

Gade et al. (1995) give an overview of order tracking theory as implemented by certain Brüel & Kjær instrumentation. They present the use of the instrumentation in four examples. The examples serve to highlight the

superiority of COT in certain applications. Gade et al. (1995) indicated the use of combining TDA and COT and make use of gated tracking, whereby COT is done on a particular angular fraction of a revolution, for complex rotating equipment such as reciprocating machinery.

Fyfe and Munck (1997) investigate the factors influencing the accuracy of the COT method. They found that higher sampling rates on the keyphasor and data signals and the use of higher-order interpolation techniques in the resampling process resulted in improved accuracy.

Saavedra and Rodriguez (2006) assessed the accuracy of the COT method using simulated data. They specifically looked at the influence of the signal and tachometer pulse sampling frequency, the amplitude interpolation method and the number of tachometric pulses per revolution. From their study they recommend multiple tachometer pulses per revolution for situations where the acceleration changes sign periodically. A higher sampling rate of the signal and pulse was also shown to decrease commonly occurring errors in the COT method.

Apart from extensively investigating approaches for producing synchronously sampled vibrations, Bossley et al. (1999) also introduce a hybrid order tracking method. This method makes use of hardware to measure the keyphasors, found in the traditional order tracking technique and uses interpolation techniques to resample the vibration data as used in COT. They show that this hybrid COT method is superior to both previous methods based on simulated data.

Groover et al. (2003) make use of the fact that a fixed frequency component such as a resonance vibration will change orders as the running speed varies. It is thus possible to eliminate rotational related components in the order domain, transform back into the frequency domain and retain an excellent resonance vibration devoid of any high-level rotational components that can make harvesting of smaller signals associated with blade vibrations in the

torsional domain easier. Groover et al. (2003) make use of the COT method as a kind of rotation component filter.

To address the high frequency sampling necessary to have good resolution for the key phasor, Bonnardot et al. (2004) suggest the use of only the vibration signals in the COT method thereby eliminating the use of the conventional key phasor signal. Investigating the location of the GMF and its harmonics, and given the number of teeth on the gear of interest the shaft speed can be estimated. The cost of analysis is reduced with this method but its drawback is that only a very small speed variation is tolerated. This drawback becomes even more pronounced when the harmonics of the GMF are used for speed estimation.

The order tracking method is a conventional vibration analysis method that directly seeks to address the effect of speed on the performance of fault detection methods.

1.2.6 Short-time Fourier transforms

The Short-Time Fourier Transform (STFT) is another time-frequency transform that represents a local spectrum of a signal. The signal is pre-windowed around a chosen time and its Fourier transform is calculated, this is repeated for each instant. This overcomes the drawbacks of the conventional Fourier transform namely its tendency to output an averaged representation of the frequency components in a signal, losing the time information essential to locate any transient signals. In comparison to the Wigner-Ville distribution, the STFT is almost free from cross-terms but does not stress the auto-terms well.

The choice of a suitable window with regards to efficiency and time-frequency resolution is a major issue concerning STFTs. Tomazic (1996) introduces a STFT with a single-sided exponential window and shows that it exhibits good time-frequency resolution.

The square of the modulus of the STFT is called a spectrogram. For each position of the window, another spectrum is obtained. Instead of totalling

these to form a time-frequency distribution, Staszewski and Tomlinson (1997) suggest a diagnosis based on the visual inspection of these spectra. Different window configurations are also used to determine the effect of different window parameters on the spectra.

No mention of speed or load related issues were found in the above articles. Once again the use of TDA could lead to errors that are not addressed.

1.2.7 Time-frequency analysis

Time frequency distributions give an account of how the energies associated with frequencies change over a period of time. This creates a very good visual representation of possible gear fault and is well suited to the analysis of non-stationary signals.

Wang and McFadden (1993i) show that the spectrogram when applied to the time domain averaged signal, gives a very clear time-frequency distribution. The window function chosen can have a significant effect on the clarity of the time-frequency distribution. Working with the residual signal produces even better results as it improves the clarity of the spectrogram. Wang and McFadden (1993ii) then further introduce a method whereby image processing is used to interpret the spectrogram. This could replace an operator, automating the process. The 'blobs' on the spectrogram are analysed by looking at their position, height, width, area, intensity and kurtosis. These factors are then used to determine whether a fault condition is present. Successful tests were done on a helicopter gearbox demonstrating the ability to detect early gear faults.

After developing a model to simulate the dynamics of a faulty gear system, Choy et al. (1996) showed the ability of the Wigner-Ville time-frequency distribution together with TDA and spectrum analysis to effectively characterize the vibration signal from a gear system.

The Wigner-Ville distribution is a bilinear distribution used initially in quantum mechanics in the 1930s. According to Hammond and White (1996) it has

however only been implemented in time-frequency analysis since the 1980s. It has good resolution capabilities but also contains interference terms when the input signal contains several components. These interference terms could lead to incorrect inferences. The pseudo-Wigner-Ville distribution is simply the Wigner-Ville distribution that is adapted to finite data lengths and employs windowing functions. Lee and White (1997) show that Wigner higher-order spectra are effective in the CM environment.

Staszewski et al. (1997) note that no effective method exists for an automatic fault detection procedure based on the Wigner-Ville distribution. Statistical and neural pattern recognition techniques were then implemented to detect different spur gear fault conditions. The weighted Wigner-Ville distribution is also tested and together with the removal of the meshing vibrations is found to simplify the result. However Staszewski et al. (1997) acknowledge that, when applied to a mining gearbox, these methods could prove less successful.

The research done in time-frequency methods has however to a large extent ignored the effect that load and speed can have on these techniques. Furthermore the majority of the research was done on spur gears. This raises doubts concerning the ability of these methods to work in a mining environment on high contact ratio helical or even double helical gears. In an attempt to remedy this, Baydar and Ball (2000) present the instantaneous power spectrum, which has a limited ability to detect fault conditions under varying load conditions.

Stander et al. (2001) present a load demodulation technique that is capable of monitoring the condition of a spur gear that is run on an experimental rig under varying load conditions. Furthermore Stander et al. (2002) presents a vibration waveform normalisation approach, which enables the use of a pseudo-Wigner-Ville distribution to indicate gear fault under fluctuating load conditions. Statistical parameters extracted from the distribution were then used to indicate linear separation for various fault conditions, which was calculated after load demodulation. Feature vectors for various fault conditions were then compiled and compared to an average vector compiled

from measured data using Mahalanobis distances. It was shown that the Mahalanobis distance could be monotonically trended to indicate fault progression. A neural network was also used to distinguish fault severity.

1.2.8 Wavelet transforms

The wavelet transform is an example of a linear time-scale decomposition of the signal and originated in the 1980s. Wavelet analysis is the localised equivalent of the Fourier transform. Where the Fourier transform moves data from a time domain to a frequency domain using sines and cosines as basis functions giving the average features of a signal, the wavelet transform decomposes the given data into a superposition of elementary wavelet functions giving localised characteristics of the signal. Because it is a linear representation of a signal, wavelets are useful for the analysis of multi-component signals. The wavelet transform provides good resolution in high frequencies offering a different time-frequency resolution compared to the Wigner-Ville distribution.

Staszewski and Tomlinson (1994) apply the wavelets to the problem of detecting a broken tooth in a spur gear and suggest that with further investigation it offers a means of fault detection. Pattern recognition and the Mahalanobis distance were used to detect fault severity. They indicate that a visual inspection of the wavelet transform can be used to localise the fault.

Wang and McFadden (1995) demonstrated that the orthogonal wavelet families are useful for detecting vibration transients, especially those transients in the meshing vibration caused by tooth fault. It was found that, due to a limited number of scales, a single wavelet map could not describe all details of the signal. Wang and McFadden suggest the use of non-orthogonal wavelet families to overcome this shortcoming.

Wang and McFadden (1996) investigated and showed that the time-scale distribution of the wavelet transform can analyse the local features of a signal, displaying both the large and small sizes in a signal simultaneously. This enables the detection of both distributed and local faults. In this respect the

wavelet transform is superior to time-frequency distributions that incorporate constant time and frequency resolutions.

The liner wavelet transform using B-spline wavelets was used to monitor crack growth by Lin and McFadden (1997). They indicate the ability of the linear wavelet transform to detect the location of a fatigue crack in a helicopter gear. They also compared the spectrum of the original time domain signal to the spectrum recovered by the B-spline wavelets after the time domain signal had been decimated by a factor of four. They thus demonstrated that the B-spline wavelet based linear wavelet transformation can successfully decompose a signal exactly.

An interesting use of wavelets was proposed by Staszewski (1998), who proposed that wavelets could be used to compress data, being especially effective for non-stationary data. He also mentioned that the compression of data could be useful for feature selection, since features are often represented by wavelet coefficients with high amplitudes.

Boulahbal et al. (1999) state that the wavelet transform is complex valued, and thus employs the phase as well as the amplitude maps of the wavelet transform to assess gear condition. They show that if both amplitude and phase maps are used in conjunction, a more positive assessment of tooth condition is accomplished. They also introduce a polar representation of the wavelet map, making the maps very intuitive.

McFadden et al. (1999) proposed that a variant to the wavelet transform, the generalised s-transform be used to decompose vibration signals. The advantage of the s-transform is that phase information about the components is easily retrieved. McFadden et al. (1999), as did Boulahbal et al. (1999), state that it is desirable to obtain local phase information in the interest of a more complete description of changes in vibrations. Given well-separated components, it is shown that near-perfect signal composition can be achieved.

Sung et al. (2000) properly verify the superiority of the wavelet transform over the short-time Fourier transform. When applying both techniques to synchronous averages of an experimental signal, and simulated signal data consisting of multi-frequency harmonics with small abrupt changes, wavelet transforms are shown to be more effective. Sung et al. (2000) mention that, based on the simulated signal performance of the wavelet transform, the gears within a gearbox should rotate close to the same speeds to facilitate fault detection.

Wavelets are also useful in improving the signal to noise ratio of vibration signals. Lin and Qu (2000) describe the use of Mortlet wavelets to de-noise a signal, thus facilitating feature extraction.

Luo et al. (2000) propose the use of the time-frequency localization of the wavelet transform in filter design. The wavelet filter together with autocorrelation enhancement allows monitoring to occur in real time due to its very short processing time. Furthermore Luo et al. (2000) state that TDA is superfluous when this method is used. Observing the natural frequencies, in time or frequency domain, the peak ratio and peak value are indicators capable of detecting a fault at an early stage.

To detect the transients from a signal with a high sensitivity, Wang (2001i) proposes a joint time-frequency-scale distribution. He suggests that due to the problem that the wavelet transform only matches time instant and length of a mother wavelet and the STFT only matches the time instant and wave shape, a fusion of the two would give full capacity to match the mother wavelet to all possible segments of the signal. Wang (2001i) demonstrates the usefulness of this transform but accedes that further research is necessary to interpret the ensuing 3D images.

The effect of speed and load variations on the Wavelet transform, being a very high-level detection technique, depends largely on the pre-processing used. Lin and McFadden (1997) consider a gear running under constant load and speed and also make use of TDA thus acknowledging a possible

problem. Boulahbal et al. (1999) mention that the change in phase modulation is a direct measure of the fluctuations of a gear's angular speed and resample the signal at constant angular positions to avoid the effect of speed variations.

1.2.9 Neural networks

The human brain, and its ability to think and solve problems, has inspired many researchers to mimic it. A result of these attempts is the artificial neural network. These Neural Networks (NNs) have then often been utilised to classify data thus eliminating the need of an operator to interpret analysed vibration data.

Paya et al. (1997) used multi-layer artificial NNs to distinguish between varieties of faults that were seeded on a model driveline. The raw data was first pre-processed by wavelet transforms before being used to train the NN. The NN was then set the task to classify the wavelet data. The NN performed well when detecting gear faults but not as well when detecting bearing faults.

Meesad and Yen (2000) mention that classical offline iterative learning classifiers require long training times and are often stuck at local minima, preventing the achievement of the optimum solution. Also, to train new data both old and new data must be used to prevent loss of the old data. A self-organising neurofuzzy network is proposed that should be able to tolerate noise, as a NN can, and deal with imprecise situations, which the fuzzy set theory can deal with. When tested on vibration data from a helicopter, the network achieved 100% correct classification.

Chen and Wang (2002) make use of multi-layer perceptrons fed with instantaneous scale-distribution patterns to detect gear faults. They state that the width of a peak pattern is not conducive to fault detection in CM, and therefore take a cross-section of a time-scale map at a specific time and refer to it as an instantaneous scale-distribution pattern. The NNs are then set to classify these instantaneous scale-distribution patterns. Chen and Wang (2002) report that this method provides adequate performance.

Samanta (2004) presents a comparative study between the performance of NN and Support Vector Machines (SVM). SVM is a statistical learning theory introduced in the 1960s. Genetic algorithms were used to extract the features for the NN and SVM. When compared the performance of the SVM is better than the NN and has a substantially shorter training time.

Since NNs are often in the final step in the vibration analysis procedure, problems linked to speed and load variations are mostly due to the analysis methods used before NNs are applied. Paya et al. (1997) do however mention that speed and load would only affect the intensity level of the signal. They do however keep load and speed constant in their testing.

1.3 Scope of the work

Vibration has in the past frequently been used to determine the condition of gears. Statistical methods, time domain averaging, phase and amplitude demodulation and a multitude of other methods have been employed. However these methods have to a large extent been based on the assumption that the gear speed is constant. If the data capture is well coordinated, then this would be a fair assumption, but errors due to fluctuating speed conditions would still occur. Recently however Stander et al. (2002) developed a method to measure the condition of gears operating under varying speed conditions, thus avoiding these errors. Effectively this allows measurements to be taken at any time during a machine's work period regardless of speed fluctuations.

In the methodology of Stander et al. (2002), gear speed data is acquired by means of a shaft encoder. Vibration data is then measured synchronous with the speed data. The angular position data then allows the acceleration data to be broken up into blocks corresponding to one revolution. A block of data is then converted to 1024 points, by interpolation. These blocks are then averaged. This technique is very similar to TDA except that angle of rotation is used and not time. Since rotation domain averaging is not time dependent, it is also independent of gear speed fluctuations. The averaged signal is then

analysed using a pseudo Wigner-Ville distribution. This allows the visualization of any gear defect that has occurred. The number of points that exceed a defect threshold during the pseudo Wigner-Ville analysis are counted and noted. These numbers are then plotted on a regular base to give a two-dimensional impression of the gear deterioration.

This methodology has been proven to be effective in detecting seeded gear damage when tested under laboratory conditions. These tests were conducted under different loading conditions, which influenced the rotational speed of the gear.

Having proved the relevance of this methodology under laboratory conditions it was necessary to apply it to a mining environment to ensure that similar results are achievable in the field. It was decided to apply the method to a dragline operating at Syferfontein, one of SASOL's open cast collieries.

However certain problems occur when this is attempted. Firstly it is not possible to install a shaft encoder on the pinion shaft, due to excessive axial motion, which would destroy the encoder. Instead two proximity sensors are used that sense the passing of the key. These proximity sensors are situated close to each other so that a change in direction can also be picked up. Using the proximity sensors instead of the shaft encoder will however significantly decrease the shaft position resolution. This would not have an effect on the method currently used by Stander et al. (2002) since it assumes constant velocity across a single revolution, but will mar any attempts to gain more precise speed information by using other interpolation techniques.

The shaft encoder is not suited to run at the mine on a permanent basis. The systems used in the laboratory would therefore need to be replaced by a capturing system suited to the electro-magnetically noisy and dusty environment aboard a dragline. The system would therefore be electro-magnetically shielded and contain air filters to remove dust from critical components such as the computer. It is difficult to inspect the gear visually and thus a comparison with currently used early detection methods is

necessary to determine whether order tracking is successful in early gear detection. Lastly data sets from 276 shaft rotations were averaged to remove noise whilst testing the order tracking methodology of Stander et al. (2002) in the laboratory, due to the change in direction occurring in the dragline data fewer shaft rotations will be useable.

The dragline is often cut from power whilst walking from one point of operation to another. It is also not operational whilst a shift rotation is in progress or whilst the caterpillar is cleaning the site. These interruptions would render the data block taken useless. Thus, as soon as data is attained from the dragline it would be necessary to check whether it is suitable. The data would be broken up into smaller blocks spanning only one revolution and sorted into forward and reverse rotating directions. Using current interpolation techniques as well as new methods of determining the speed fluctuation within one revolution, the acceleration data would be manipulated so that it is independent of speed. Order domain averaging would then be applied followed by FFT analysis to interpret the results. Finally a link between forward and reverse results will be investigated.

1.4 Summary

Ever since vibration monitoring was used for condition monitoring, many different methods and approaches have been utilised. Very few of these approaches deal with condition monitoring of varying speed components, such as gears, as well as those methods based on order tracking.

1.5 Dissertation overview

This dissertation is broken up into 5 chapters dealing with the literature, the setting up of the monitoring station, the order tracking methods and their development, the data analysis and the conclusion.

The first chapter dealt mainly with the literature pertaining to vibration monitoring. It covered many approaches to vibration monitoring and highlighted the niche into which the order tracking techniques fall. The order tracking techniques were also discussed in depth.

The second chapter deals with the development and implementation of the monitoring station aboard the dragline at the Syferfontein colliery. It discusses the hardware used and justifies the choice of equipment in light of the environment aboard the dragline. The acquisition software developed to capture data is introduced and the testing that was done prior to installing the station on the dragline is described.

The third chapter deals with the order tracking methods that are already established and relate the development of a new approach. The data from the dragline is also analysed to ascertain whether the captured data can be related to the dragline activity.

The fourth chapter covers the data processing and analysis of the captured data. The different order tracking approaches are compared and a gear deterioration graph is constructed. Correlation between forward and reverse rotating directions are also deliberated.

The fifth and final chapter concludes the dissertation and discusses accomplishments, shortcomings and recommendations.

CHAPTER 2 ONLINE MONITORING HARDWARE

In order to begin with the research, it was of paramount importance that the monitoring station at SASOL's Syferfontein colliery be implemented as soon as possible. The data acquired would be necessary to adjust and modify existing theoretical speed estimation techniques so that they would work successfully on the dragline data. The captured data would also provide insight into the development of a new speed estimation technique. This was thus the first major step en route to completion of the research.

The monitoring station was to work aboard the largest dragline in the southern hemisphere, a Dresser 8200 Marion dragline. Three of these draglines are in operation at the Syferfontein colliery. Figure 2.1 shows the Marion 1, aboard which the monitoring station was placed. This dragline has a bucket capacity of 150 tons.

Figure 2.1: The Marion 1 dragline on location at the Syferfontein colliery.

To operate successfully in the mining environment the monitoring station would have to comply with a number of specifications. The station should be robust enough to handle the opencast mining environment; this includes shock, dust and high electro-magnetic interference fields. It should be capable of sampling at a high frequency so that no relevant information is lost; this

applies especially to the vibration readings. Finally it should be able to detect the direction of rotation of the pinion of interest.

The activity of setting up the monitoring station is classified into three sections: hardware employed, software development and preliminary testing. The following subsections will cover these three aspects in depth.

2.1 The hardware employed

The hardware part of the monitoring station encompasses all mechanical and electrical components necessary to support the operation of the data acquisition software. The software requires adequate sensory input and significant storage space.

To be able to run the software, a number of hardware units were acquired or built. Sensors capable of relaying speed, direction and vibration data were required. A low pass filter would have been indispensable to prevent aliasing of the measured data. An analogue to digital (A/D) conversion card capable of a sufficiently high sampling frequency would have been vital to accept the data relayed by the sensors. And a computer capable of housing and protecting the A/D card and supplying an interface between the software and the A/D card would have been necessary.

2.1.1 The sensors

The main role of the sensors is to relay speed, directional and vibration information to the A/D card. Two types of sensors would be capable of meeting the requirements of this research. Typically an accelerometer would be sufficient to measure the vibration data and a proximity sensor would be capable of supplying speed data.

The accelerometer is preferred to velocity and displacement sensors since it is capable of measuring higher frequencies typically encountered when monitoring machinery. Commonly a radial as well as an axial reading are taken when monitoring rotating machinery. Thus two 100mV/g Integrated

Circuit Piezoelectric (ICP) accelerometers were selected for the task. Each accelerometer needs a signal-conditioning box to amplify the output of the accelerometers.

According to McFadden (1986) it is usual to mount a transducer on the exterior housing of the gearbox, since direct measurement on the gear itself is not practical. At the Syferfontein colliery the accelerometers were mounted with studs onto aluminium platelets that were bonded to the pinion housing on the drive end of the drag motor in radial and axial directions as shown in Figure 2.2. A galvanised steel plate box was also constructed and glued in place over the accelerometers to prevent accidental damage to the sensors. The different locations of the drag and hoist drums are indicated in Figure 2.3. The position of the drive end and non-drive end of the motor is illustrated in Figure 2.4.

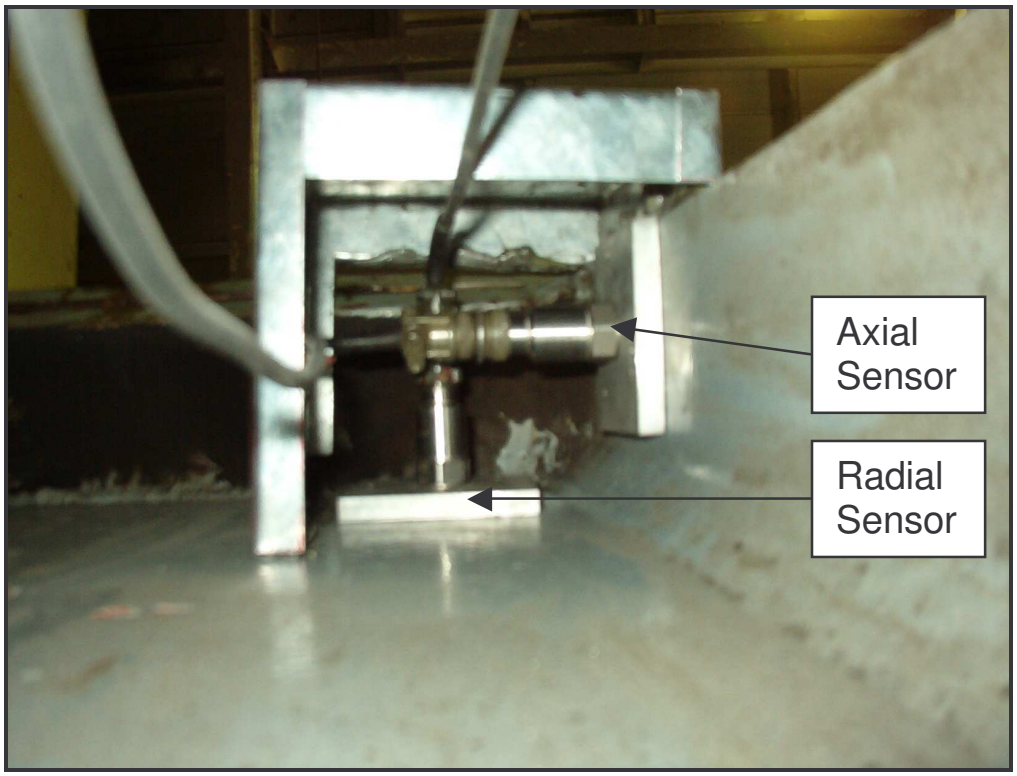

Figure 2.2: The positioning of the accelerometers against the pinion housing as seen from below

Figure 2.3: A view inside the dragline.

.

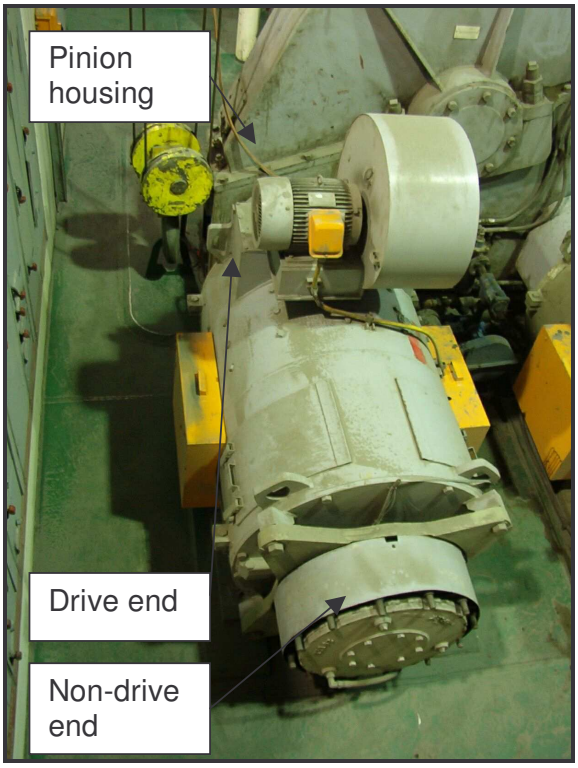

Figure 2.4: The instrumented DC motor aboard the dragline.

The pinion housing, indicated in Figure 2.4, also houses another gear assembly and this could lead to an increase in the complexity of the measured signal. This problem however is minimised by the use of signal averaging in the order domain when processing the data.

The measurement of the speed of the pinion requires the use of a proximity sensor. A key is present on the pinion shaft, which is employed to trigger the proximity sensor once per revolution. The square signal received from a sensor can easily be converted into speed information since the distance travelled between pulses is constant and an indication of average speed is obtainable by simply dividing the time taken between pulses into the distance travelled. This average speed over one revolution is however not accurate, and suggests the use of interpolation techniques to gain more precise information about speed fluctuations within one revolution. The positioning of the proximity sensors for speed-readings is arbitrary and would be dictated by the requirement to determine rotational direction.

To determine the rotating direction of the pinion it is necessary to have another proximity sensor additional to the one used to determine speed. Each proximity sensor will be measured on a different A/D channel. The two proximity sensors should be mounted next to each other. As the key triggers the two adjacent sensors it is possible to identify which sensor was triggered first and thus a direction is obtainable. If the proximity sensors were placed 180° apart from one another it would be impossible to determine in which direction the shaft is moving. The sensors were thus placed approximately 9° apart from each other, this was partly due to the ease with which the sensors could be attached to a single bracket.

To measure both direction and speed two M18 Pulsotronic inductive sensors capable of switching at 1 kHz were acquired. It has been observed, from preliminary data acquisitioning on the dragline at the Syferfontein colliery, that the pinion rarely rotates faster than 20 Hz, thus the switching frequency of these sensors are adequate.

At Syferfontein the proximity sensors were mounted on a mild steel bracket at the non-drive end of the motor between the motor and the brake as shown in Figure 2.5.

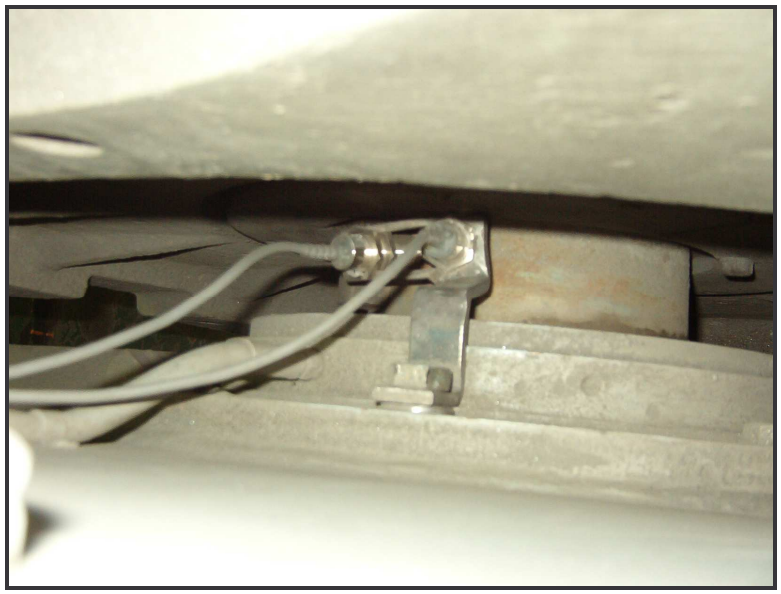

Figure 2.5: The situation of the two proximity sensors at the non-drive end of the motor.

The operating temperature of the proximity sensors is in the region of 50 °C since heat from the motor is conducted to the sensor. These operating conditions are acceptable as the proximity sensors are rated to working in an environment where temperature fluctuations of –25 to 70 °C occur.

2.1.2 The low pass filter

The purpose of the low pass filter is to avoid amplitude and frequency errors due to aliasing. Aliasing occurs when frequencies higher than half the sampling frequency are present in the analogue time history of the captured signal. Aliasing causes the signal to appear to be of a much lower frequency than it actually is. This will create false readings at lower frequencies in a FFT. This scenario must be avoided and thus the low pass filter is indispensable.

The low pass filter is only necessary for the vibration data relayed by the accelerometers since the data received from the proximity sensors has a very low frequency range and will not be analysed by a FFT. The low pass filter is positioned between the accelerometers and the A/D card as illustrated in Figure 2.6.

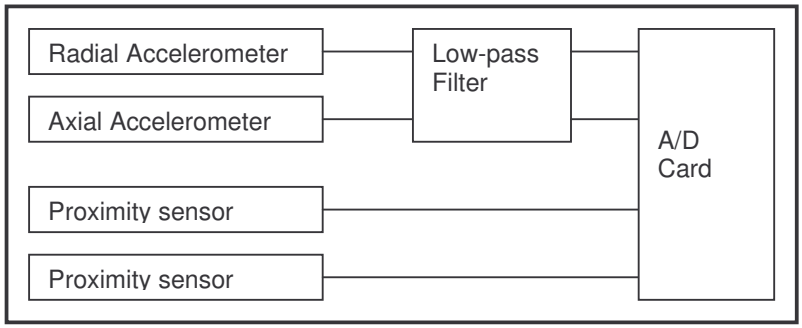

Figure 2.6: The position of the low pass filter in the hardware set-up.

The cut off frequency is determined by the frequency of interest and the number of higher harmonics of this frequency that are required. For the set-up at the Syferfontein colliery the GMF of the pinion is being investigated to detect fault conditions. The GMF is a function of rotation speed and number of teeth on the pinion as shown in equation 2.1.

$$Gearmesh = Speed \times Teeth \tag{2.1}$$

The speed of the pinion on the dragline will rarely exceed 20 Hz and it has 25 teeth. Thus the frequency of interest is 500 Hz. To include the first four harmonics the cut off frequency of the low pass filter was chosen at 2500 Hz.

Several filter types with different characteristics can be used. Two commonly used filter types are the Chebyshev and Butterworth filters. The Chebyshev filter has a steeper roll off at the cut off frequency than the Butterworth filter but does not have such a flat characteristic within the pass band, as does the Butterworth filter. The choice of the filter order is a trade off between pass band flatness and steeper roll off. With increasing order there appears an increasing disturbance in the flatness of the pass band along with a steeper roll off at the cut off frequency. The steeper roll off is laudable but comes at an increasing cost of pass band accuracy.

Another factor that plays a role in the choice of filters is phase distortion. All non-ideal filters introduce a time delay between the input and output terminals. This delay can be represented as a phase shift if a sine wave is passed through the filter. The phase shift typically alters with the input frequency; it would thus be desirable to have a linear phase response so that

all frequencies are similarly delayed. The Butterworth filter's phase response is more linear than that of the Chebyshev filter and is thus a better choice in this regard. To uphold the integrity of the data and avoid introducing any amplitude modulating effects, an 8th order Butterworth filter was chosen. Figure 2.7 shows the characteristics of the filter used, as designed with Microchip's FilterLab program, available at www.microchip.com.

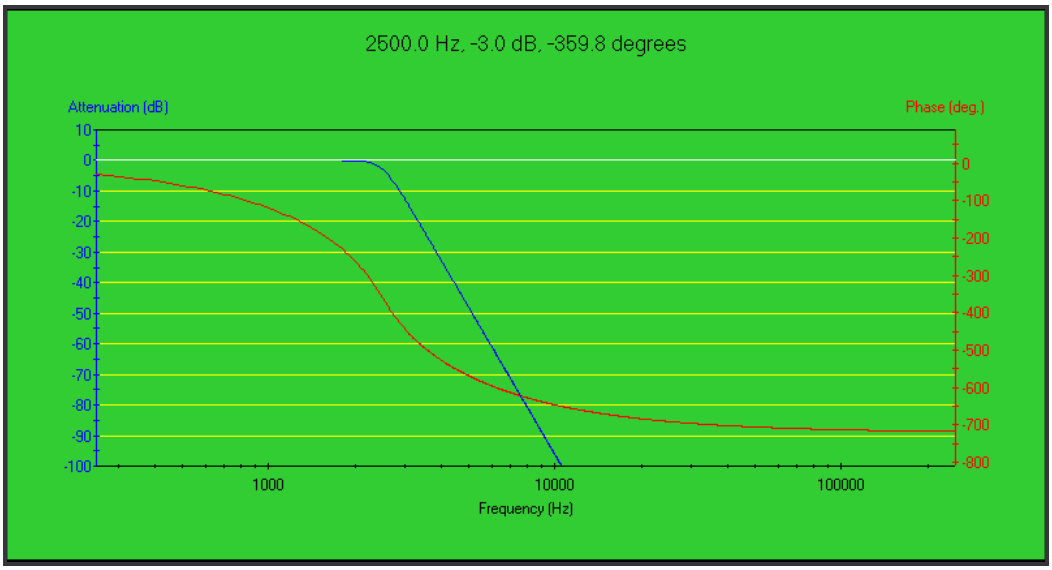

Figure 2.7: The characteristics of an 8th order Butterworth filter showing attenuation and phase response.

However, the effect of the phase distortion on the signal must still be quantified. The change in phase is normally represented through the group delay concept. Group delay is the derivative of the phase shift through the filter with respect to frequency. The normalised group delay response of various 8th order filters is indicated in Figure 2.8. It was retrieved from www.freqdev.com.

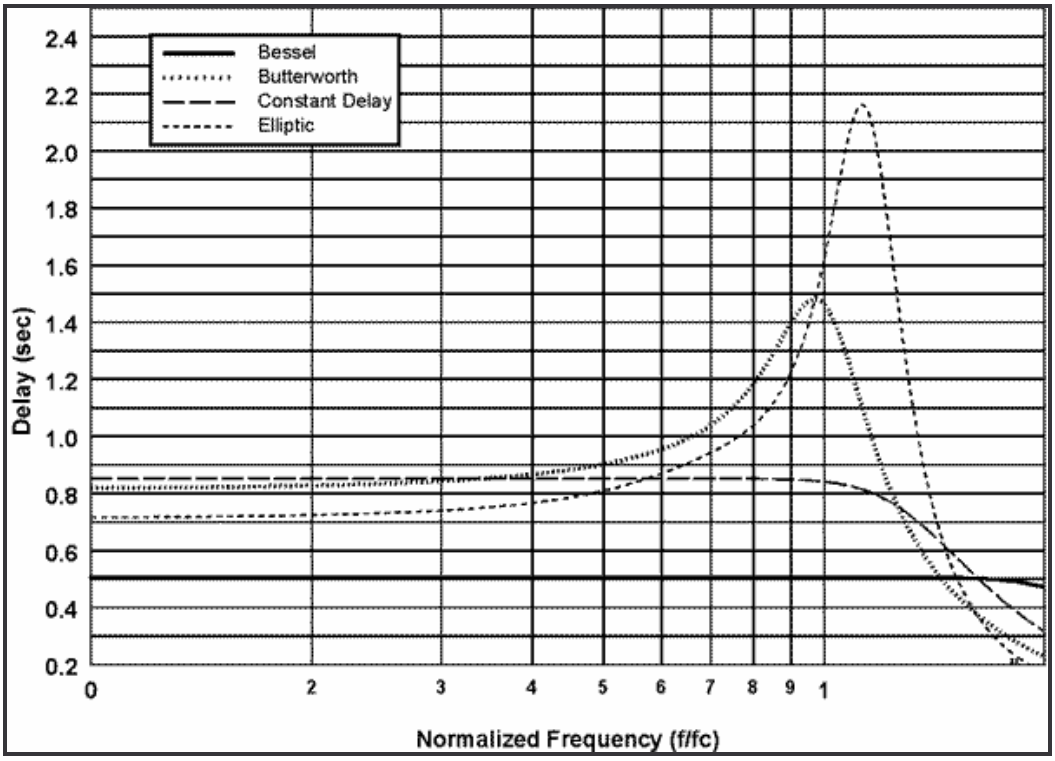

Figure 2.8: Group delay data of 8th order Bessel, Butterworth, Constant Delay and Eliptic filters.

The actual delay for a point on Figure 2.8 through the filter is the normalised group delay divided by the cut off frequency. The worst delay for an 8th order Butterworth filter typically occurs close to the cut off frequency and is approximately 1.5 seconds. The actual delay can thus be determined:

$$ActualDelay = \frac{1.5s}{2500Hz} = 0.0006s/Hz \qquad (2.2)$$

At top speed the pinion rotates at approximately 20 Hz. This represents a period of 0.05 seconds between speed pulses received from the proximity sensors. The delay due to phase distortion will thus have a negligible effect on the outcome of this dissertation. Furthermore the first 1000 Hz, 0-0.4 f/f_C on Figure 2.8, where the first two GMF will be found has a very similar delay, thus further limiting the effect of phase distortion in the context of this dissertation.

2.1.3 The analogue to digital (A/D) conversion card

The most common modern vibration analysis techniques rely heavily on digital data processing. Thus it is imperative that the analogue signal supplied by the

accelerometers and proximity sensors be converted to digital values. The accuracy of the conversion is dependent on the sampling rate and the A/D card's quantification of the amplitude.

The sampling frequency that the A/D card should comply with depends on the signal to be captured. Since the sampling frequency is more critical in the case of the accelerometer data than in the proximity sensor data, the vibration data will be the limiting factor. The low pass filter will cut off at 2500 Hz encompassing the first 4 harmonics of the gear mesh signal. Since filters are far from perfect it is recommended that the sampling frequency should be from 2.56 to 4 times higher than the –72 dB frequency point on the filter transfer function, which is 7050 Hz. Thus the sampling frequency should be at least 18 050 kHz, ensuring that the frequency analyses are not compromised. However if the waveform itself is of interest, so that time domain parameters can be accurately determined, it is recommended that the sampling frequency be much higher. Thus a sampling frequency of 50 kHz should suffice. The A/D card should therefore be able to control four inputs, of which two should be sampled at a rate of at least 50 kHz.

The quantification of the analogue amplitude depends on the resolution capability of the A/D card. For example if a 12 bit A/D card is set for an input range of –10 V to 10 V then the smallest increment quantifiable is 4.88 mV as calculated in equation 2.3.

$$\frac{10V-(-10V)}{2^{12}} = 4.88mV \qquad (2.3)$$

If the resolution of the A/D card is too low, the amplitude of the digital signal can be significantly distorted hampering fault detection. This is due to the fact that a range of fixed integer steps, the size of which is the smallest increment quantifiable, represents the analogue signal. The analogue amplitude could thus be distorted by as much as one quantifiable step. Thus the higher the resolution of the A/D card, the better the digital quantification of the signal.

The A/D card chosen was a National Instruments PCI 6023E card. This card has a resolution of 12 bits, is capable of controlling 16 analogue inputs and

has an aggregate sampling rate of 200 kHz. Thus if four input channels are required, two for the accelerometers and two for the proximity sensors, the sampling rate of each channel is 50 kHz. This is equal to the required sampling frequency needed to obtain quality vibration data.

However the Bayonet Neill Concelman (BNC) cables from the sensors cannot be directly linked to the A/D card. For this a BNC adapter is necessary. The BNC adapter also serves to simplify the connection between the sensors and the A/D card. The BNC-2110 was chosen to be the linking device between the sensors and the A/D card. This device provides BNC connectors for up to eight analogue input channels. The BNC-2110 is capable of operating over a temperature range from 0 to 70 °C and will thus have no problem in the warm environment aboard the dragline. The BNC adapter cannot handle an input voltage larger than 42 V. This will not occur since the largest output will be received from the proximity switches and will not exceed 12 V.

2.1.4 The computer

The computer has two basic functions to fulfil as part of the online monitoring station; it serves as a housing unit for the A/D card and as an interface between the A/D card and its controlling software. The main components of a computer comprise a case, the motherboard and central processing unit (CPU), random access memory (RAM) and a storage device. An uninterrupted power supply (UPS) and screen are also necessary.

To be able to provide sufficient protection to the internal components and to the A/D card, the computer case must be able to withstand shock loading, it should be well ventilated and allow as little as possible dust to enter and contaminate the internal components. It was decided that an industrial rack mounted case would be sufficient to the task. This case provides additional clamps to keep cards secure to the motherboard of the computer and thus provides shock resistance. The case also has an air filter mounted in front of the chassis fan to prevent dust build up within the computer. The fan also provides air circulation to cool down the internal components. The case has a rugged exterior, which serves as an adequate shield against impact. The

power and reset buttons as well as the CDROM drive are situated in a recess in the case that is covered by a lockable-hinged plate. This prevents the computer from being switched on or off by an accidental contact.

A 1.8 GHz CPU was selected to handle the functions needed to acquire and store data. An INTEL Celeron processor runs at a low temperature and was thus deemed the best CPU suited to the mining environment. A suitable motherboard with on-board graphics onto which the CPU and A/D card could be mounted was then chosen.

RAM acts as a buffer between the storage device and the CPU. Thus the operation time of any program running on the computer is affected by the amount of RAM that it has at its disposal. The number of RAM modules installable on the motherboard is limited and too much RAM is not cost effective. 256Mb of RAM were installed onto the motherboard for the data acquisition.

A storage device is necessary to store information required by the operating system and by all programs running within the operating system. It is also necessary to store the recently acquired data until such time as it can be written to compact disk for more permanent storage. It also serves well as a transportation device in the event that large and/or numerous files need to be transferred. No connection to a local area network or Internet was available. This is due to the dragline roaming around the mine during operation. Transferring the data by radio was also infeasible. From preliminary measurements it is known that a single 2-minute data sample will be 48 Mb large. A simple calculation can be made to determine the number of samples that can be stored.

$$\frac{80Gb \times 1024Mb/Gb}{48Mb} = 1706 \qquad (2.4)$$

From equation 2.4 an 80 Gb will last for 28 months if two samples per day are taken and stored. This is more than enough. Two 80 Gb hard drives were bought as well as two removable hard drive slots. Whilst one hard drive would be aboard the dragline storing, the other would be useful for data

manipulation. This also allows for short visits to the mine when all that is necessary is to switch the onboard hard drive with the spare hard drive when the latest data is required. This means that the data can be written to compact disks on regular occasions. A 20 Gb hard drive, to store the information required by the operating system and any installed programs, was bought.

The electricity supply aboard the dragline is not constant due to frequent power cuts when the umbilical cable supplying power to the dragline is severed during relocation. The large direct current (DC) motors aboard the dragline also cause power fluctuations. An uninterrupted power supply (UPS) is thus a prudent precaution. The 1 kW UPS acquired will supply power to the computer and the screen for at least 20 minutes. This would span the minor power interruptions and smooth out any spikes and troughs in the supplied power. The UPS will however not supply sufficient power for lengthy interruptions.

Due to the environment a new screen was not utilised aboard the dragline. The DC motors aboard the dragline emit large amounts of electromagnetic interference, large enough to distort the image seen on the screen by deflecting the electrons within the tube of the screen. The screen was thus placed within a metal cupboard that serves as a faraday cage. An additional screen was also kept at the mine in the event that the one aboard the dragline failed. Simple 14” video graphic array (VGA) monitors were used.

2.1.5 Hardware housing

Almost all the hardware, excluding the sensors, was housed in the control room aboard the dragline. Figure 2.9 depicts the screen, the rack mountable computer case and the UPS.

Figure 2.9: The computer as situated in the control room aboard the Marion 1.

In the compartment just left of the one housing the computer, the signal conditioners for the accelerometers, the low pass filter and the power supply for the proximity sensors and the signal conditioners were housed. As shown in Figure 2.10, the two boxes taped together with red duct tape are the signal conditioners, and the black box to the rear houses the low pass filter.

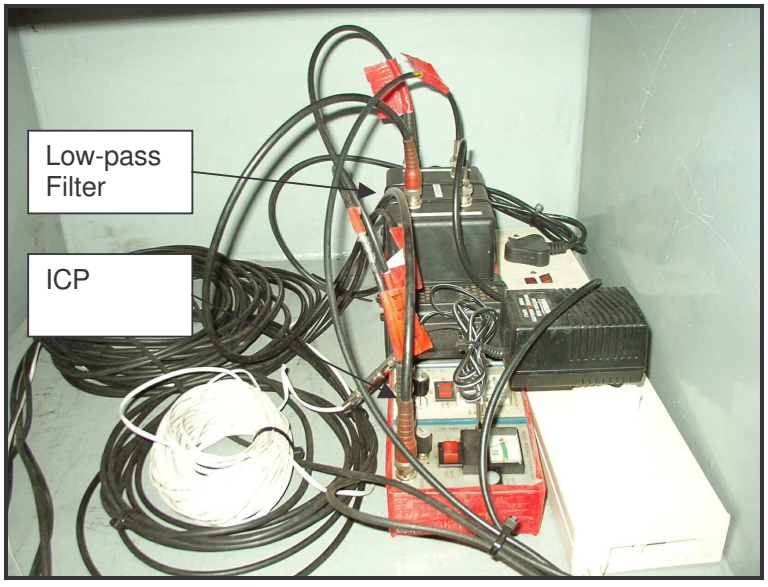

Figure 2.10: The compartment housing the signal conditioners, the low pass filter and the power supplies.

2.2 Software development

Having attained all the hardware requirements for the dragline online monitoring station, the next step is to select and develop suitable software to complement the hardware. Firstly the programming language must be chosen with which the capturing programmes will be written. Secondly the operating system of the computer must be selected and lastly the capturing programmes must be written.

2.2.1 The programming language

This research project was conducted within the DSG (Dynamic Systems Group) at the University of Pretoria, where there is a wealth of Matlab knowledge available, allowing research to proceed efficiently. Matlab has proven to be an effective platform to develop mechanical signal processing methodologies. Signal capturing and processing algorithms can thus be implemented with ease.

Matlab's data acquisition toolbox is also compatible with the National Instruments A/D card that is utilised for this research project, thus no compatibility problems will arise.

2.2.2 The operating system

Windows 2000 was chosen as the operating system to be installed on the computer aboard the dragline, as it does not have memory leakage. Memory leakage is the term used to describe the lack of available RAM space when the operating system does not delete unused data stored in the RAM, causing lethargic system operation. Windows 2000 was also deemed the most stable platform available at the time and has the added advantage that a critical error does not result in system wide inoperativeness.

2.2.3 The capturing program

The capturing program to be installed and used must meet certain requirements. It must be capable of sustained data capturing over an indefinite period of time. It must be capable of capturing a fixed amount of

data at specific times, and it should be able to store the data with informative file names.

To be able to capture data over an indefinite period of time it is necessary to make use of an 'if' loop. Increasing or decreasing the time span used to capture data controls the amount of data to be captured. To capture at specific times, the program makes use of the system clock. The timing is simplified by keeping the time period between captures constant, i.e. if capturing occurs at 6 am then a second capture should occur at 6 pm. The logic behind the capturing program aboard the dragline is illustrated in Figure 2.11.

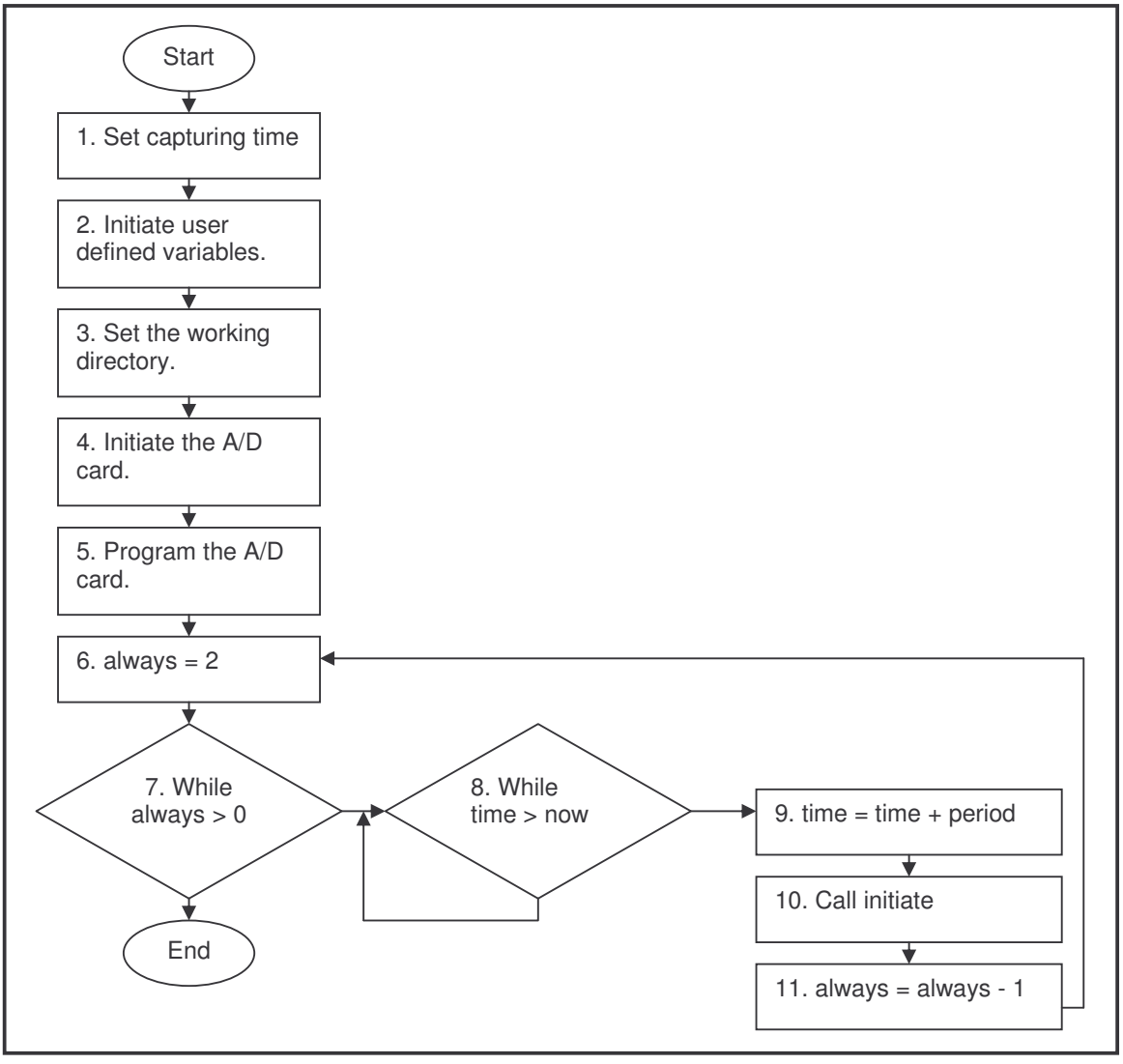

Figure 2.11: The flowchart of the capturing program aboard the dragline.

At the start of the program the initial time of capturing and the period between captures is set. Other user-defined variables such as the time span are also defined. The working directory is then set, ensuring that the captured data is stored in an assigned location on the hard drive. The NI 6023E A/D card is then activated and the range of channel inputs is programmed. To ensure an infinite loop a variable 'always' is assigned the value 2. A 'while' loop is then engaged which can only be broken by user intervention. This is due to the fact that the variable 'always' will continue to be larger than zero, keeping the while loop in tact. A second 'while' loop, that will loop continuously until the time for capture is reached, is then engaged. When the time of capture is reached, the next time of capture is defined by adding the user-defined period to the time of capture. A subprogram named 'initiate' is then called, which captures data of the four channels for the assigned time span. To satisfy Matlab's requirement that the 'while' loop should be breakable, the variable 'always' is reduced by 1. This completes the indefinite capturing loop.

2.3 Pre-operative testing

Before taking the hardware to the Syferfontein colliery it was necessary to run several tests to highlight any possible problems that could compromise reliable operation of the system aboard the dragline. The length of data to be taken had to be chosen based upon tests and dragline observation. This is necessary to determine the largest possible sample length that can be captured, whilst retaining the ability to effectively manipulate the captured data. The low-pass filter needed testing to ensure that the correct cut off frequency was present and then the system needed to be tested as a whole.

2.3.1 The sample length

The length of the sample is measured in seconds. The longer the sample the larger the space it requires for storage and the more RAM is required to load and manipulate the sample. Loading is the process whereby the data acquisition format is rewritten so that Matlab can identify the variables contained within the data. Thus the longer the data sample the longer the period required to manipulate the data. If the captured data sample is too

large then the computer becomes unresponsive and the data cannot be analysed.

Two computers were available for this research, the office computer and the data acquisition computer. The office data processing computer had a 550 MHz CPU with 128 Mb of RAM. The data acquisition computer had a 1.8 GHz CPU with 256 Mb of RAM. The ability of both machines was tested using various sample lengths.

A random signal generator fed two channels of the A/D card, simulating the accelerometer data. Another signal generator fed another two channels of the A/D card with a square wave. The sampling frequency of the A/D card was set at 50 kHz, precisely as it would be set when aboard the dragline at Syferfontein. This was done to simulate the data that would be received from the dragline. Starting with an initial sample length of 5 seconds, 32 data sets were captured each lasting 5 seconds longer than the previous one. This gave a time range from 5 to 175 seconds and a data size ranging from 7830 kB to 64554 kB.

Both machines were set to load and plot the data in its entirety whilst the time taken to do so was noted. Plotting all the data points at once is a sufficiently intensive task that would simulate the data manipulation to take place once the data capturing at Syferfontein was completed.

The ability of the available computers to load and manipulate the captured data is critical in attaining the ability to detect gear fault, thus a system crash due to data loading must be avoided. Figure 2.12 shows the time taken for each computer to load varying periods of data successfully.

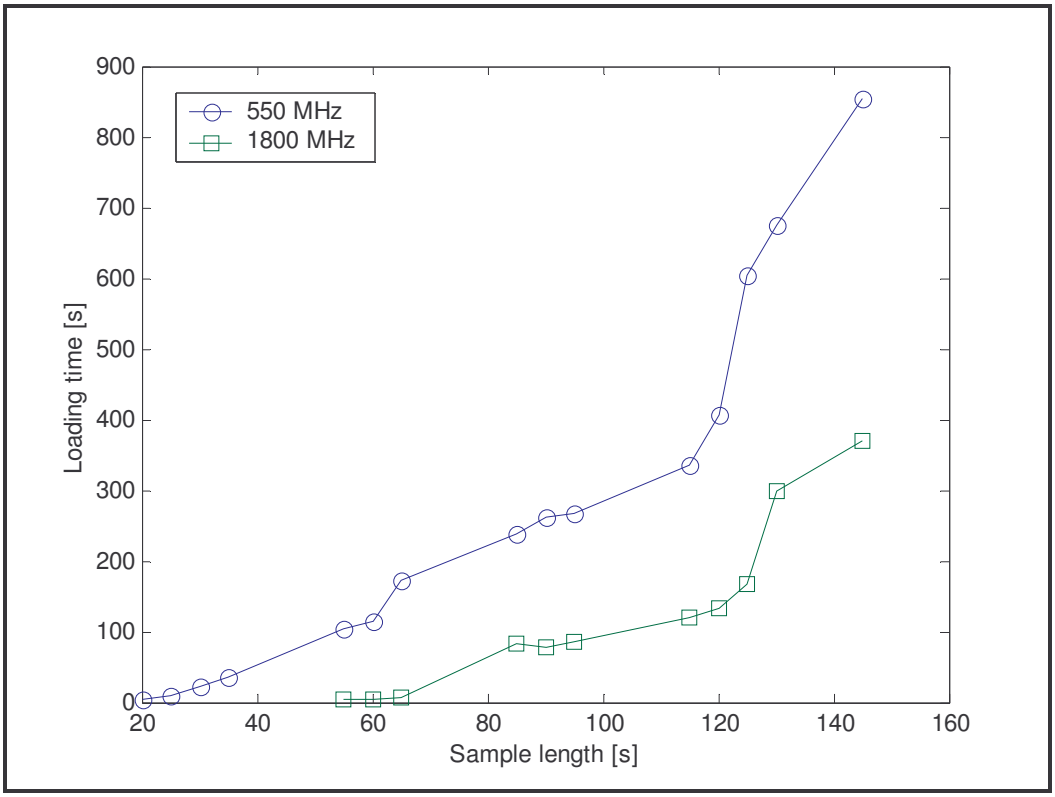

Figure 2.12: Comparing the loading performance of a 550 MHz and 1.8 GHz computer.

For both machines a dramatic increase in the computation time occurs for samples longer than 120 seconds, thus 120-second samples are a good trade off point between sample length and loading time.

A complete cycle of the dragline was observed to be typically 69 seconds. This was taken when the angle between the pick up point and the drop off point was 148°. In other words the boom of the dragline moved through 148° when viewed from above during one cycle. The vibration technicians at the colliery were confident that 120 seconds would be more than sufficient to capture at least one cycle of the dragline, i.e. pick up, drop and pick up again.

It was thus decided to take 120-second data samples. This period of data would encompass a complete cycle of the dragline, ensuring that no dynamics might be missed, and is optimal when considering loading times.

2.3.2 The low-pass filter test

Having constructed the low-pass filter to cut off at 2 500 Hz it was also necessary to test whether the filter does indeed cut off at this frequency. Incorrect assembly of the components making up the filter and flawed or damaged components could cause discrepancies affecting the cut off frequency.

A signal generator was used to generate a chirp signal ranging up to 20 kHz. This signal was then split and put through both channels of the filter. The outputs were inputted into an FFT analyser. From the captured transfer function it was clear that both filter channels were functioning as designed.

2.3.3 The system test

The final test to be performed before implementing the online monitoring station on the dragline was a system wide test. This encompassed the observation of the entire system, as it would be working on the dragline, and the fixing of any unforeseen errors.

A large motorised metal wheel with a diameter of approximately 2m, which was available in the lab, was used to test the entire system. A piece of metal was bonded to the shaft of the wheel to simulate a key. The two proximity sensors where then held in position to detect the key by a simple metal harness. The proximity cables where attached to the BNC-2110, which relayed the signal to the A/D card. The accelerometers were attached to the bearing housing of the shaft in the axial and radial directions. The accelerometer cables where attached to the input of the low-pass filter, which was in turn also attached to the BNC-2110 relaying the signal to the A/D card. All power supplies where activated and the data acquisition program was initialised.

The system was kept running for approximately 18 hours taking 120-second data samples every five minutes. This intensive use of the system did not highlight any large technical difficulties or malfunctions and apart from fine-tuning the capturing program, nothing was changed to the set-up. The data

samples that were captured where plotted and found to be coherent. The system was thus ready to be implemented aboard the Marion 1 dragline at the Syferfontein colliery.

2.4 Summary

The establishment of a monitoring station aboard a dragline is critical to the completion of this research. The individual hardware and software components that make up the monitoring station such as the computer, the sensors, the analogue filter, the data acquisition hardware, the operating system and the capturing program were selected and/or developed.

The system was then tested and a suitable sample size of 120 seconds was chosen based on these tests.

CHAPTER 3 ORDER TRACKING METHODS

3.1 Relating the dragline activity to sensor data

To successfully develop methods for a specific environment it is beneficial to fully understand the environment. It is important to be able to derive the dragline activity from the captured sample, as it will enable quicker error detection in the process of developing a new method. Fluent interpretation of the data will also aid in detecting a monitoring station system error aboard the dragline. This detection capability is critical in assuring captured data quality. To better understand the data received from the dragline, the 120-second sample block was captured and related to the mining activity of the dragline.

Figure 3.1: Layout of a dragline.

As seen in Figure 3.1, the dragline has two pairs of cables. Each pair is connected to one of two drums aboard the dragline. Each pair of cables from the two drums is also attached to the dragline bucket. One pair of cables is attached to the top of the bucket and controls the vertical motion of the bucket. This drum and the gearbox controlling it are given the prefix: hoist. The other pair of cables is attached to the front of the bucket and controls the

buckets horizontal traversing. This drum and gearbox is given the prefix: drag. The accelerometers were capturing data from one of the six motors driving the drag-gearbox. Thus the information captured is related to the horizontal traverse of the bucket.

Video footage was taken and compared to the captured signals to be able to determine what the dragline is doing during the daily capture times.

3.1.1 Relating captured data with video footage

A Hi-8 digital video camera was used to take video footage of the Dragline during operation at the Syferfontein Colliery. A wristwatch was synchronised with the timer aboard the monitoring station and the data acquisition software written in Matlab was set to take data once off at a specified time. Then video footage was taken of the bucket for the two-minute duration of the sample. Four such data sets were taken.

Using a video capturing and editing program the video footage was captured and converted into .mpeg format. This allows the video to be played by any computer that has access to the correct compression-decompression algorithms. Playing the video on a computer allows faster jumps to specific intervals allowing easier comparison between the video footage and the measured vibration data.

To aid in comparison it is necessary to present the vibration signal in a short-time RMS (root mean square) representation. The 120-second vibration signal is broken up into 556 smaller pieces and the RMS is calculated for each segment. Then these 556 RMS points are plotted yielding an uncluttered view of the vibration intensity.

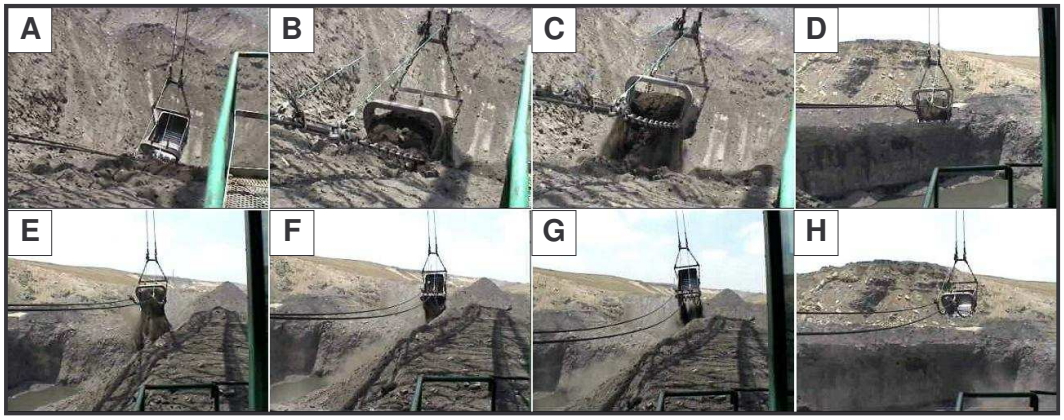

Figure 3.2: A series of stills taken from the dragline operation video.

Figure 3.2 illustrates a common cycle of the dragline consisting of dropping the bucket and dragging it through the ground to shovel dirt into the bucket (A-C in Figures 3.2 and 3.3). Then the bucket is hoisted and the dragline swings to the dumping position where the drag-cables are paid out to dump the dirt (D-G in Figures 3.2 and 3.3). The dragline then returns to the pick up point to restart the cycle (H in Figures 3.2 and 3.3). On occasions the dragline does deviate from this basic cycle.

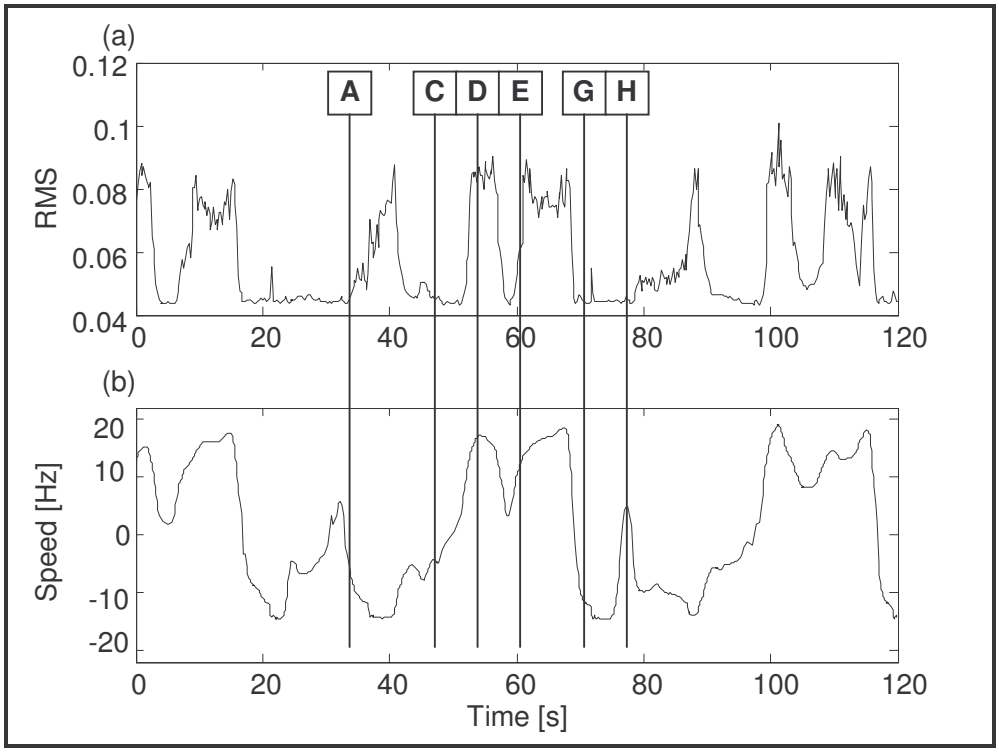

Figure 3.3: (a)The RMS fluctuation of a vibration sample. (b)The speed fluctuation of one sample.

The RMS fluctuation plot, shown in Figure 3.3(a), illustrates the vibration intensity levels. The vibration intensity levels of both vibration channels are so

similar that differentiating between them does not contribute to this evaluation. Specific dragline actions are identifiable by the different peaks. The peak occurring between point A and C and the peak occurring immediately after point H in Figure 3.3(a) are diagnostic of the pick up process since a gradual increase of the vibration intensity levels occurs and the negative speed in Figure 3.3(b) indicates that the bucket is being pulled towards the dragline.

The peak occurring at point D and again at 100-103s in Figure 3.3(a) is diagnostic of dirt transport between the pick up and drop off areas. This is due to the fact that it occurs after the peak identified as the pick up point and that the positive speed in Figure 3.3(b) indicates that the bucket is moving away from the dragline. The intensity level of the vibration during this phase indicates that the bucket is loaded with dirt.

The peaks occurring at 4-18s, and again between points E and G and at 108-117s in Figure 3.3(a) are diagnostic of dropping dirt. This can be seen due to the 'bull horns' on these peaks caused by increased vibration intensity at the start and end of each peak. The first 'horn' occurs when the drag cable is panned out, thus dropping the dirt. The second 'horn' occurs when the drag cable is again retracted to level the bucket after the dirt has been dropped. The dip in between the two 'horns' is due to the relatively inactive state of the drag cable whilst the operator is waiting for the dirt to completely evacuate the bucket. This phase is also identified due to the positive speed peak, as seen at 18s, 68s and 117s in Figure 3.3(b), shortly before dropping to a negative speed peak. This change from positive to negative speed is always associated with the second 'horn' on the RMS peak representing the dropping of dirt.

The lack of vibration intensity between point G and H and after every dropping peak in Figure 3.3(a) is associated with moving the empty bucket from the dropping point to the pick up point. The vibration levels are low due to the fact that the bucket is empty.

Understanding the dragline cycle and its constituents significantly aids in the development of an online monitoring technique and also enhances the ability to detect flaws and inconsistencies within the captured data sets.

3.2 Reviewing existing and developing new processing programs

Having developed an understanding of the dragline, its functions and environment, the next step involves developing programming that aids in the assessment of gear damage aboard the dragline. The Dynamic Systems Group (DSG) at the University of Pretoria has done work in the field of order tracking and existing programs are available for review and editing to suit the requirements of this research. The reviewing and subsequent editing is described in this section.

3.2.1 The speed estimation program

Stander wrote the existing program used to convert pulse to speed data in the Matlab environment called Puls2SpeedDragline.m. The program was used in the investigation that led to the article published by Stander et al. (2002). The program required the sampling frequency and the number of pulses per revolution along with the pulse signal as input. It cycles through the pulse vector and detects amplitude changes denoting a pulse. The time taken from one pulse to the next is then used to calculate the average speed between the pulses. The disadvantage is that this program has long processing times.

A new program called sigspd.m was developed to improve on Puls2SpeedDragline.m. As with Puls2SpeedDragline.m it starts off with the pulse vector shown in Figure 3.4(a). Sigspd.m then differentiates the pulse data giving a signal with clear spikes to indicate the start and end of a pulse as illustrated in Figure 3.4(b). The beginning of each pulse is thus transformed into a positive spike, and the end of each pulse into a negative spike. The time taken between two positive spikes is then divided into the traversed rotational angle between the spikes yielding the constant speed between the start of one pulse and the start of the next pulse. The same process is

repeated with the spikes in the negative direction in Figure 3.4(b) yielding a second set of speed data. The two sets are then combined as shown in Figure 3.4(c). As there is little difference between the two speed sets, only one was used in the pre-COT procedure. This further reduces the processing time and the reduced program complexity enables quicker faultfinding.

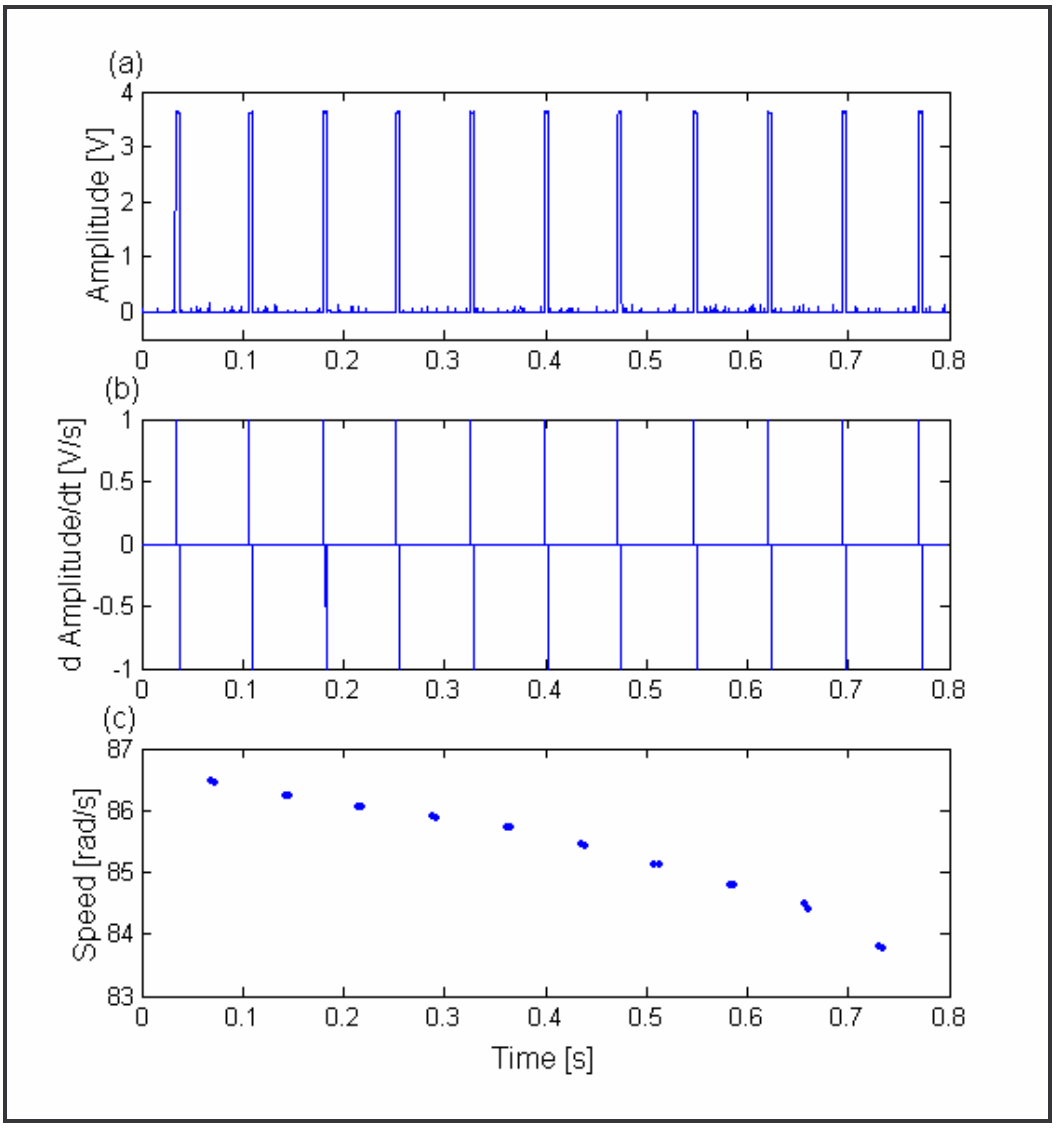

Figure 3.4: The processing progression. (a) Pulse signal, (b) Differentiated pulse signal and (c) Speed signal.

The processing time required by sigspd.m to obtain a speed signal from a pulse on an Athlon XP 2.6+ CPU computer is 5 seconds for a pulse vector with 6 million data points. The traversed angle between consecutive pulses is

easily modified thus giving sigspd.m the flexibility to process pulse data originating from multiple, equally spaced, proximity sensors.

3.2.2 The order tracking program

Several interlinking programs were also written by Stander to complete the Stander et al. (2002) article. These programs did COT by assuming that the speed variation between pulses remains constant. This assumption was acceptable due to the fact that 1024 pulses per revolution were utilised. However the monitoring station aboard the dragline only receives one point per revolution, thus interpolation techniques become critical. This program was rewritten to be able to do COT using linear, cubic and moving window order tracking (MWOT) interpolations. Displacement driven velocity interpolation (DDVI), a speed correction subroutine was also added.

3.3 Introducing existing interpolation techniques

COT is a method whereby the speed signal is used to re-sample the vibration data acquired from the rotating machine. The accuracy of the speed is thus of paramount importance. However since there are always a fixed number of pulses per revolution when using digital encoders for angular measurement, interpolation techniques have been implemented.

In the case of this study only a single pulse per revolution is available. This suggests the use of interpolation techniques to ensure accurate speed estimation. Constant, linear and cubic interpolation methods have been used in the past and will be presented and discussed in this section.

3.3.1 Constant interpolation

This is the simplest form of interpolation; it assumes that the shaft speed remains constant over each revolution. The time taken to complete one shaft revolution is converted to the average speed. This average shaft speed is then assumed to hold true for the entire revolution. Figure 3.5 illustrates the constant speed interpolation technique as used in this dissertation, where it is

used to interpolate one of the sample sets received from a single proximity sensor.

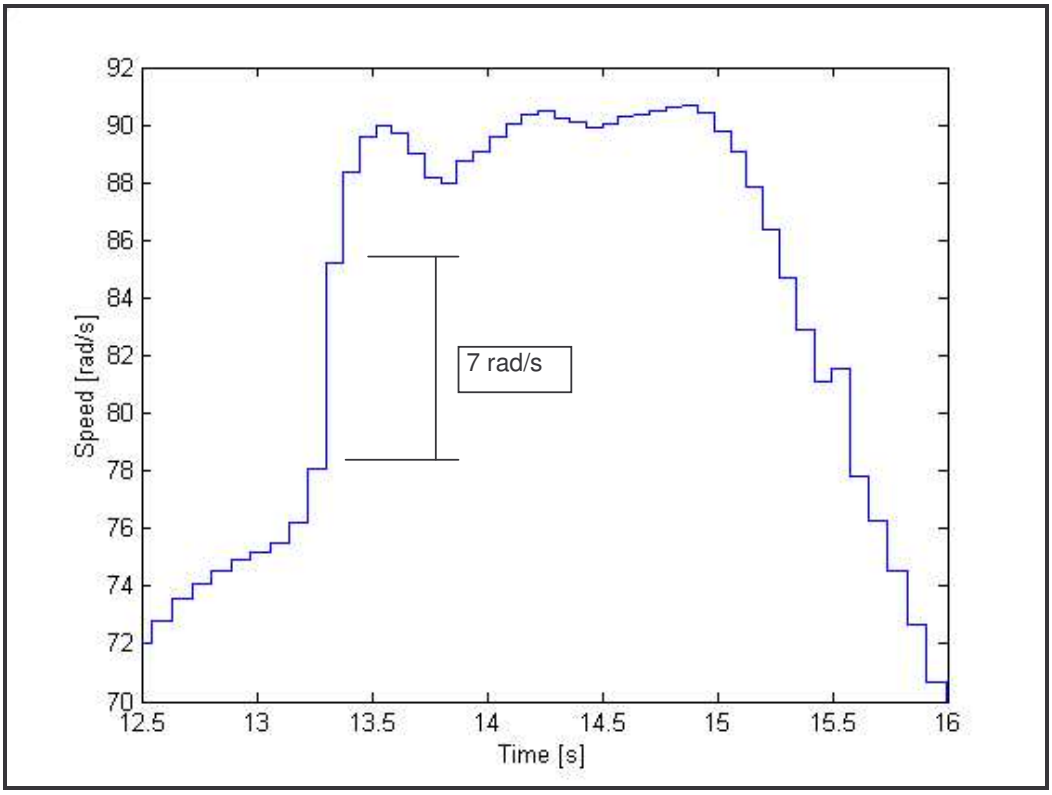

Figure 3.5: The constant speed interpolation technique.

The biggest shortcoming of this method however is that it disregards any intra-revolutionary speed fluctuation. In the case of the dragline this is unacceptable since, as indicated in Figure 3.5, the speed change from one revolution to the next can be as large as 7 rad/s. This represents a change in speed of 9%. The information contained within one revolution could be vital to the implementation of COT to the dragline. This prompts the use of more sophisticated interpolation techniques

3.3.2 Linear interpolation

This interpolation method assumes that shaft acceleration is constant. Given constant acceleration, speed can only vary linearly. Bossley et al. (1999) state that linear interpolation is the simplest, cheapest and one of the most popular signal interpolation methods.

To implement linear interpolation a series of discrete points describing the pinion shaft motion must be attained. In the case of this research two proximity sensors, which are triggered by a key, captured the discrete points. A linear connecting line is now inserted between two adjacent points to form a continuous estimation of the shaft speed. Figure 3.6 is constructed using the same data used to construct Figure 3.5. It exhibits the effect of the linear interpolation method in that the graph is much smoother. However the discontinuity at 15.5 seconds and 81 rad/s hints that a higher order interpolation would better suit the data.

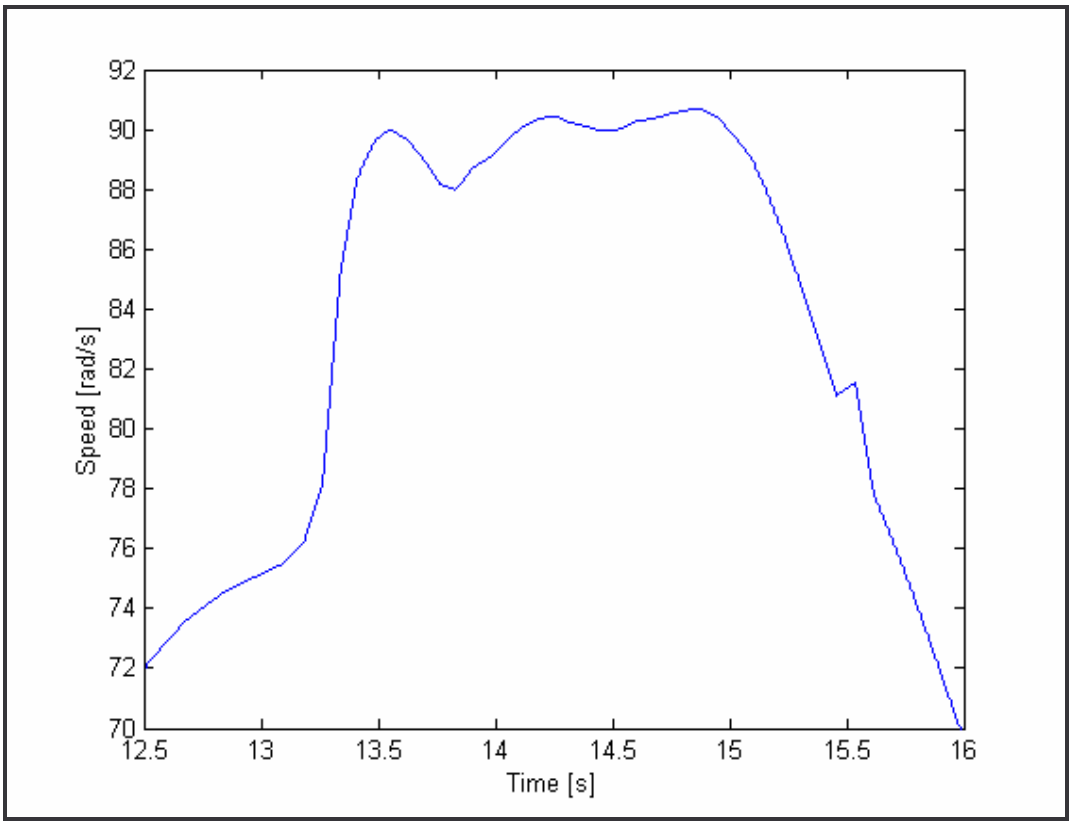

Figure 3.6: The linear speed interpolation technique.

3.3.3 Cubic interpolation

There are two approaches to cubic interpolation. Piecewise cubic interpolation considers a local and block-wise cubic spline interpolation a holistic approach.

Piecewise cubic interpolation makes use of two points on either side of the interpolation point and fit a curve. This is done for successive interpolation points. This technique is significantly more accurate than linear interpolation.

Block-wise cubic spline interpolation mentioned by Fyfe and Munck (1997) considers a large block of data and fits a series of cubic splines to it. This ensures that the first and second derivatives of the interpolated curve are continuous. Within this research the piecewise cubic interpolation was used.

3.4 Development of a new speed interpolation technique

The task of developing a speed interpolation technique that would allow sufficient accuracy for the successful application of order tracking was approached from three viewpoints, numerical integration optimisation, filter optimisation and moving window speed determination.

3.4.1 Numerical integration optimisation

Assuming that the dragline and all its components, that affect the inertia of the system, can be represented as a simple single degree of freedom model, such a model might then be refined and used to predict the speed fluctuation of the system accurately enough that computed order tracking (COT) can be successfully implemented.

The procedure to implement the numerical integration optimisation method starts at the same point as the interpolation methods described in section 3.3 namely with the captured pulse signal. As with the interpolation methods the pulse signal is converted to a velocity signal using sigspd.m, the Matlab program specifically developed for this purpose. However the numerical integration optimisation procedure differs in that the velocity signal is differentiated to obtain an acceleration signal. This acceleration signal is then inputted into the proposed single degree of freedom system. After having optimised the other unknown components in the system such as mass, damping constant and spring constant, the system outputs an interpolated velocity signal. A flowchart of this procedure is presented in Figure 3.7.

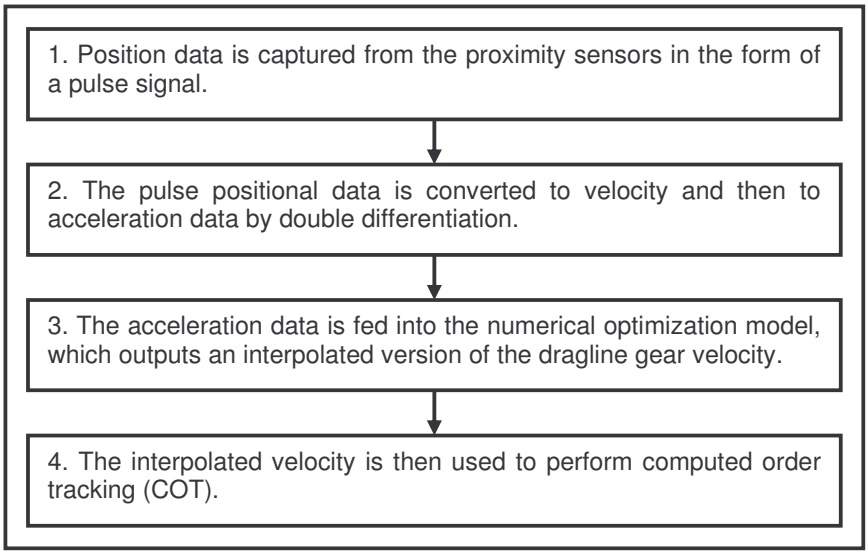

Figure 3.7: A flowchart to demonstrate the numerical integration optimisation method.

This was the first attempted approach to an interpolation method.

3.4.1.1 Model construction

The equation of motion of this single degree of freedom model can be expressed as:

$$I\ddot{\theta}(t) + C_T\dot{\theta}(t) + K_T\theta(t) = f(t) \tag{3.1}$$

To facilitate numerical integration equation 3.1 must be rewritten in first order form. By defining the velocity and displacement as part of a single unknown quantity, this is achievable.

$$\Theta = \begin{Bmatrix} \theta(t) \\ \dot{\theta}(t) \end{Bmatrix} \tag{3.2}$$

Rewriting equation 3.1 as:

$$\ddot{\theta}(t) = -\frac{K_T}{I}\theta(t) - \frac{C_T}{I}\dot{\theta}(t) + \frac{f(t)}{I} \tag{3.3}$$

and using the identity:

$$\dot{\theta} = \dot{\theta} \tag{3.4}$$

equation 3.1 can then be written in a first order, state space form:

$$\dot{\Theta} = \begin{Bmatrix} \dot{\theta}(t) \\ \ddot{\theta}(t) \end{Bmatrix} = \begin{bmatrix} 0 & 1 \\ -\frac{K_T}{I} & -\frac{C_T}{I} \end{bmatrix} \begin{Bmatrix} \theta(t) \\ \dot{\theta}(t) \end{Bmatrix} + \begin{Bmatrix} 0 \\ \frac{f(t)}{I} \end{Bmatrix} \tag{3.5}$$

The angular speed output of the model is the angular velocity vector that forms part of $\dot{\Theta}$ in equation 3.5.

The unknown system characteristics K_T, I and C_T must however first be determined before numerical integration, to find the interpolated angular speed, can commence. This is achieved by mimicking the data gathering process in use on the dragline, which allows the estimation of the system characteristics. An arbitrary angular speed vector representing the speed of a simple flywheel under varying torque is created. This represents the actual speed of the gear system on the dragline. This speed is then sampled at a lower frequency than the frequency used to create the 'actual' speed vector. The sampled speed is then linearly interpolated and fed to the model as input. The sampled speed is interpolated to provide the same number of points as the 'actual' speed. The unknown system characteristics are then adjusted using an optimisation technique until the output of the model closely resembles the 'actual' speed created.

When the unknown system characteristics have been found they would be inserted into equation 3.5, which would subsequently be numerically integrated so that the interpolated angular speed is outputted. Paragraphs 3.4.1.2 and 3.4.1.3 describe the attempts to find the system characteristics using different optimisation approaches.

3.4.1.2 R-squared optimisation

In this attempt the generated 'actual' speed and the speed outputted by the model are compared, to gauge the accuracy of the characteristic estimation process, by making use of optimisation. The function value, which is to be minimized by optimisation, is defined using the R-squared value.

The R-squared value is a measure of the relative predictive capability of a model and is expressed as a fraction between 0 and 1. The closer the R-squared value is to 1, the better the model fits the data. The R-squared value is determined by calculating two variables, the sum of squares due to error (S) and the sum of squares about the mean (T). S is the variability of the data set with respect to the predicted model and T is the variability of the data set with respect to its own mean. Microsoft® Excel 2000 utilises R-squared value to

determine the goodness of some trend line fits. Microsoft® Excel Help indicates that given a data set Y_j and its fit $\hat{Y}_j$ with n elements, the R-squared value is defined as:

$$R^2 = 1 - \frac{S}{T} \tag{3.6}$$

where,

$$S = \sum \left(Y_j - \hat{Y}_j \right)^2 \text{ and } T = \left(\sum Y_j^2 \right) - \frac{\left(\sum Y_j \right)^2}{n} \tag{3.7}$$

The function value described in equation 3.6 was minimised using Matlab's unbounded optimisation function fminsearch.m. This program requires initial characteristic values and another sub-program that runs in parallel with it and supplies the function value for a given set of characteristic values. The function value is the R-squared value and compares the current model output to the known 'actual' value.

The initial characteristic values and system state values were required. The data that will be captured from the operating dragline goes through a pre-processing period where it is separated into unidirectional segments so that each segment starts at an initial velocity of zero. The starting position for each segment is also selected to be zero. This is an arbitrary choice since the gear fault detection method proposed in this document relies on change in speed and is thus independent of the number of shaft revolution. The system state values, position and speed, were thus always set to zero.

The 'actual' speed, from which a sampled set will be used as input to the model, was generated using the torque variation over 200 seconds as presented in Figure 3.8. This torque variation was also applied to the system, which was created using characteristics calculated by the optimisation program, to determine speed which would then be compared to the 'actual' speed using the R-squared function value. This process would then be repeated until an optimised value for the function value is achieved.

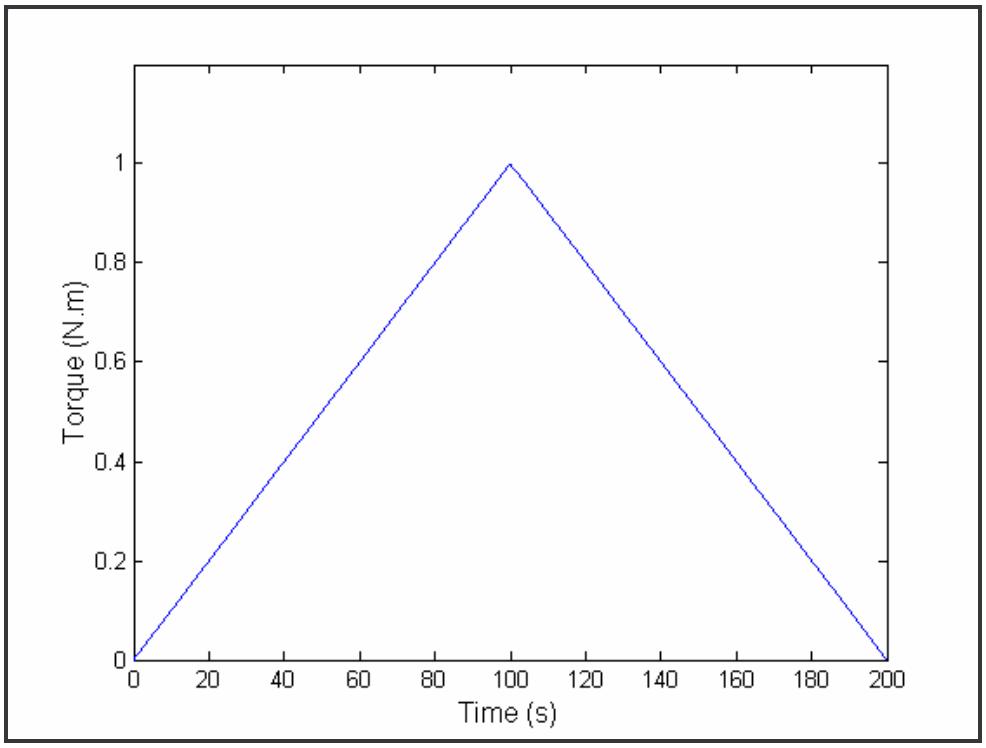

Figure 3.8: The torque variation used as input into the optimisation model.

Having defined the function value and the initial characteristics of the model optimisation can commence. The optimisation was started using three initial characteristic values. The choice of these values does have an effect on the ability of the optimisation program to find a global minimum for the function value. Three of the initial characteristic value sets with the corresponding optimised characteristic values and function value are shown in Table 3.1.

Table 3.1: R-squared optimisation result.

Initial Characteristic Value			**Optimised Characteristic Value**			**Function Value**
m	**c**	**k**	**m**	**c**	**k**	
0	0	0	0.171	0.053	0.157	0.999
1	1	1	0.999	1.031	1.001	0.999
1	1	100	1.049	1.000	100.307	0.999

Immediately apparent is the fact that the optimised function value did not vary with varying initial characteristic values. This could be due to poor initial characteristic value choice, but this suggestion is disputed by the large

variation in k, shown in Table 3.1, as well as similar function values achieved when large changes are made to m, c and k.

It is possible that the insensitivity of the function value to the initial characteristic values is due to too many constraints, which restrict the optimising algorithm to a domain in which no minimum is present. Filter optimisation is possibly a method that would allow a sufficiently large search domain to find a minimum.

3.4.2 Filter optimisation

Due to the lack of success described in the previous section, the state space model approach was abandoned. Instead a straightforward filter was used.

As depicted in Figure 3.9 below, the initial procedures remain the same as those used for the state space optimisation method. The generated 'actual' data is again sampled at a lower frequency and linearly interpolated before the filter is applied to it. The filter output is then compared to the 'actual' data.

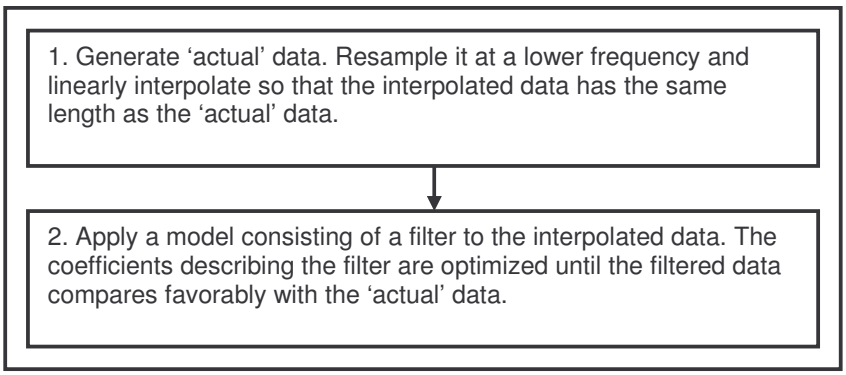

Figure 3.9: The filter optimisation flowchart.

Using Matlab's filter.m for the filter which is described by the following equation:

$$a(1)\times y(n) = b(1)\times x(n) + b(2)\times x(n-1) + b(3)\times x(n-2) + \ldots \qquad (3.8)$$

Once again Matlab's fminsearch.m was used. The initial values where the filter's coefficients, a and b. The modified R-squared value was again used to compare the output to the 'actual' value.

Having run the filter optimisation method it became evident that the function value diverged repeatedly. Thus after the optimisation was completed, no perceptible change had occurred when comparing the input to the output.

This method likely fails due to the fact that the filter input is so close to the desired output, that the optimisation does not find any characteristic values that are essentially sensitive to sampling rate. Any method utilising optimisation in this manner is thus unlikely to succeed. A totally different approach is required.

3.4.3 Moving window speed determination

All methods employed so far in this section, used only the proximity sensors' data converted to continuous real speed values as primary input. However a part of the vibration data can also be a valuable source of rotational speed information.

When a gear runs on a shaft at a constant speed, noticeable energy levels will be seen in the frequency domain at the shaft speed, even more so at the GMF. The GMF is found by multiplying the shaft running speed with the number of teeth on the gear of interest as shown in equation 3.9.

$$GMF = Speed \times Teeth \tag{3.9}$$

Thus if the shaft rotates at 15 Hz and the gear of interest has 25 teeth, then there will be significant energy seen in the frequency domain at 375 Hz. This occurrence will be tested to see if it can be of use in determining sufficiently accurate speed so that computed order tracking can be successfully implemented.

Bonnardot et al. (2004) report attempting to use purely the acceleration signal in performing COT, they process the contact shocks that gears make whilst rotating, in order to locate the position of the gear with respect to time. Interpolation is then used to estimate the angular acceleration required to perform COT. However they mention that although this approach is cheap, lacking the hardware required by traditional order tracking methods, it is vulnerable to high fluctuations in angular speed. The shaft of interest on the

dragline at the Syferfontein colliery however has large speed fluctuations ranging from about 0 to 20 Hz. This exceeds the capability of the method proposed by Bonnardot et al. (2004).

A major obstacle to overcome is the speed fluctuation. The location of the GMF within the frequency domain, given a fixed shaft speed, remains constant. However with large fluctuations, as those observed on the dragline, a method must be developed to determine the location within the frequency domain of the GMF. From observation of data retrieved from the dragline, a precise frequency is not required since the GMF should be the dominant phenomenon for a bandwidth of at least 50 Hz. Thus an approximate frequency band is required within which a search can be made for the dominant peak in the frequency domain. This should then yield the GMF.

Once the GMF is determined it is then substituted into equation 3.9 along with the number of teeth of the gear of interest. The equation is then solved for the unknown shaft speed required by the COT method.

Having two proximity sensors attached to the motor, a rough indication of the speed is fortunately easily obtainable. Using the sigspd.m program, an approximation of the speed is calculated. This program however can only return one point per revolution. This is insufficient since speed fluctuations from one revolution to the next frequently exceed 1.9 Hz. Using equation 3.9 and taking into account that the gear of interest has 25 teeth it can be shown that this speed fluctuation represents a shift in the GMF of 47.5 Hz. This is too large a frequency band within which to search for the GMF as it could easily lead to the identification of another, incorrect peak in the frequency domain as being the GMF. Thus the speed attained by the sigspd.m program must be interpolated to give an indication of the shaft speed between pulses. In this case a cubic interpolation was used.

Once a satisfactory speed approximation has been achieved, the next step is to window the available acceleration data into segments small enough so that the speed variation across the segment is insignificant. This avoids the

smearing of the GMF across several frequencies making it considerably harder to get any meaningful speed related data. Smaller windowed sections will also lead to a higher resolution in determining the speed. However it must be noted that if the segment is too small there are not enough tooth on tooth impacts causing the amplitude of the GMF to dwindle when compared to resonance frequencies, resulting in an inaccurate pinpoint of the GMF.

To minimise the effect of detecting a false GMF, the first, second and third GMF are identified using the above-described method and the average shaft speed calculated and used in the COT method. Figure 3.10 gives an overview of the proposed method, which shall be referred to as the Moving Window Order Tracking (MWOT) method.

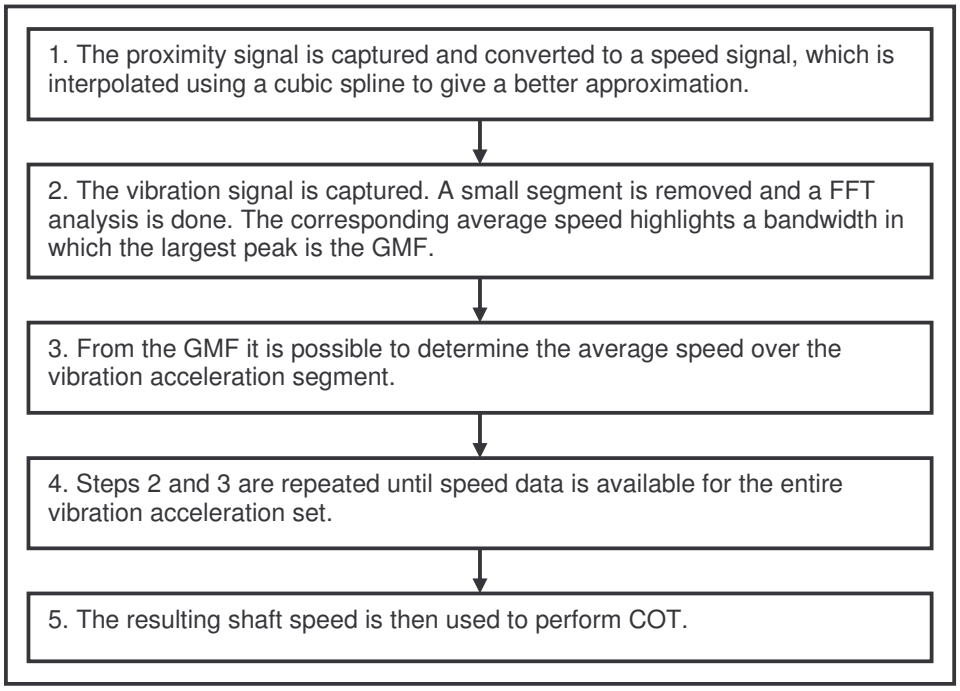

Figure 3.10: An overview of the MWOT method to calculate shaft speed.

By applying the MWOT method it becomes clear that the resulting speed is similar to the speed calculated by sigspd.m from the proximity sensors as is to be expected, however smaller fluctuations in speed become visible which could be significant when applying computed order tracking. Figure 3.11 shows a section of about 3 seconds of the speed as calculated by MWOT and sigspd.m respectively, clearly highlighting the difference.

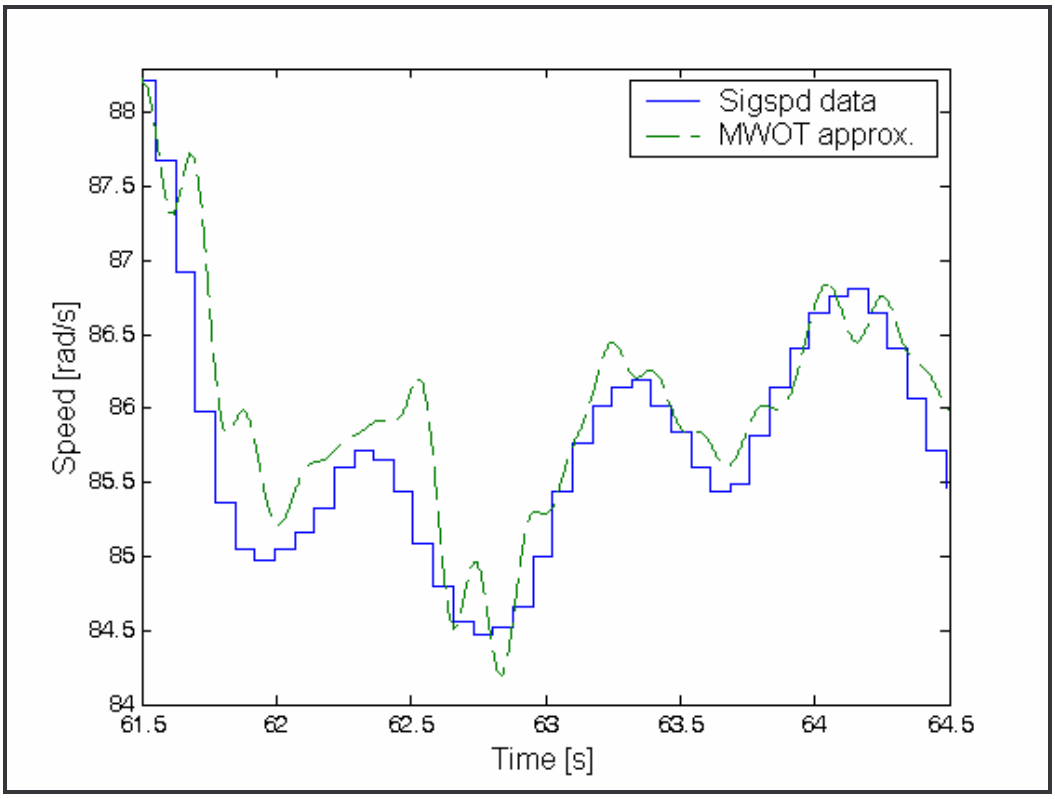

Figure 3.11: Showing the difference between sigspd.m data and MWOT data using segments with a length of 4096 points.

The MWOT method adds a facet of information to the speed that is otherwise lacking with the normal interpolation techniques. Although the cubic spline interpolation technique smoothes out the speed, it is essentially generated data. With MWOT however every fluctuation in speed can be traced back to the measured data giving it higher credibility when compared to the other interpolation techniques.

The segment length chosen for MWOT however has a profound effect on the accuracy. This is demonstrated in Figure 3.12 where a 1 024-point segment size was used to calculate the GMF and subsequently the speed.

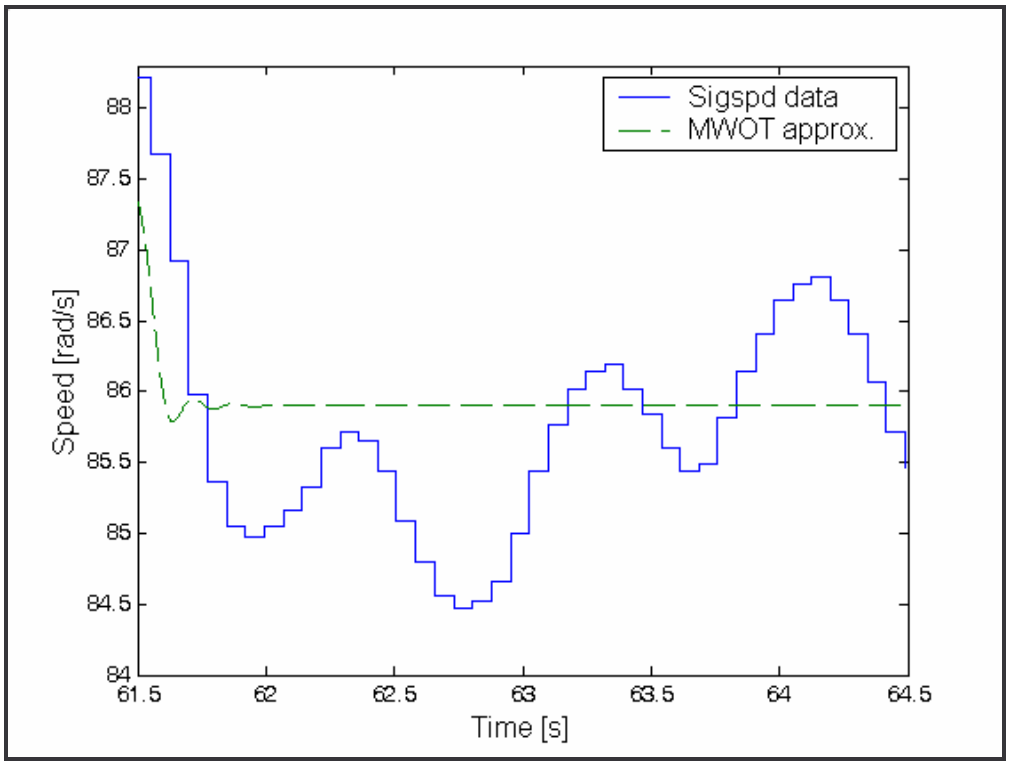

Figure 3.12: Showing the difference between sigspd.m data and MWOT data using segments with a length of 1024 points.

Even the relatively good speed approximation, achieved if 4 096-point segments are used as in Figure 3.11, is not accurate enough as it is possible that a non-GMF peak is chosen. However the amplitude of a non-GMF peak would still fluctuate with the speed, thus even though the speed itself may not be accurate, the speed profile will contain valuable data.

It is thus necessary to add an additional process to the pre-COT procedure that will capture the speed profile whilst ensuring accurate speed. This is possible if Displacement Driven Velocity Interpolation (DDVI) is used.

3.4.4 Displacement driven velocity interpolation, a speed adjustment algorithm

Given the limited amount of information available from the proximity and vibration sensors and the uncertainty inherent in the lack of sufficient rotational speed resolution, it is wise to exploit all concrete facts to ensure that the highest possible accuracy is achieved. One such fact is that the angle

rotated by the shaft between two consecutive pulses from the proximity sensor is precisely 6.2832 radians or 360 degrees.

To determine whether the velocity data attained after processing holds true to this fact, it is necessary to graphically represent the angle between each pulse received from the proximity sensor. Integrating the area beneath the speed graph between two adjacent pulses does this. This exercise was applied to a dragline data set after it had been converted to speed and cubically interpolated. The results are depicted in Figure 3.13.

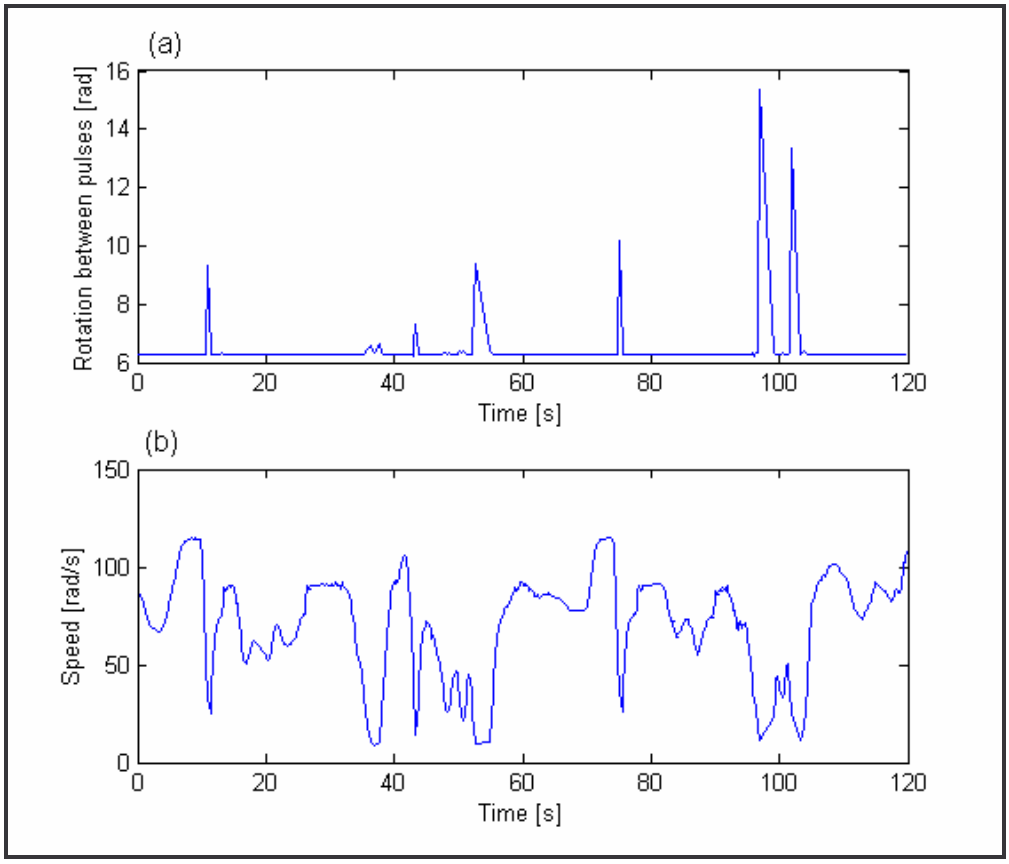

Figure 3.13: (a) Depicting the deviations in area beneath each velocity segment.(b) Depicting the concurrent speed of the data set.

From Figure 3.13 it is clear that there are distinct segments of the speed graph where 6.2832 radians is not the result of the integral of speed between adjacent pulses. From careful observation it becomes clear that the largest deviations occur when the speed approaches 0 rad/s. This is due to the fact that the motor aboard the dragline may become motionless between pulses indicating one revolution. It may even cycle back and forth within one

revolution, thus the angle traversed between pulses at low speeds is not necessarily 6.2832 radians. It is thus important that the speeds approaching 0 rad/s within the data sample are not used to do COT as it would compromise accuracy.

If unreliable speed data only occurs at low speeds then no further processing, apart from excluding low speeds in the COT analysis, need be done. However, when a closer view is taken of Figure 3.13 it becomes clear that further processing would be advisable. Figure 3.14 clearly indicates that there are rotation angle fluctuations from pulse to pulse even at higher speeds.

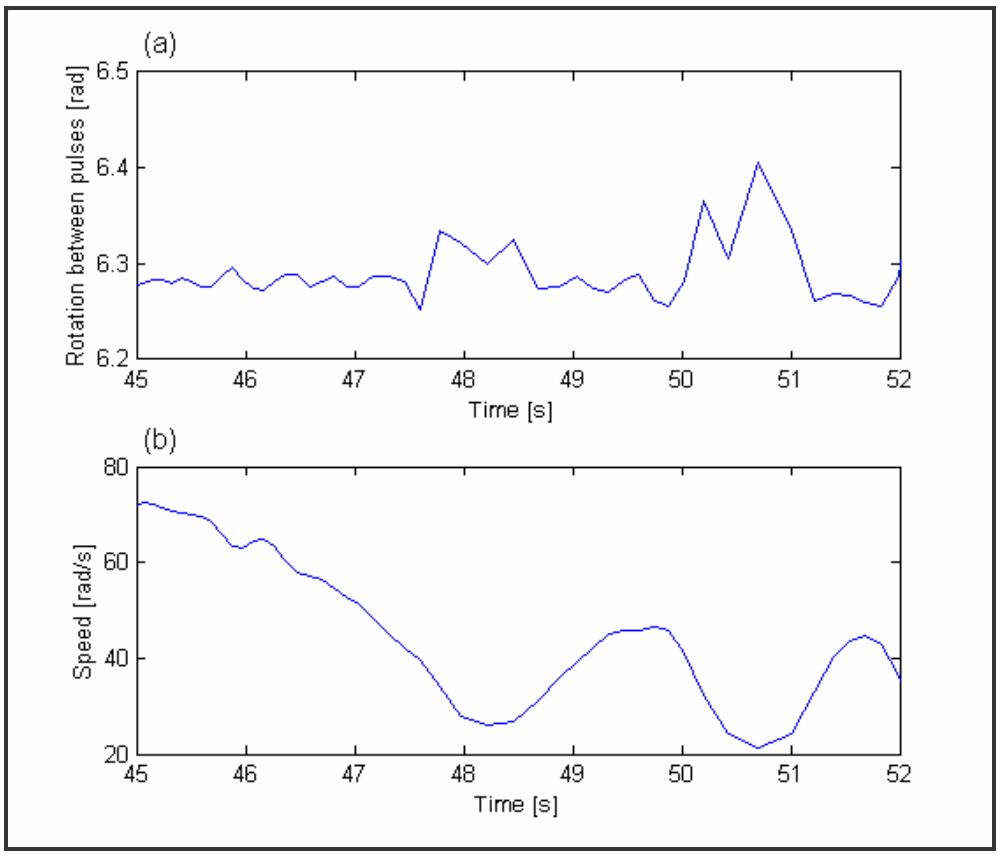

Figure 3.14: (a) A closer view of the rotation angle between pulses. (b) The corresponding speed graph.

This is mainly due to the interpolation scheme that is used to give a closer approximation of the real speed, which often estimates the real speed incorrectly. The need for a suitable algorithm thus exists to ensure that the speed used for COT reflects 6.2832 radians between adjacent pulses. DDVI is an algorithm that was developed to address this shortcoming of the applied

interpolation schemes. The basic steps taken in applying DDVI are outlined in Figure 3.15.

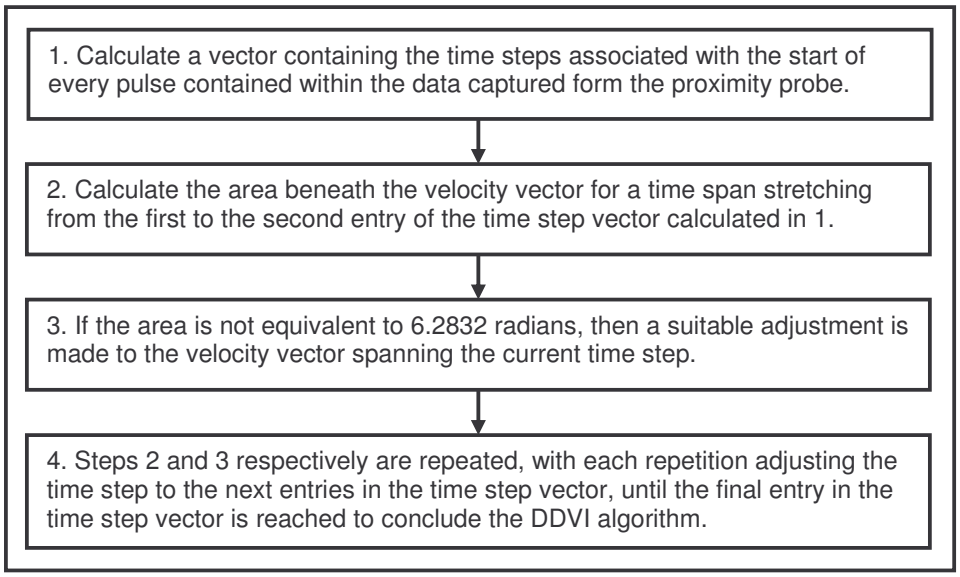

Figure 3.15: A flowchart of the DDVI process

The raw data received from the sensors, 2 channels of vibration data and 2 channels of pulse data, is necessary to complete the first step. To be able to work through every revolution of the interpolated velocity, obtained by applying MWOT or one of the traditional interpolation techniques to a data set, it is required to know where every revolution begins and ends. One of the channels containing raw pulse data, received from a proximity probe, must be differentiated marking the start and end time of each pulse with a distinct spike (Refer to Figure 3.4). This method is identical to that used in the sigspd.m program. These spikes are easily found using Matlab's 'find' function resulting in a vector containing time instants that relate the start and end of each pulse in the data set.

Using a 'for' loop, each consecutive time segment of the velocity is integrated. The integration result is compared to the ideal result, namely 2π or 6.283 radians. A deviation value is then calculated by subtracting the integration result from the ideal result as seen in equation 3.10.

$$Deviation = abs(2\pi - Integration\ result) \tag{3.10}$$

A boxcar windowing function normally used to split vibration data is now employed to adjust the velocity vector by making use of addition. This window

has the same number of entries as the velocity vector of each segment and is adjusted every time a new segment is being analysed. However the area underneath the windowing function must also be adjusted so that it coincides with the deviation calculated in equation 3.10. An adjustment factor must therefore be obtained which will result in the correct area beneath the window function if it is multiplied by the window function. This adjustment factor is simply the deviation divided by the area underneath the window function as shown in equation 3.11.

$$Adjustment\ Factor = \frac{Deviation}{\int (Window \quad function)dt} \tag{3.11}$$

Finally the velocity segment in consideration is adjusted up or down, as required, by adding the product obtained by multiplying the boxcar window function with the adjustment factor. This process is then repeated until the entire velocity vector has been analysed and suitably altered. Figure 3.16 depicts the changes that DDVI made to the speed signal after it underwent cubic interpolation.

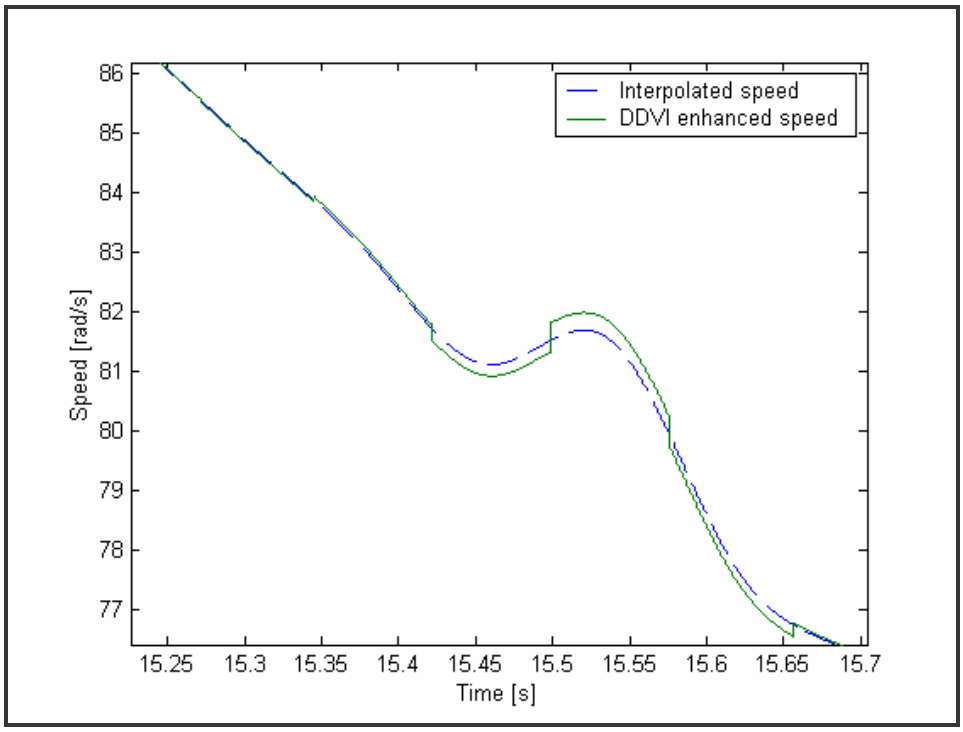

Figure 3.16: Illustrating the effect of DDVI when applied to a cubic interpolation of the shaft speed.

The smallest data size that DDVI analyses and adjusts is one revolution. The speed segment corresponding to each revolution is adjusted as a whole, independently to other segments. It is thus possible that DDVI adjusts one speed segment upwards and the next downwards as is clearly displayed in Figure 3.16. The border between these two speed segments thus shows a clear discontinuity.

The discontinuities do not affect the following COT process as it re-samples the vibration data per revolution. This means that only the data between the discontinuities is used for the COT evaluation ensuring accurate results.

3.5 Summary

To aid in fluent interpretation of subsequently captured data an investigation was launched. During the investigation video footage of the dragline activity was captured in conjunction with vibration signals from the drag gearbox. The vibration intensity levels were successfully linked to specific dragline activities.

Having developed an understanding of the dragline a review of existing and development of new programming within the Matlab environment was undertaken. Programs that were developed included a pulse to speed conversion program and a COT program. A review of existing speed interpolation methods was also done.

A new speed interpolation technique was then developed. Initial attempts included numerical integration optimisation and filter optimisation. These attempts were unsuccessful due to the insensitivity of the function value to the initial characteristic values. Subsequently MWOT was successfully developed. This method makes use of both the pulse as well as the vibration data to interpolate the speed between two pulses. To improve the accuracy of the method an additional algorithm, DDVI, was developed. DDVI determines whether the area beneath the determined speed between two pulses corresponds to 360 degrees, as it should, and adjusts the speed to suit if necessary.

CHAPTER 4 RESULTS

The results derived from the completed analysis of the data captured aboard the dragline for approximately one year are presented in this chapter. The chapter covers four major sections: convergence, inspection of the damaged gears, rotational domain averaging and the spectrum results. Within this chapter the 4 methods described in chapter 3 will be examined and their effects estimated. The performance of the methods in both rotating directions will also be investigated. Furthermore the effect of the number of averages and the MWOT window size will also be discussed.

4.1 The effect of number of averages taken

Determining the number of pinion shaft revolutions available within the captured data sets is important since it determines the number of rotation domain averages (RDA) that can be taken during COT. The higher the number of rotations present in a mono-directional segment, the more averages can be achieved improving the coherency of the results.

Each 120-second data set captured contains speed information of the gearbox running in two directions. Each data set segment with only mono-directional speed can thus be isolated. To shorten the time spend searching through the data captured for a suitable set, a Matlab program was written that analysed the data sets and then determined how many revolutions were available within each mono-directional segment of each data set. This now allowed sets with a certain number of mono-directional rotations to be easily identified.

Figure 4.1 indicates the largest number of rotations available in both directions for each data set. Clearly the higher the number of rotations required the smaller the number of data sets available for analysis. This graph shows that if an indicator of gear deterioration was required then it would be difficult to use more than 200 rotational averages once RDA has been

completed since very few data sets have been captured containing more than 200 rotations in both operating directions.

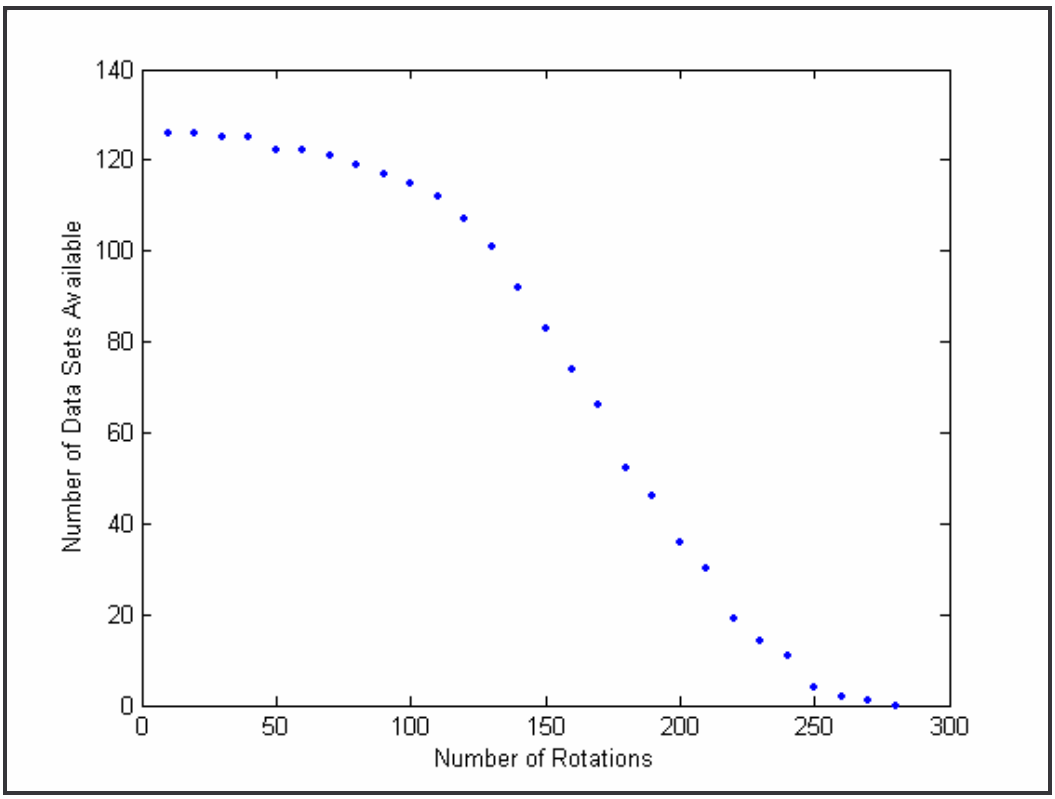

Figure 4.1: Available data sets as a function of required averages.

Only 36 data sets are available if 200 averages are required, furthermore these 36 data sets are not spread uniformly throughout the year of monitoring. Certain months are better represented than others, thus to get a good indication of wear progression the data sets available must be normalised with reference to the month with the fewest data sets. In other words if a month is represented by only one data set, then only one data set per month is used. Due to this elimination procedure the largest number of rotational averages that can be considered when working with both directions is 200. In months where more than one data set was available, a data set was chosen so that the time between the adjacent chosen data sets was as close as possible to 30 days.

Although it has been established that, given the captured data sets, it would be difficult to do COT with more than 200 averages it has yet to be determined whether 200 averages are good enough. This can be established

by plotting successive spectra of a single mono-directional segment. Each successive spectrum is calculated using a different number of averages.

Figure 4.2 presents such a mono-directional data segment taken on 30 May 2003, and will indicate graphically whether 200 averages are enough. The mono-directional segment was also selected such that the speed variance stays approximately between 12.4 and 14.6 Hz to avoid GMF smearing. The data segment was broken up into revolutions. These were then averaged a varying number of times ranging from 10 to 250 averages. From Figure 4.2 it is clearly seen that as the number of averages increase, the frequency content that is synchronous to the shaft revolution is emphasised as the noise or non-synchronous signal is eliminated. It is clear that averaging more than 100 times would be a waste, as stability of the GMF located between 310 and 365 Hz is reached at approximately this point.

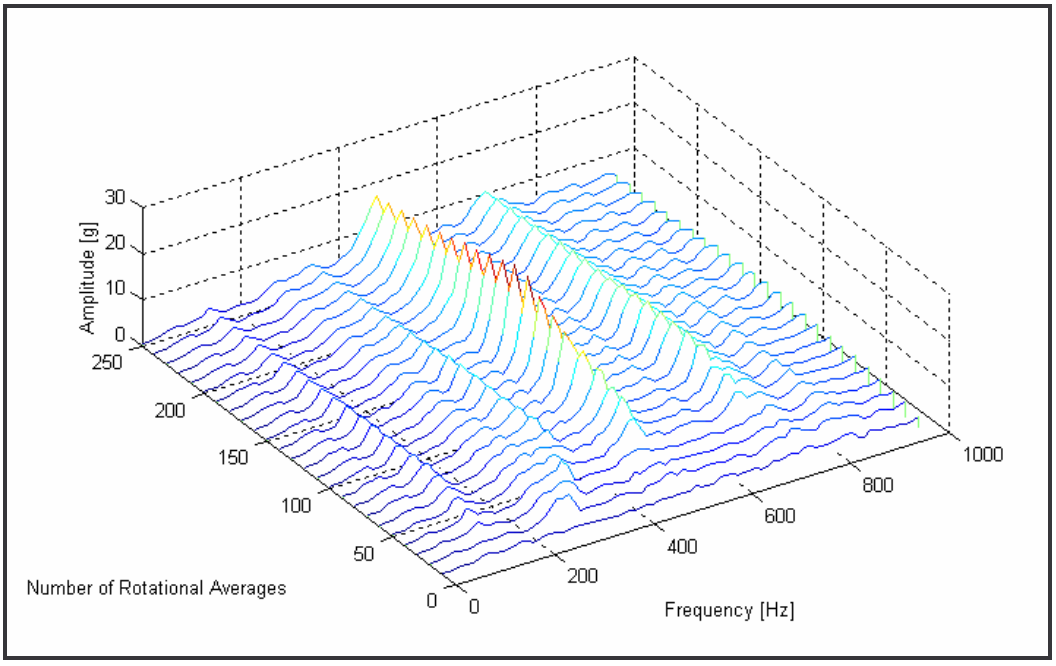

Figure 4.2: The effect of number of averages on the FFT of vibration from a single shaft rotation.

The initial general amplitude increase of the peaks up to 60 averages and the subsequent drop from 200 averages is due to speed fluctuating between 12.4 and 14.6 Hz during the 20 s sample period.

Another approach is to determine the response present around the GMF. This is done by calculating the area beneath the GMF present within each spectrum that forms part of the cascade plot in Figure 4.2. From the raw data used to generate Figure 4.2 it is known that the first GMF will range between 310 and 365 Hz since there are 25 teeth present on the pinion. This area beneath the individual FFTs in this frequency range can now be plotted and presented as in Figure 4.3. The initial exponential increase highlights the effectiveness of averaging but is also partially due to the speed fluctuations present in the sample. Figure 4.3 also indicates that if only the first GMF were to be taken into consideration, approximately 70 averages would be sufficient to obtain trustworthy COT results.

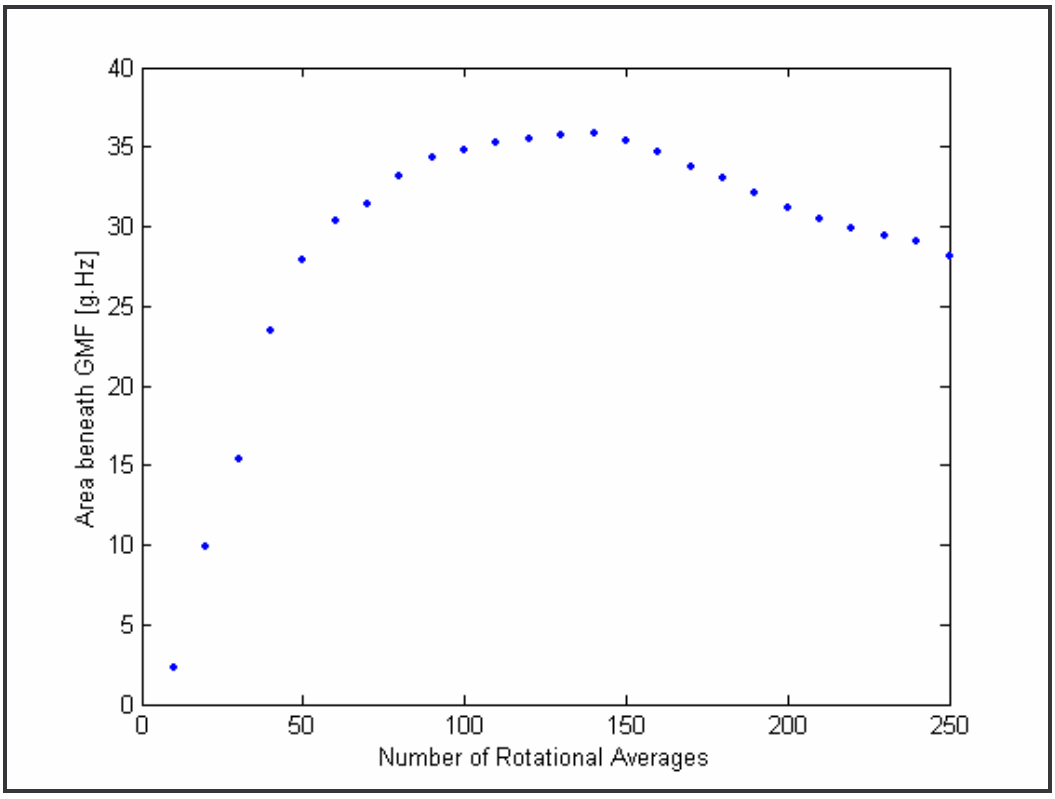

Figure 4.3: The change in gear mesh frequency as a function of number of averages.

The fluctuation in the GMF response after the initial rise is due to the fact that the data used to present Figures 4.2 and 4.3 was raw data. This means that although a relatively constant speed, mono-directional section was used, the slight variations in speed of approximately 2 Hz is enough to hinder perfect convergence to a single response level.

4.2 The effect of window size in MWOT

The MWOT method determines shaft rotational speed by calculating the GMF of consecutive windows or segments of the vibration data. The size of this window affects MWOT accuracy by determining sensitivity to speed changes and affecting spectrum resolution, which is vital to the functioning of the MWOT method. These two factors are in conflict with one another. If window size is increased, a better spectrum for finding the GMF is achieved but the ability of the method to pinpoint small speed changes for the COT analysis can be compromised.

To begin this investigation, several spectra were generated from the captured data. From these spectra it became clear that the GMF is difficult to pinpoint if a spectrum of less than 1 024 points was generated. Thus the window sizes to be investigated should be larger than 1 024 points. Four different window sizes were chosen ranging from 1 024 up to 8 192 points. The points were deliberately chosen as powers of two so that the FFT process inherent to MWOT can be completed efficiently. Figure 4.4 shows the speed over the entire data set captured on the morning of 30 May 2003.

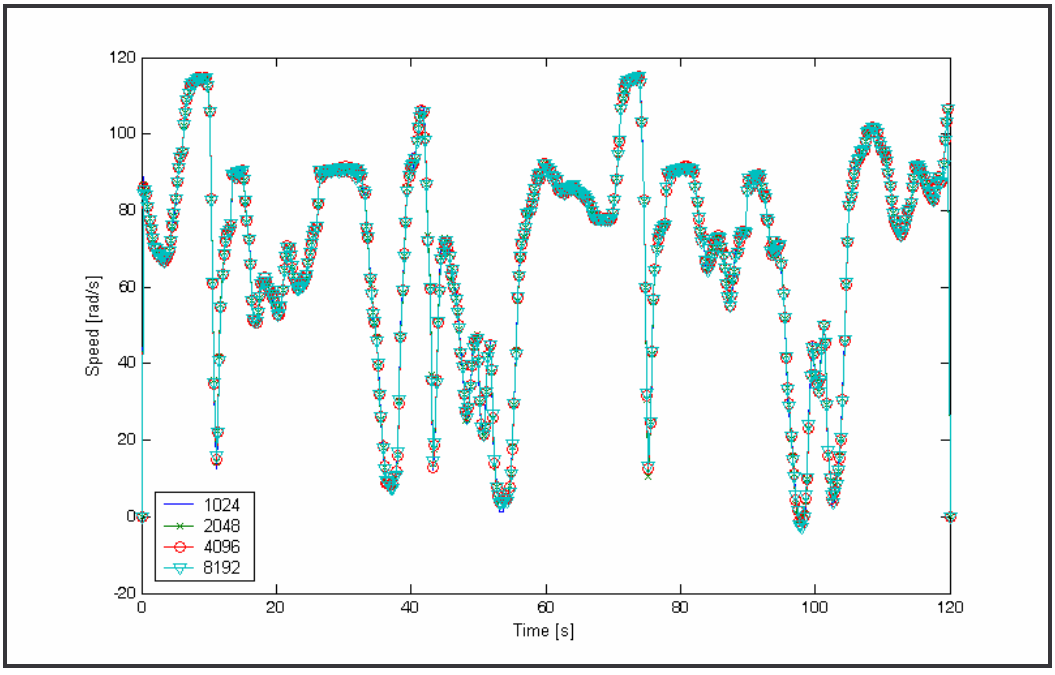

Figure 4.4: Comparing the speed generated by MWOT using four different window sizes.

Globally there is no discernible difference between the four window sizes, but if one were to zoom in closer, as was done in Figure 4.5, a separation between window sizes becomes evident.

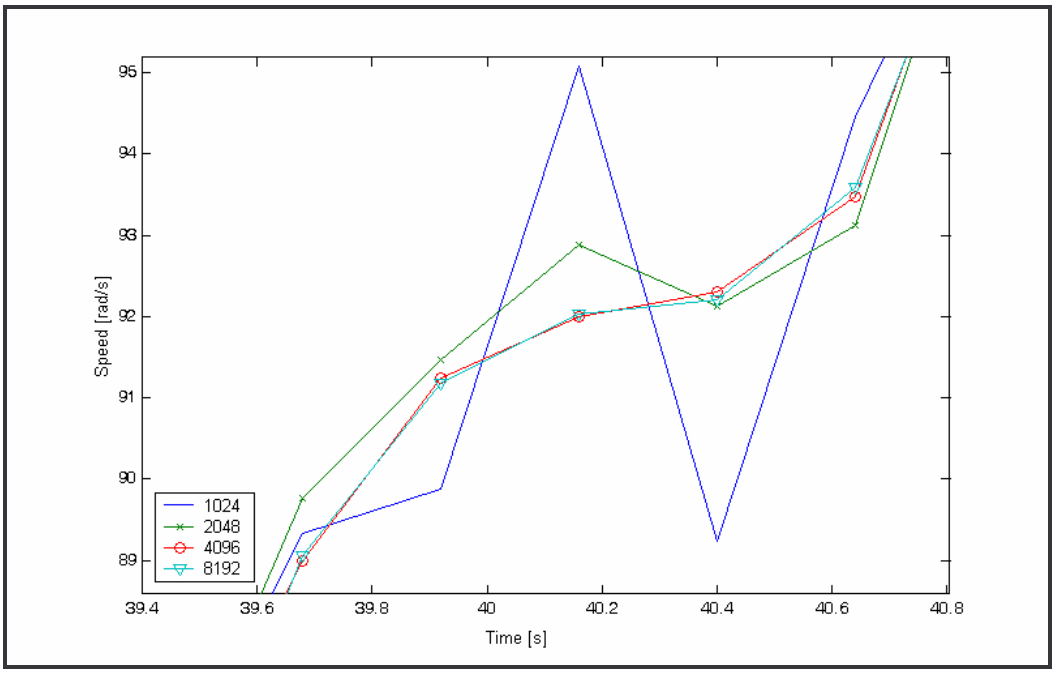

Figure 4.5: Taking a closer view at the differences between MWOT window size.

From this Figure it becomes clear that larger window sizes have a similar effect as a low pass filters. Due to the speed being averaged over a longer period, speed fluctuations are smoothing out. The distance between the starting positions of each window is 1 000 points. Thus if the window size increases, every segment of data will be evaluated more often. The amount of fresh data evaluated for each window is thus decreased, creating the evident smoothing effect. It is evident that 4 096-point spectra perform as well as 8 192-point spectra, thus eliminating the use of 8 192-point spectra due to an increase in processing time with little or no gain in accuracy.

The sensitivity to change in speed is affected in another way, namely, the smaller the window size the higher the resolution of the velocity vector. If the shaft were to be rotating at a maximum speed of 20 Hz, then a revolution occurs once every 0.05 s. If the window has 1 024 points then it analyses every 0.02 s, which is 2.5 times per revolution at top speed. Whilst this is advantageous the FFT resolution drops significantly to the extent that it

becomes difficult to clearly distinguish the GMF to be able to estimate speed. A window size of 4 096 points was thus chosen when estimating shaft speed using MWOT. This determination can now be used to effectively analyse and interpolate the shaft speed by implement MWOT.

4.3 Convergence in the rotational domain

The test for convergence indicates how fast the order tracking method implemented settles down to a stable RDA.

If a data set containing 240 rotations were averaged, convergence is applied by splitting these into two daughter sets of 120 sets apiece. The daughter sets are then incrementally averaged, that is to say first two are averaged then three and so forth. After each incremental average the resulting RDA from each daughter set is subtracted from the other. The answer is evaluated using RMS to get a single value that makes up the convergence graph.

Figures 4.6 to 4.9 show how the captured data fares when a convergence test is undertaken. Each Figure shows all four methods in a specific direction with either damage or no damage to the gear at the time the data was captured. The two data sets used, captured on the evening of 4 June 2003 and the morning of 24 February 2004, had 240 rotations in both inward and outward bucket motion. In June 2003 the pinion was still relatively new whilst the pinion failed shortly after February 2004, thus ensuring that convergence is tested on data from both the non-damaged and the damaged pinion.

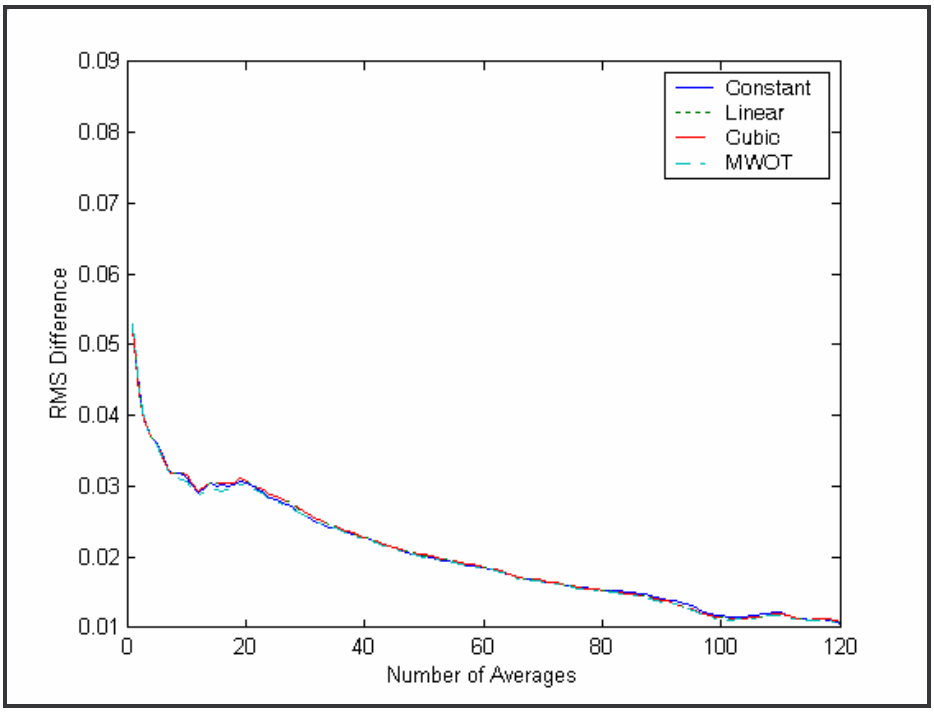

Figure 4.6: The convergence results of all four methods in the inward bucket motion direction with no gear damage present.

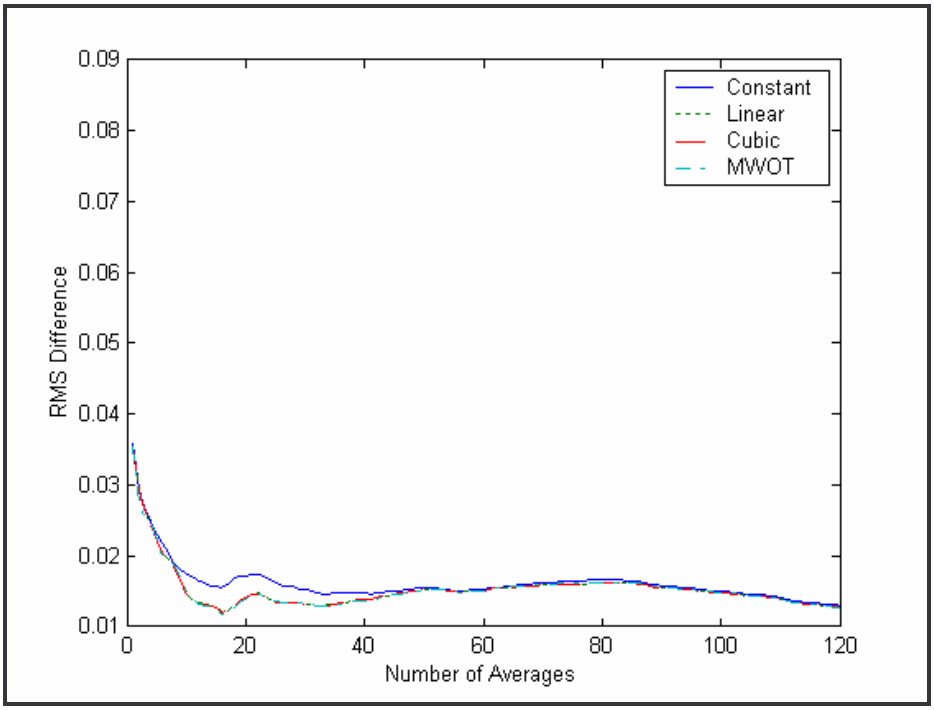

Figure 4.7:The convergence results of all four methods in the outward bucket motion direction with no gear damage present.

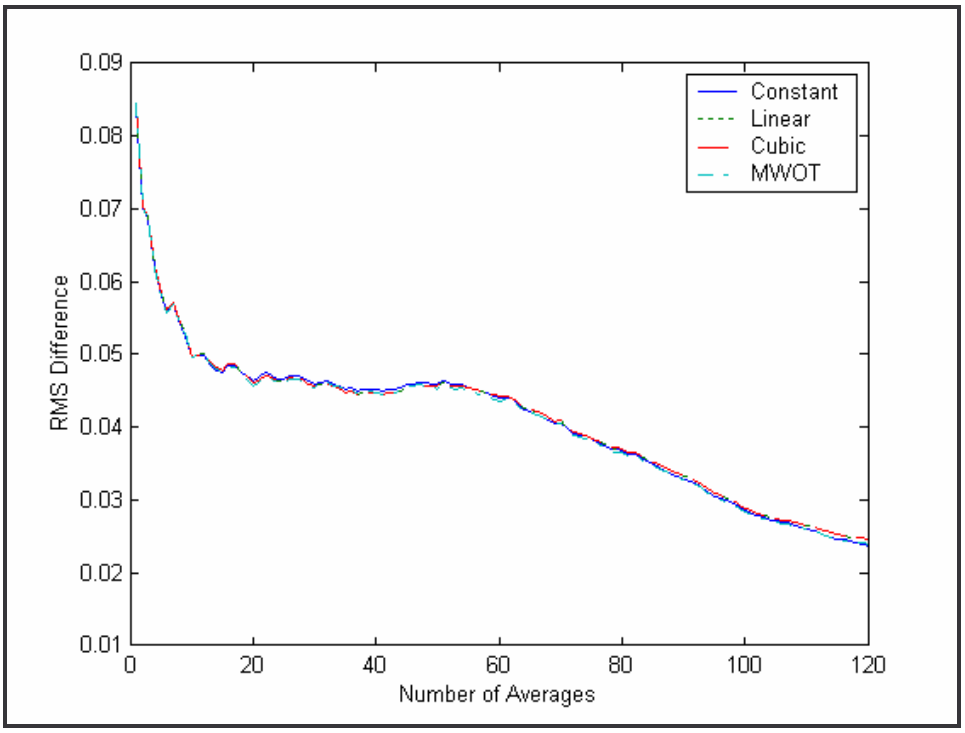

Figure 4.8: The convergence results of all four methods in the inward bucket motion direction with gear damage present.

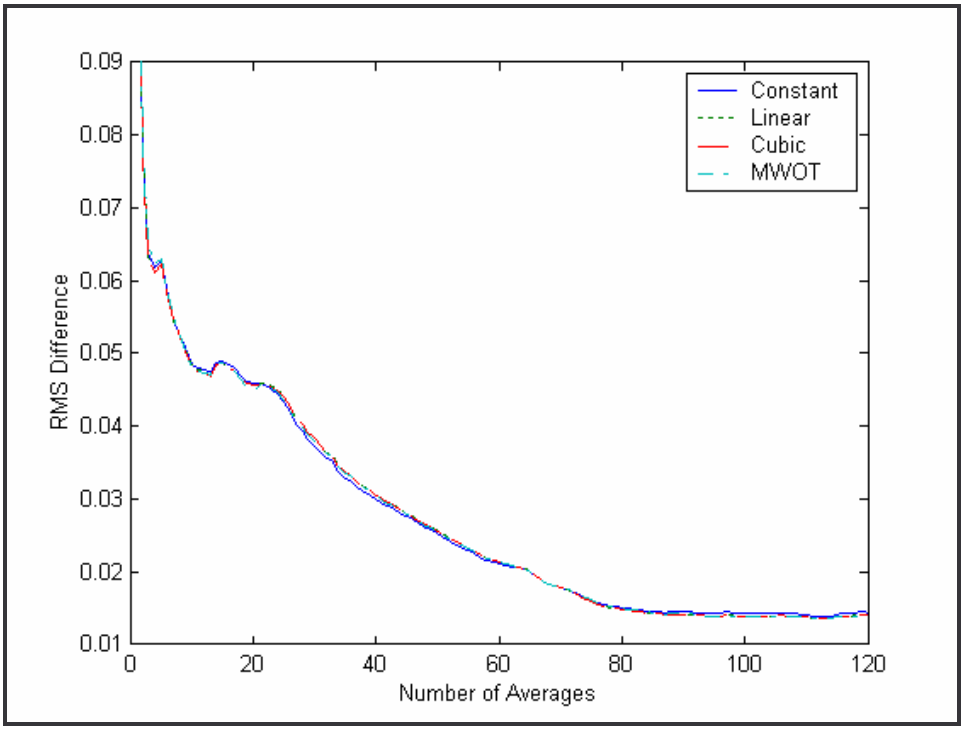

Figure 4.9: The convergence results of all four methods in the outward bucket motion direction with gear damage present.

In all four cases all four methods successfully converge to a stable RDA. It is difficult to discern individual method performance as they perform similarly. At arbitrary points during the number of averages taken any method could be seen as performing best. The only method that could be said to have performed worse than the others is the Constant interpolation method and that only in the outward bucket motion with no damage as indicated in Figure 4.7. Interestingly Linear and Cubic interpolation yield almost identical convergence graphs indicating the suitability of linear interpolation as a candidate that is reasonably accurate and computationally inexpensive. Having established that all methods converge satisfactorily, it is possible to carry on to the RDA with confidence that any results achieved are not marred by incompetent implementation of interpolation methods.

4.4 Inspection of defective gears

On 14 May 2004 two pinions, one of which was monitored, and a bull gear were removed and inspected. These three gears formed part of a single gear system where the two pinions drove the larger bull gear. Figures 4.10 to 4.13 show pertinent pictures indicating the damage found on these three gears.

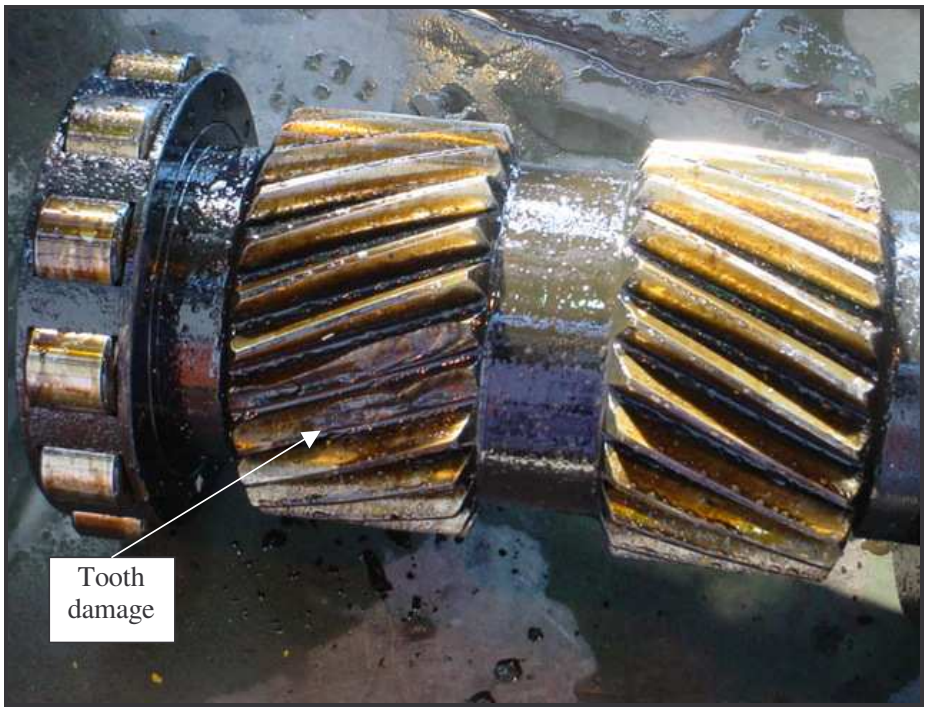

Figure 4.10: Tooth damage on the left gear set of the monitored pinion.

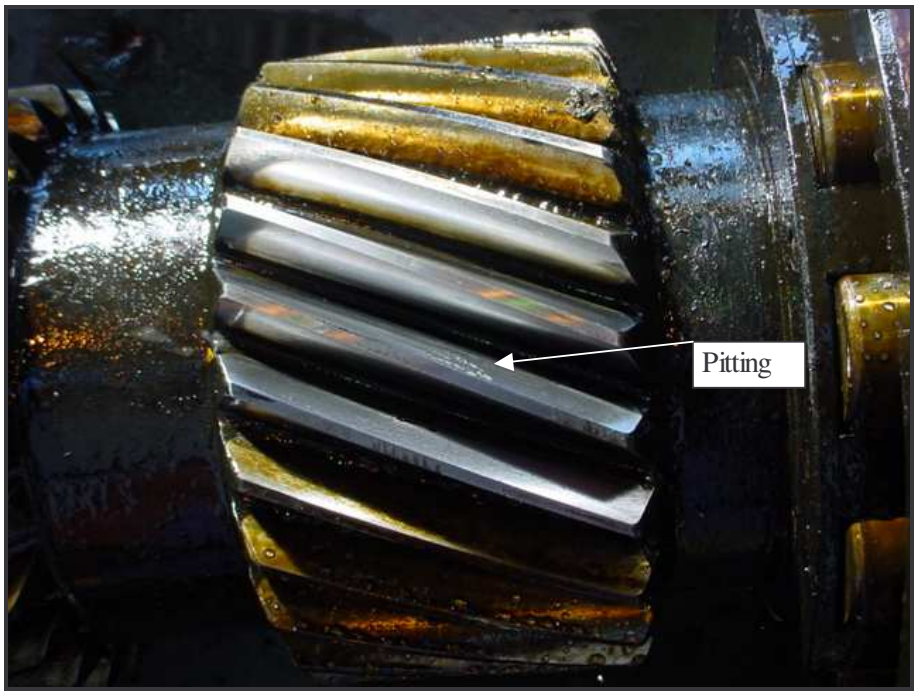

Figure 4.11: Pitting damage on the right set of the monitored pinion.

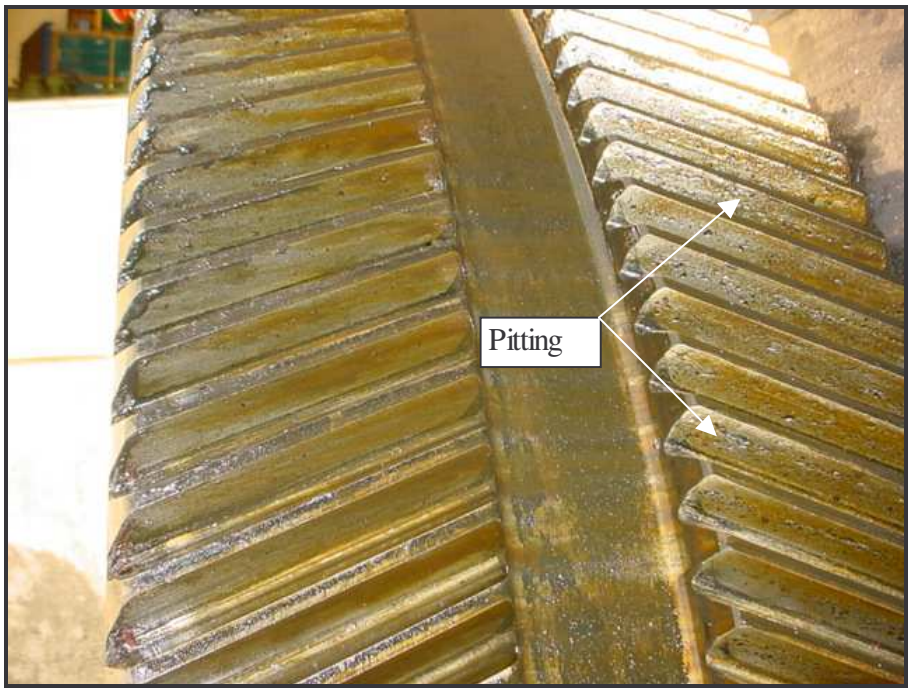

Figure 4.12:Bull gear showing pitting on one set of teeth.

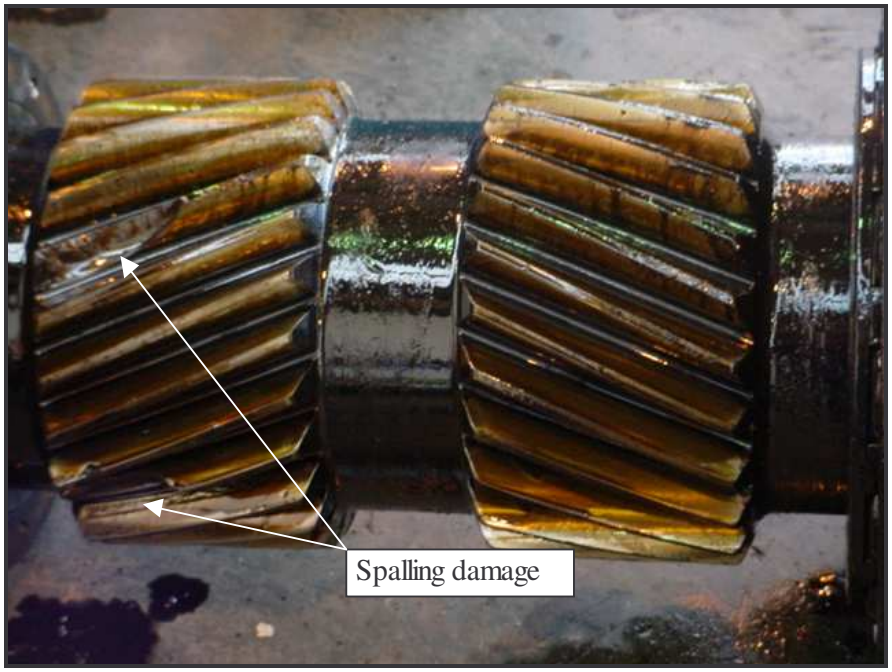

Figure 4.13: Spalling damage on unmonitored pinion.

Two gear defects occurring on the inspected gears are spalling and pitting. Kuhnell (2004) mentions that no common definitions have been established to distinguish between pitting and spalling, it is however generally accepted that pitting is caused by surface contact fatigue cracks and spalling by subsurface cracks propagating under the work hardened surface.

Pitting tends to occur on high spots of gear faces that are subjected to excessive contact stress. Both pitting and spalling can be due to the manufactured geometry of the gears since high points are subject to high stresses; furthermore the surface roughness of the gear has a significant impact on the gear life. Kuhnell (2004) also mentions that misalignment has the same severe impact as improper gear geometry. The damage seen in Figures 4.10 to 4.13 is thus caused by improper geometry, misalignment or a combination of these two factors.

The monitored pinion shown in Figures 4.10 and 4.11 shows severe spalling on two adjacent teeth on the left set of teeth. The right set showed minimal pitting damage. This indicates that the left set of teeth was subjected to higher stresses than those on the right. The bull gear showed severe pitting on only

one set whilst the other remained relatively unscathed. The unmonitored pinion also showed more severe spalling damage on only one set of teeth.

The bull gear and both pinion gears showed preferential damage to one set only. This is a strong indicator that misalignment is the root cause of the damage to the gears in this system. The bull gear shows less severe damage because each of the 235 teeth mesh less frequently than the 25 teeth on each pinion. The damage on the two pinions is more severe than that on the bull gear indicating the higher workload of the pinions. The cursory gear inspection thus indicates that gear misalignment is the cause of pinion failure.

4.5 Rotation domain averaging

Once the convergence of the methods is proven, the next step is to have a look at the rotation domain average that is produced using the four different speed interpolation techniques. As with the convergence, damage- and no damage scenario will be presented in both operational directions.

The rotation domain averages shown in Figures 4.14 and 4.15 are a result of 240 averages. Two data sets were used; the first set was captured on 4 June 2003 when there was relatively little gear damage. The second set of data was taken on 24 February 2004 and certainly had damage since slightly more than a month later on the 14 May 2004 the pinion was removed from the dragline with two broken teeth, as shown in Figures 4.10 and 4.11.

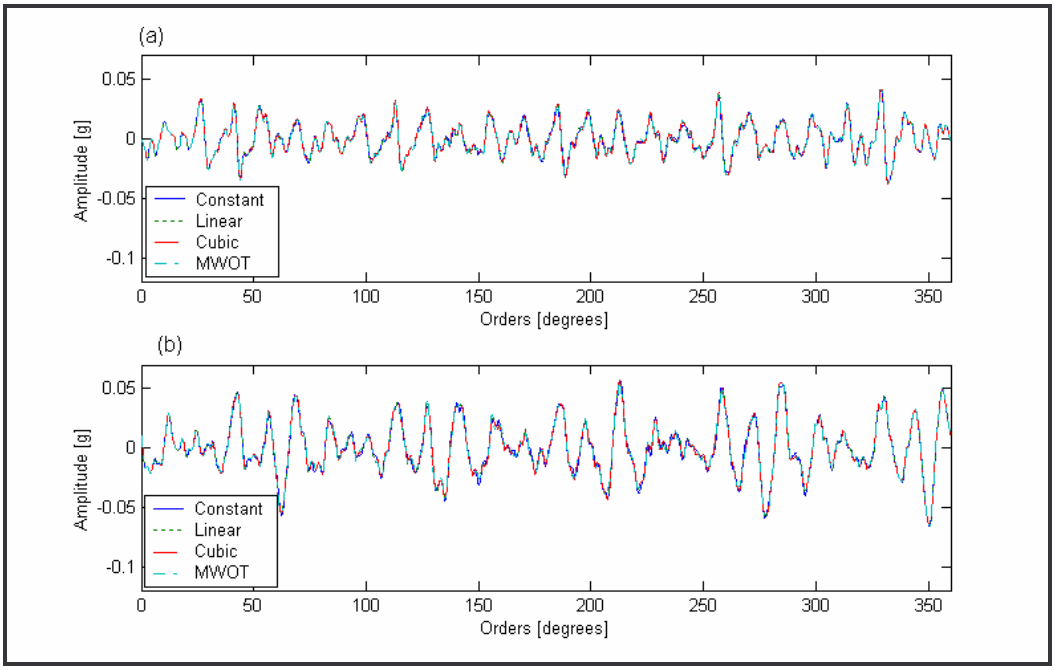

Figure 4.14: The rotational domain average using constant, linear, cubic and MWOT interpolations. (a) without and (b) with damage. Dragline bucket motion is inward.

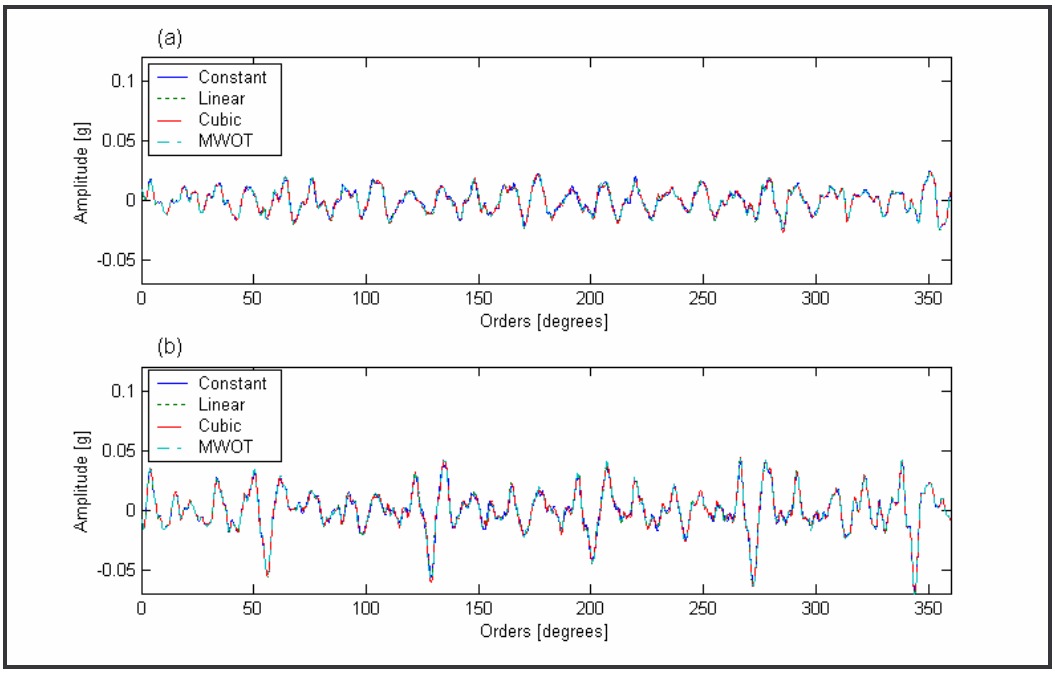

Figure 4.15: The rotational domain average using constant, linear, cubic and MWOT interpolations. (a) without and(b) with damage. The dragline bucket motion is outward.

The regular signal that is evident in Figures 4.14(a) and 4.15(a) has 25 peaks corresponding to the tooth impacts of the pinion. These impacts are also visible in Figures 4.14(b) and 4.15(b) but are slightly distorted due to the

damaged condition of the pinion, as illustrated in Figures 4.10 and 4.11. This was expected and is a further indication, apart from convergence, that computed order tracking has been successfully implemented aboard the dragline.

In both cases, damaged and undamaged, the slight distortion of the tooth impact peaks is likely due to the fact that the pinion is a double helix gear. This means that the manufacturing tolerances of the gear could affect the RDA especially if the teeth from the two sides do not mesh in complete unison. RDA would not filter out this type of distortion since it is periodically synchronous with the shaft rotation. The slight amplitude modulation seen in the undamaged cases is probably caused by gear misalignment. The presence of misalignment is also supported by the inspection of the damaged gears.

Figures 4.14(b) and 4.15(b) indicate the data taken with damage present. The effect of the damage is clearly visible as the RDA has increased in amplitude and shows clear amplitude modulation. The increased amplitude is likely caused by increased overall surface wear of the pinion teeth, leading to larger meshing tolerances. Higher tooth impact energies would result as evident in Figures 4.14(b) and 4.15(b). The amplitude modulation seen is accentuated by local tooth defects. The amplitude modulation has a period of 1/5 revolution and should thus be seen on a COT FFT at 5 orders. Furthermore, according to White (1991), the sidebands developing due to this amplitude modulation should be seen at 5 orders either side of the GMF. The four methods used are all depicted in Figures 4.14 and 4.15.

Once again there is little difference between the methods. This lack of variation in results obtained from using the different interpolation schemes is likely due to the meagre 2 pulse per revolution speed information obtained from the proximity sensors. This trend continued throughout the research. All subsequent graphs will thus only present results as obtained by using MWOT.

4.6 Fast Fourier transforms and cascade plots

To be able to see the performance of the computed order tracking method the resulting RDAs are transformed into the frequency domain. The FFTs of RDAs stretching over the one-year monitoring period are then presented as a cascade plot.

The data sets were chosen according to suitability; only those samples were chosen that contained 200 or more revolutions in both rotating directions. The data sets used were captured at the dates and times indicated in Table 4.1.

Table 4.1: Indication of the capturing date and time of data sets used.

Sample Number	Date of Capture	Time of Capture
1	30 May 2003	06:02
2	09 June 2003	06:02
3	17 August 2003	18:02
4	11 September 2003	05:02
5	11 October 2003	18:02
6	18 December 2003	05:02
7	31 January 2004	17:02
8	13 February 2004	05:02
9	24 February 2004	05:02
10	06 March 2004	17:02
11	23 March 2004	05:02
12	11 April 2004	17:02
13	13 April 2004	17:02

The rotating directions are described with reference to the dragline bucket motion, which either moves outwards, away from the dragline, or inwards, towards the dragline.

To serve as comparison, Figures 4.16 and 4.17 show the precise same data sets that are to be analysed using COT. They depict the vibration emanating from the gearbox during a single revolution. In general the overall noise levels are high and no discernible deterioration trend is visible, especially in the case

of an outward moving bucket. However with some of the sets, in both directions, the GMF at 25 orders is discernible.

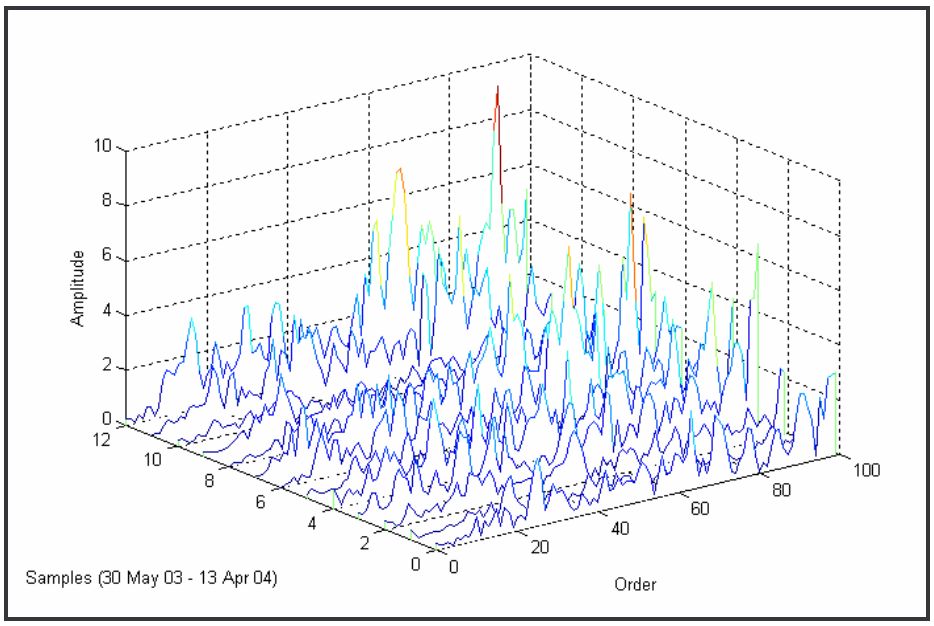

Figure 4.16: The cascade plot of the vibration data emanating from the gearbox during one revolution whilst the dragline bucket is moving inward.

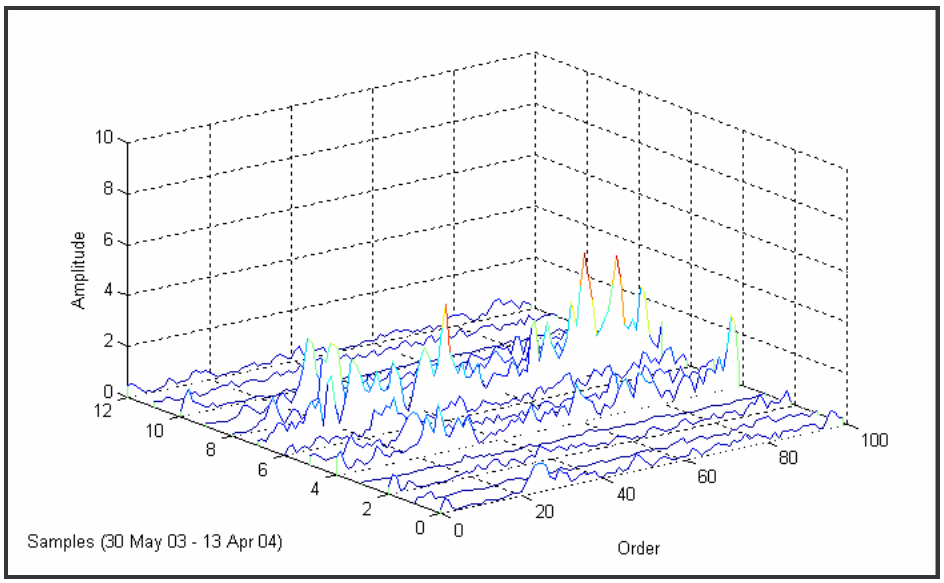

Figure 4.17: The cascade plot of the vibration data emanating from the gearbox during one revolution whilst the dragline bucket is moving outward.

4.6.1 Cascade plots using 200 RDA

Figure 4.18 and 4.19 show the cascade plots generated using MWOT with 200 RDAs.

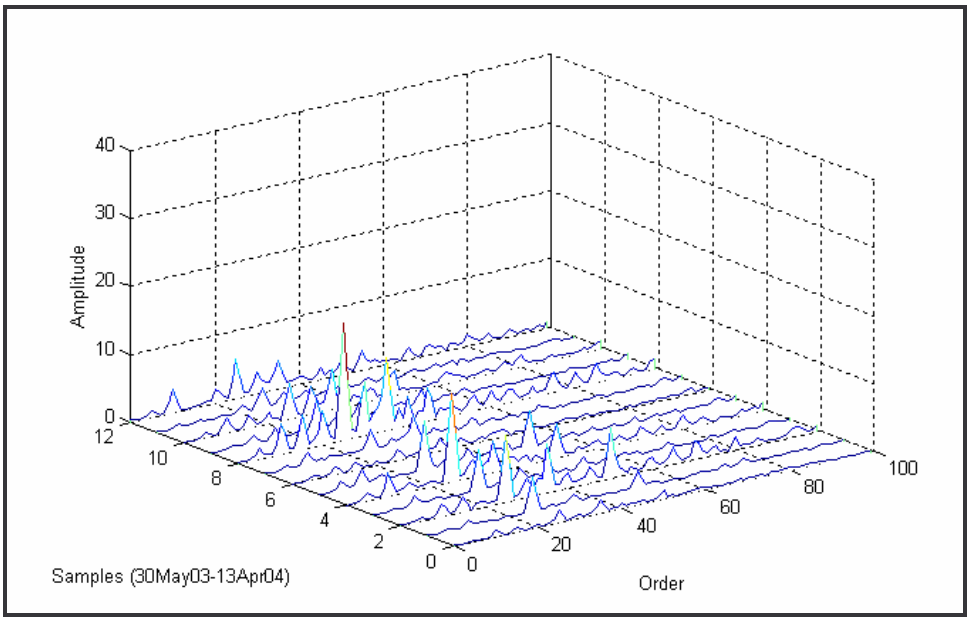

Figure 4.18: The cascade plot of 200 RDAs that were generated using MWOT speed interpolation. The bucket motion is inward.

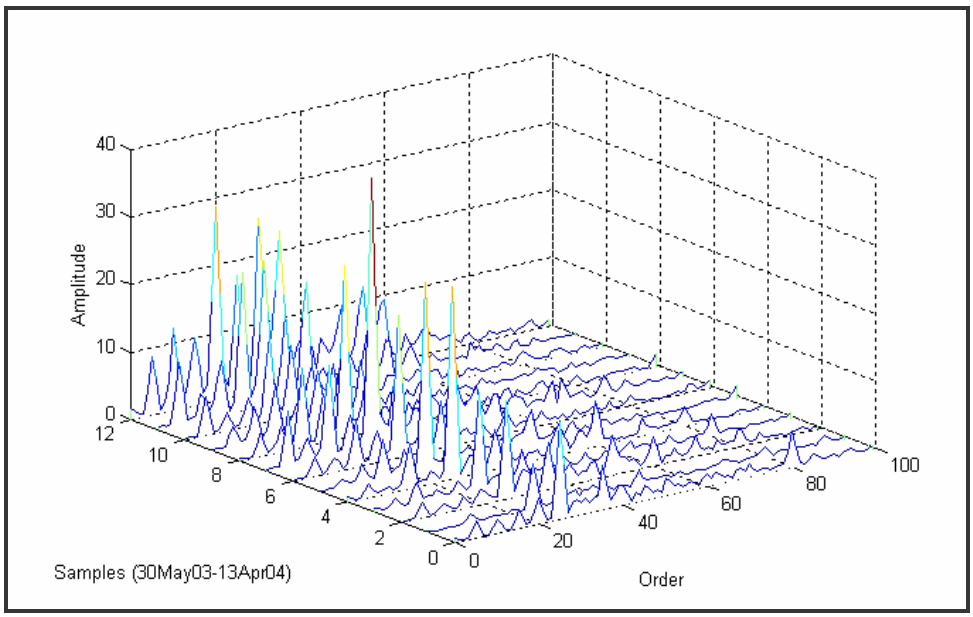

Figure 4.19: The cascade plot of 200 RDAs that were generated using MWOT speed interpolation. The bucket motion is outward.

When compared to the non-averaged signal presented in Figure 4.17, a noticeable decrease in noise and an improvement in amplitude is present. Furthermore the outward moving signal shown in Figure 4.19 is less erratic and shows clear increase in amplitude indicating pinion fault advancement.

There is a considerable difference between the results from COT and the vibration data emanating from the gear over one revolution, as shown in Figure 4.14 and 4.15. All methods produced results similar to Figures 4.18 and 4.19. All methods showed an overall increase in vibration levels across the order spectrum indicating gear fault. The GMF at 25 orders is clearly visible throughout the cascade plots in both directions.

The sidebands however show a significant increase in all cascade plots giving a clear indication of fault progression. The sidebands are visible at 5 orders either side of the 1st and 2nd gear mesh frequencies. There is thus a modulating frequency of 5 orders, which is clearly visible in the advanced wear RDA graph depicted in Figures 4.14(b) and 4.15(b). Modulation is typically caused by local tooth defect, misalignment or load variation. Loading is not a likely cause since the load profile of the dragline is not consistent across one shaft revolution. Local tooth defect would certainly increase the extent of the modulation but can not account for the slight modulation seen early in the pinion life span as shown in Figures 4.14(a) and 4.15(a). Misalignment of the pinion is a more likely root cause for the modulation.

It is probable that initial misalignment caused high stress on a small number of teeth causing them to break. In turn the broken teeth accentuated the modulation. This chain of events is supported by the assessment of the removed gears earlier in this chapter, which showed strong indications of misalignment. The root cause of the pinion failure is thus initial misalignment rather than defective gear components.

The inward bucket motion vibration has approximately half the amplitude of that from the outward bucket motion. This is due to the fact that for the inward bucket motion no load is present in the bucket except for a short period when the bucket is dragged through the dirt to load it. Since the sampling process was not synchronised with the dragline operation, it stands to reason that most inward bucket motion samples would not have been captured whilst the pinion was subjected to high loading conditions. Furthermore the same gear face that is subjected to high loads whist loading the bucked also sees load in

the outward bucket motion. This is due to the fact that gravity and not the dragline motor moves the bucket in the outward bucket motion direction. Thus the motor acts as a brake controlling the speed at which the bucket moves. The braking force would thus act on the same tooth faces as the dragging force produced by the motor in the inward bucket motion. Thus the direction in which the defects would be most clearly identifiable would be the outward bucket motion, since the outward bucket motion is always under load, not just periodically.

4.6.2 FFT based deterioration graph

Although the cascade plots in the previous section are interpretable, a more intuitive portrayal of the gear wear progression is necessary. This is achieved by trending a number of components in the cascade plot and plotting these separately. The following two graphs show the trend of the maximum amplitude peak in the spectrum in both directions.

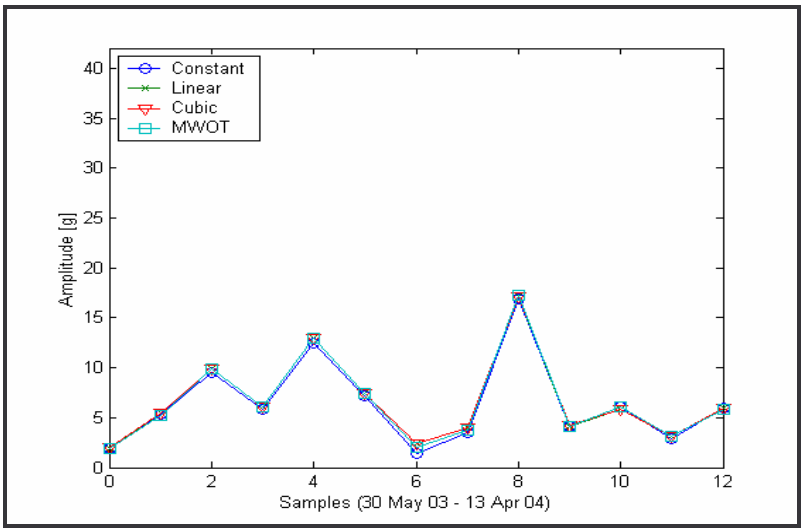

Figure 4.20: The maximum amplitude of the FFT taken from all four methods in the inward bucket direction.

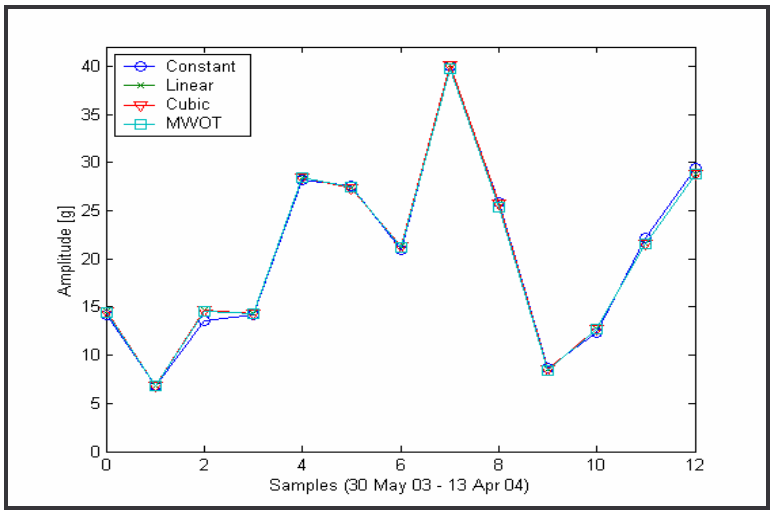

Figure 4.21: The maximum amplitude of the FFT taken from all four methods in the outward bucket direction

Neither Figure 4.20 or 4.21 shows much of a trend although the outward bucket motion data shows a marked amplitude increase over the last 4 data points. The lack of significant amplitude in the inward bucket motion is due to the fact that for the most part this direction of motion is under no load. The maximum peak in the FFT could vary with load, rendering this manner of deterioration determination unreliable. The first GMF sideband amplitude shown in Figures 4.22 and 4.23 is a better indication of damage advancement.

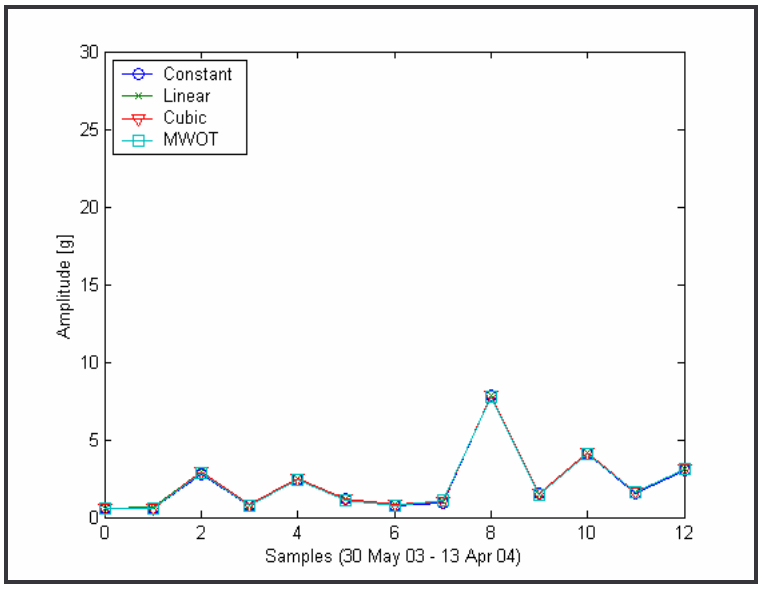

Figure 4.22: The gear deterioration graph derived from the sum of the 1st GMF sidebands in the inward bucket direction.

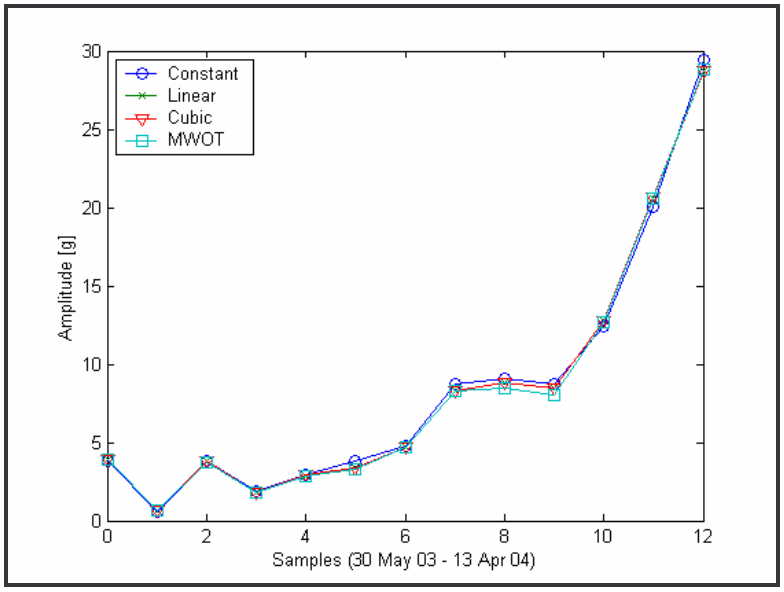

Figure 4.23: The gear deterioration graph derived from the sum of the 1st GMF sidebands in the outward bucket direction.

Again the deterioration in the outward bucket motion is better defined compared to that of the inward bucket motion. In both cases the 1st GMF sideband amplitude gives a better indication than overall maximum amplitude. Figure 4.23 clearly shows the exponential increase in wear towards the end of the gear lifespan. The second GMF sidebands are shown Figures 4.24 and 4.25.

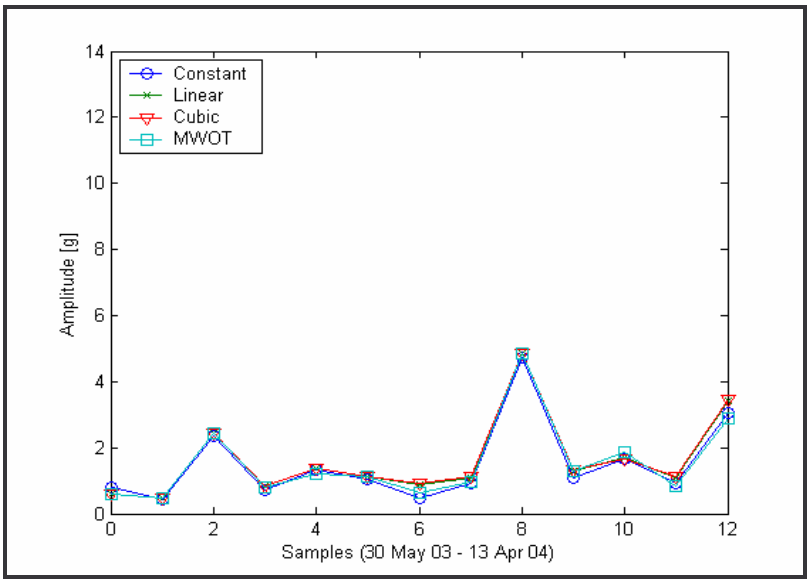

Figure 4.24: The deterioration graph constructed from the sideband amplitudes surrounding the 2nd GMF with the bucket moving inwards.

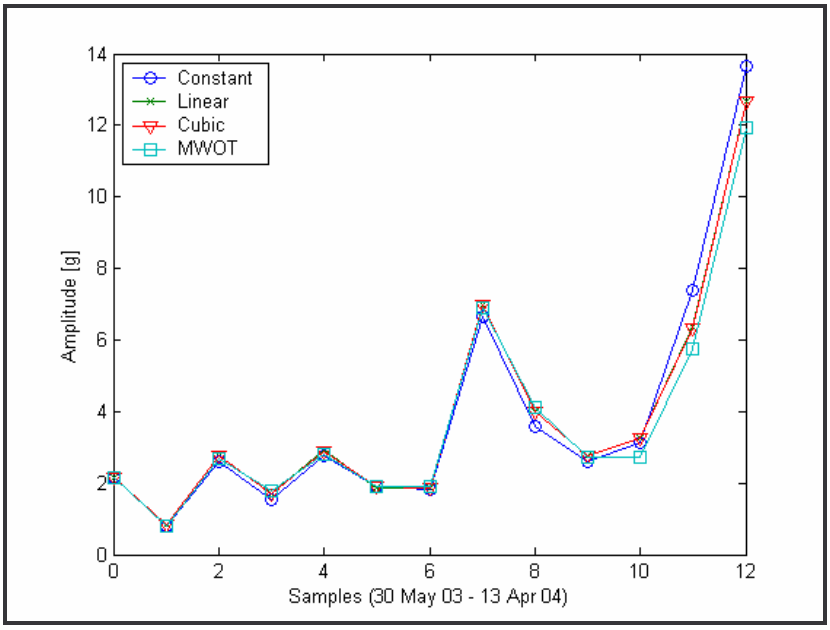

Figure 4.25: The deterioration graph constructed from the sideband amplitudes surrounding the 2nd GMF with the bucket moving outwards.

The 2nd GMF sidebands amplitudes are comparable to those generated from the 1st GMF sidebands. The peak observed at set number 7 could possibly indicate the spalling effect of one tooth. This assumption is supported by the fact that the sideband levels are higher for sets 8 to ten than those from sets prior to set 7. The drop in sideband amplitude from set 7 to set 8 could be due to the break 'wearing in', thus lowering vibration levels.

There is higher amplitude present at the 1st GMF than at the second, making the deterioration graph composed from the 1st GMF sideband amplitude in the outward bucket motion the premier fault propagation indicator. All four methods performed uniformly, small differences are however shown by summing all the points in the above 6 Figures for each method. The result is tabulated in Table 4.2.

Table 4.2: Comparing the four interpolation methods using three different deterioration graph techniques.

	Max FFT Amplitude		1st GMF Sidebands		2nd GMF Sidebands	
Bucket Direction	**Inward**	**Outward**	**Inward**	**Outward**	**Inward**	**Outward**
Constant	83.19	263.92	27.89	109.93	19.54	50.63
Linear	86.36	264.93	28.68	108.82	21.08	50.08
Cubic	86.40	264.92	28.71	108.85	21.31	50.07
MWOT	85.64	263.84	28.34	107.88	19.91	48.16

From Table 4.2 it could be concluded that MWOT performs the worst compared to the other three methods. However it should be noted that the performance difference between the methods is so small that it is inconsequential.

The lack of significant difference between the methods could be attributed to the meagre twice per revolution speed information. All interpolation methods considered made use of the speed captured from the proximity sensors. It is possible that the small changes made by the interpolation techniques are overshadowed by the lack of sufficient speed information. In the application of COT to the dragline with the equipment used it is possibly most efficient to use the basic constant speed interpolation technique.

4.7 Summary

Before obtaining the final results it was necessary to determine an appropriate number of RDAs to be taken. The captured data was analysed to determine the number of sets available with sufficient mono-directional rotations to present an indication of pinion wear progression over time. It was determined that sufficient data sets were available if the number of averages were restricted to 200. It was subsequently shown that 200 averages would be good enough to obtain trustworthy COT results by plotting successive spectra of a single mono-directional segment, each successive spectrum being calculated using a different number of averages.

Furthermore the vibration data window size used to interpolate between two pulses was chosen. This was done by investigating the speed resolution and accuracy obtained by using various window sizes. The chosen optimum window size was 4096 points.

Next a test for convergence in the rotational domain was done. Four methods, including MWOT, were tested. All methods successfully converged to stable RDAs proving that the rotational domain averaging was implemented correctly and that the pending results are believable. The actual RDAs produced at different stages of wear progression by using the four different speed interpolation techniques showed very little difference between the RDAs produced by each method. Visual inspection of the RDAs also indicated clear signs of wear progression in the form of amplitude modulation and distorted tooth impact peaks.

13 data sets captured at relatively regular intervals throughout the lifetime of the pinion were used to create RDAs. These RDAs were then transformed into the frequency domain using FFTs. The successive FFTs were depicted as a whole using a cascade plot. From a visual inspection of the cascade plot indications of wear progression were observable. A clear difference was also noted between the cascade plots originating from different pinion rotating directions.

To present a more intuitive portrayal of the wear progression a number of components were extracted from the cascade plots and trended individually. The trends giving the best indication of wear progression were those of the 1st and 2nd GMF amplitudes.

CHAPTER 5 CONCLUSION

It has been shown that computed order tracking can be successfully employed to detect fault progression of a pinion gear in the drag gearbox of a dragline. The work done to verify the above statement was broken up and spread over four chapters. Each chapter dealt with a different aspect of the work namely the literature study, the preparation of a monitoring station, the development of order tracking methods and the analysis of the data.

Overviews of numerous fault-detecting methods were introduced in the first chapter. These methods were ordered into families of related work. Statistical methods, neural networks, time-frequency analysis, short-time Fourier transforms, wavelet transforms and autoregressive modelling are all fault finding methods that were discussed. Method groups that are more relevant to the research done include synchronous averaging, demodulation techniques and order tracking.

Demodulation techniques were used to check the data after order tracking was completed. Fatigue cracks often manifest themselves in the measured vibration signal as amplitude and phase modulation; these modulations were used to determine whether gear damage was present. Synchronous averaging is a process whereby a data set is averaged to filter out any noise and to highlight periodic disturbances related to faults in the rotating machinery. Synchronous averaging is usually done with regard to time, in this dissertation however it was done with regard to rotational position, this method is called order domain averaging. Due to the fluctuating nature of the rotational speed, orthodox as well as new order tracking methods were used and evaluated.

To be able to exclude human error and acquire reliable vibration data, an automated on-line monitoring station was set up. This equipment was stationed on the dragline for the approximate lifetime of the drag pinion. The hardware employed consisted of proximity sensors, accelerometers, a low-

pass filter, an analogue to digital conversion card and an industrial computer. The merits and uses of each hardware component utilised were discussed in the second chapter. Software developed to acquire vibration data was also introduced. The ideal sample size to be captured with the available system was determined to be 120 s. The ability of the low-pass filter to cut off frequencies higher than 2500 Hz and a general system test were all performed prior to the monitoring station being employed.

Having set up the monitoring station and acquired the first data sets, the development of tools to analyse the data was described in the third chapter. To facilitate understanding of the specific environment and to enable quicker error detection during the development process it was necessary to relate the acquired data to the dragline activity. To this end video footage was taken synchronous to several 120 s sampling periods. The data block was then divided into a number of finite time periods. The RMS of each finite time period was then taken. The RMS values where then plotted and compared to the video footage enabling identification of periodic increases in vibration intensity to be related to physical dragline actions.

The next development step was to improve existing order tracking programs available by modifying them to suit the data captured. An efficient speed estimation program was also developed. This program supplied the basic speed information that would be interpolated and adjusted so that order tracking could be performed.

In the case of this study only a single pulse per revolution is available to derive angular speed. Interpolation techniques were thus critical to facilitate accurate speed estimation. Orthodox methods such as constant, linear and cubic interpolation techniques were introduced and the merits of each were discussed. In the pursuit of a new speed interpolation technique, numerical integration optimisation and filter optimisation were investigated without success. However by making use of the speed information inherent in the vibration data coupled with the limited information of the shaft rotation, moving window speed determination was developed. This speed interpolation

technique makes used of the shaft pulse to locate the likely position of the GMF in the FFT of a small part of the captured vibration data. The GMF is then pinpointed and reverted back to speed information.

Displacement driven velocity interpolation is another method that was developed to aid the interpolation techniques. DDVI makes use of the fact that granted that the motion of the pinion is in one direction, the angular displacement between two pulses is precisely 2π rad. Thus the integration of the speed-time graph, between two time instances related to two pulses, should be a multiple of 2π. If this is not the case then DDVI adjusts the speed accordingly.

The results derived from the completed analysis of the data captured aboard the dragline for approximately one year were presented in the fourth chapter. It was necessary to determine the minimum number of rotation domain averages that would still yield satisfactory results since the experimental data did not allow for a large number of averages to be taken. To this end a single data set was averaged a number of times, each time using a different number of averages. The power of the GMF achieved in the FFT for each situation was then evaluated. It was found that approximately 70 averages would be sufficient to obtain trustworthy COT results.

The window size used in the MWOT method was determined to be 4096 data points large. This determination was necessary since the window size affects the spectrum used to find the GMF and the ability to detect small changes in the speed. Since an increase in window size improves the spectrum to the detriment of the ability to detect small speed changes a golden middle path had to be found.

Prior to implementing order tracking, the ability of the interpolation techniques to yield stable results was tested by splitting a single data set into two daughter sets. Each daughter set is then incrementally averaged and the average of one daughter set is subtracted from the corresponding average of

the other. All implemented methods performed satisfactorily, constant interpolation was the only method to have performed worse than the others.

Rotation domain averaging was then applied to a number of data sets that were chosen for their abundance of suitable data ranges. The data sets were also chosen to ensure an even spread of samples throughout the monitoring time. This was done so that a progression in fault severity could be spotted. A sample of the averaged data was shown which clearly indicated the amplitude modulation caused by each of the 25 teeth on the pinion.

Cascade plots were then drawn up to show changes in the FFT of the RDA data over the lifetime of the pinion. It was clearly visible that the vibration power of the GMF increased indicating fault progression. It was also noted that the outward bucket motion was a better indication of gear fault due to the fatigue cracks being opened wider by the meshing action of the gears whilst subjected to load. It was shown that the most likely cause of pinion failure was due to misalignment. The misalignment would cause to uneven load distribution and subsequent spalling of the drag pinion.

Although the cascade plots were interpretable, a clearer portrayal of the pinion wear progression was necessary. To this end a number of components of each set in the cascade plot were plotted separately. Maximum amplitude was less sensitive to the fault than the power at the 1^{st} and 2^{nd} GMFs.

In this dissertation the suitability of COT to detect fault progression aboard a dragline has been demonstrated. Furthermore a relationship between the different rotating directions has been established, although it was clear that one direction is more sensitive to fault progression.

The lack of distinction between the four interpolation techniques can be assigned to the meagre speed data available.

5.1 Recommendations

Based on this study the following should be noted with regard to any work in this field or could be investigated additionally:

- The effect of vibration data interpolation on COT could be investigated.
- Care should be taken when choosing vibration segments for analysis of gears rotating in two directions since the early detection of gear faults could be hampered if the insensitive direction is chosen.
- To yield better differentiation between interpolation methods future work done under similar circumstances should be based on more substantial speed information.

REFERENCES

ANDRADE, F.A., ESAT, I., BADI, M.N.M. 2001. A new approach to time-domain vibration condition monitoring: gear tooth fatigue crack detection and identification by the Kolmogorov-Smirnov test. *Journal of Sound and Vibration,* 2001, 240(5), p. 909-919.

BAYDAR, N., CHEN, Q., BALL, A., KRUGER, U. 2001. Detection of incipient tooth defect in helical gears using multivariate statistics. *Mechanical Systems and Signal Processing,* 2001, 15(2), p. 303-321.

BONNARDOT, F., EL BADAOUI, M., RANDALL, R.B., DANIERE, J., GUILLET, F. 2004. Use of the acceleration signal of a gearbox in order to perform angular resampling. *Mechanical Systems and Signal Processing,* Article in Press.

BOSSLEY, K.M., MCKENDRICK, R.J., HARRIS, C.J., MERCER, C. 1999. Hybrid computed order tracking. *Mechanical Systems and Signal Processing,* 1999, 13(4), p. 627-641.

BOULAHBAL, D., GOLNARAGHI, M.F., ISMAIL, F. 1999. Amplitude and phase maps for the detection of cracks in gear systems. *Mechanical Systems and Signal Processing,* 1999, 13(3), p. 423-436.

CHEN, D., WANG, W.J. 2002. Classification of wavelet map patterns using multi-layer neural networks for gear fault detection. *Mechanical Systems and Signal Processing,* 2002, 16(4), p. 695-704.

CHOY, F.K., POLYSHCHUK, V., ZAKRAJSEK, J.J., HANDSCHUH, R.F., TOWNSEND, D.P. 1996. Analysis of the effects of surface pitting and wear on the vibration of a gear transmission system. *Tribology International,* 1996, Vol. 29, No. 1, p. 77-83.

DEMPSEY, P.J. 2000. A comparison of vibration and oil debris gear damage detection methods applied to pitting damage. *NASA/TM-2000-210371.* http://gltrs.grc.nasa.gov/citations/all/tm-2000-210371.html

FYFE, K.R., MUNCK, E.D.S. 1997. Analysis of computed order tracking. *Mechanical Systems and Signal Processing,* 1997, 11(2), p. 187-205.

GADE, S., HERLUFSEN, H., KONSTANTIN-HANSEN, H., WISMER, N.J. 1995. Order Tracking Analysis. *Brüel & Kjær Technical Review No.2.*

GROOVER, C.L., TRETHEWEY, M.W., MAYNARD, K.P., LEBOLD, M.S. 2003. Removal of order domain content in rotating equipment signals by double resampling. *Mechanical Systems and Signal Processing,* Article in Press.

HAMMOND, J.K., WHITE, P.R. 1996. The analysis of non-stationary signals using time-frequency methods. *Journal of Sound and Vibration,* 1996, 190(3), p. 419-447.

HONGXING, L., HONGFU, Z., CHENGYU, J., LIANGSHENG, Q. 2000. An improved algorithm for direct time-domain averaging. *Mechanical Systems and Signal Processing,* 2000, 14(2), p. 279-285

KUHNELL, B.T., 2004. Wear in Rolling Element Bearings and Gears - How Age and Contamination Affect Them. *Machinery Lubrication* Magazine. September 2004

LEE, S.K., WHITE, P.R. 1997. Higher-order time-frequency analysis and its application to fault detection in rotating machinery. *Mechanical Systems and Signal Processing.* 1997, 11(4), p. 637-650.

LIN, J., QU, L. 2000. Feature extraction based on Mortlet wavelet and its application for mechanical fault diagnosis. *Mechanical Systems and Signal Processing,* 2000, 234(1), p. 135-148.

LIN, S.T., MCFADDEN, P.D. 1997. Gear vibration analysis by b-spline wavelet-based linear wavelet transform. *Mechanical Systems and Signal Processing,* 1997, 11(4), p. 603-609.

LUO, G.Y., OSYPIW, D., IRLE, M. 2000. Real-time condition monitoring by significant and natural frequencies analysis of vibration signal with wavelet filter and autocorrelation enhancement. *Journal of Sound and Vibration,* 2000, 236(3), p. 413-430.

MA, J., LI, C.J. 1996. Gear defect detection through model-based wideband demodulation of vibrations. *Mechanical Systems and Signal Processing,* 1996, 10(5), p. 653-665.

MCFADDEN, P.D. 1986. Detecting Fatigue Cracks in Gears by Amplitude and Phase Demodulation of the Meshing Vibration. *Journal of Vibration, Acoustics, Stress, and Reliability in Design*, April 1986, Vol. 108, p. 165-170.

MCFADDEN, P.D. 1987i. A revised model for the extraction of Periodic waveforms by time domain averaging. *Mechanical Systems and Signal Processing,* 1987, 1(1), p. 83-95.

MCFADDEN, P.D. 1987ii, Examination of a technique for the early detection of failure in gears by signal processing of the time domain average of the meshing vibration. *Mechanical Systems and Signal Processing,* 1987, 1(2), p. 173-183.

MCFADDEN, P.D. 2000. Detection of gear faults by decomposition of matched differences of vibration signals. *Mechanical Systems and Signal Processing,* 2000, 14(5), p. 805-817.

MCFADDEN, P.D., and SMITH, J.D. 1985. A signal processing technique for detecting local defects in a gear from signal average of the vibration. *Proc Instn Mech Engrs,* 1985, Vol. 199, No C4, p. 287-292.

MCFADDEN, P.D., COOK, J.G., FORSTER, L.M. 1999. Decomposition of gear vibration signals by the generalised s transform. *Mechanical Systems and Signal Processing,* 1999, 13(5), p. 691-707.

MEESAD, P., YEN, G.G. 2000. Pattern classification by neurofuzzy network: application to vibration monitoring. *ISA Transactions,* 2000, 39, p. 293-308.

OGUAMANAM, D.C.D., MARTIN, H.R., HUISSOON, J.P. 1995. On the application of the beta distribution to gear damage analysis. *Applied Acoustics,* 1995, 45, p. 247-261.

PADOVESE, L.R. 2004. Hybrid time-frequency methods for non-stationary mechanical signal analysis. *Mechanical Systems and Signal Processing,* 2004, 18, p. 1047-1064.

PARKER, B.E.JR, WARE, H.A., WIPP, D.P., TOMPKINS, W.R., CLARK, B.R., LARSON, E.C., POOR, H.V. 2000. Fault diagnosis using statistical change detection in the bispectral domain. *Mechanical Systems and Signal Processing,* 2000, 14(4), p. 561-570.

PAYA, B.A., ESAT, I.I., BADI, M.N.M. 1997. Artificial neural network based fault diagnostics of rotating machinery using wavelet transforms as a pre-processor. *Mechanical Systems and Signal Processing,* 1997, 11(5), p. 751-765.

POSTE, P. 2001. Can Condition Monitoring improve your plant performance? *World Pumps,* September 2001, p. 40-47.

ROAN, M.J., ERLING, L.G., SIBUL, L.H. 2002. A new, non-linear, adaptive, blind source separation approach to gear tooth failure detection and analysis. *Mechanical Systems and Signal Processing,* 2002, 16(5), p. 719-740.

SAAVEDRA, P.N., RODRIGUEZ, C.G. 2006. Accurate assessment of computed order tracking. *Shock and Vibration,* 2006, 13(1), p. 13-32.

SAMANTA, B. 2004. Gear fault detection using artificial neural networks and support vector machines with genetic algorithms. *Mechanical Systems and Signal Processing,* 2004, 18, p.625-644.

STANDER, C.J., HEYNS, P.S., SCHOOMBIE, W. 2001. Fault detection on gearboxes operating under fluctuating load conditions. *Condition Monitoring and Diagnostic Engineering Management. Comadem 2001. Proceedings of the 14th International Congress.* Manchester, 4-6 September 2001, p. 457-464.

STANDER, C.J., HEYNS, P.S., SCHOOMBIE, W. 2002. Using vibration monitoring for local fault detection on gears operating under fluctuating load conditions. *Mechanical Systems and Signal Processing,* 2002, 16(6), p. 1005-1024.

STASZEWSKI, W.J. 1998, Wavelet based compression and feature selection for vibration analysis. *Journal of Sound and Vibration,* 1998, 211(5), p. 735-760.

STASZEWSKI, W.J., TOMLINSON, G.R. 1994. Application of the wavelet transform to fault detection in a spur gear. *Mechanical Systems and Signal Processing,* 1994, 8(3), p. 289-307.

STASZEWSKI, W.J., TOMLINSON, G.R. 1997. Local tooth fault detection in gearboxes using a moving window procedure. *Mechanical Systems and Signal Processing,* 1997, 11(3), p. 331-350.

SUNG, C.K., TAI, H.M., CHEN, C.W. 2000. Locating defects of a gear system by the technique of wavelet transforms. *Mechanism and Machine Theory,* 2000, 35, p. 1169-1182.

TOMAZIC, S. 1996. On short-time Fourier transform with single-sided exponential window. *Signal Processing*, 55 (1996), p. 141-148.

WANG, W.J., MCFADDEN, P.D. 1993i. Early detection of gear failure by vibration analysis-I. Calculation of the time-frequency distribution. *Mechanical Systems and Signal Processing,* 1993, 7(3), p. 193-203.

WANG, W.J., MCFADDEN, P.D. 1993ii. Early detection of gear failure by vibration analysis-II. Interpretation of the time-frequency distribution using image processing techniques. *Mechanical Systems and Signal Processing,* 1993, 7(3), p. 205-215.

WANG, W.J., MCFADDEN, P.D. 1995. Application of orthogonal wavelets to early gear damage detection. *Mechanical Systems and Signal Processing,* 1995, 9(5), p. 497-507.

WANG, W.J., MCFADDEN, P.D. 1996. Application of wavelets to gearbox vibration signals for fault detection. *Journal of Sound and Vibration,* 1996, 192(5), p. 927-939.

WANG, W., WONG, A.K. 2000. Linear prediction and gear fault diagnosis. *Condition Monitoring and Diagnostic Engineering Management. Comadem 2000.* p. 797-807.

WANG, W.J. 2001i. Wavelets for detecting mechanical faults with high sensitivity. *Mechanical Systems and Signal Processing,* 2001, 15(4), p. 685-696.

WANG, W. 2001. Early detection of gear tooth cracking using the resonance demodulation technique. *Mechanical Systems and Signal Processing,* 2001, 15(5), p. 887-903.

WHITE, G. 1991. Amplitude Demodulation - A New Tool for Predictive Maintenance. *Sound and Vibration*, September 1991, p. 14-19.